UNIVERSITY OF MESSINA
DEPARTMENT OF VETERINARY SCIENCES

THE PhD COURSE IN VETERINARY SCIENCES
MORPHOPHYSIOLOGY AND APPLIED BIOTECHNOLOGY

LARVAL PERFORMANCE AND SKELETAL DEFORMITIES IN FARMED GILTHEAD SEABREAM: THE POTENTIAL EFFECTS OF MELATONIN

by
Kamel Mhalhel

A Dissertation Submitted for the Degree of
Doctor of Philosophy in Veterinary Sciences

Tutor
Prof. Giuseppe Montalbano

PhD Coordinator
Prof.ssa Rosaria Laurà

Messina, November 2022

UNIVERSITY OF MESSINA
DEPARTMENT OF VETERINARY SCIENCES

THE PhD COURSE IN VETERINARY SCIENCES
MORPHOPHYSIOLOGY AND APPLIED BIOTECHNOLOGY

LARVAL PERFORMANCE AND SKELETAL DEFORMITIES IN FARMED GILTHEAD SEABREAM: THE POTENTIAL EFFECTS OF MELATONIN

by
Kamel Mhalhel

A Dissertation Submitted for the Degree of
Doctor of Philosophy in Veterinary Sciences

Tutor
Prof. Giuseppe Montalbano

PhD Coordinator
Prof. Rosaria Laurà

Messina, November 2022

Present doctoral thesis in numbers

Number of preliminary pages: XIII

Number of total pages: 135

Number of figures: 21

Number of tables: 3

Number of references: 180

The results of this dissertation have been published in:

Mhalhel, K., Germanà, A., Abbate, F., Guerrera, M. C., Levanti, M., Laurà, R., & Montalbano, G. (2020). The Effect of Orally Supplemented Melatonin on Larval Performance and Skeletal Deformities in Farmed Gilthead Seabream (*Sparus aurata*). International Journal of Molecular Sciences, 21(24). https://doi.org/10.3390/ijms21249597

(Copy in Appendice)

Keywords

Sparus aurata; seabream; melatonin; fish-farming; growth; bone; mineralization; IGF-1; deformities; operculum; opercular complex; *PTHrP*; *mlc2*; *bglap*

Abstract

The gilthead seabream larval rearing in continuous light is a common practice in most Mediterranean hatcheries to increase food intake, improves the conversion rate, and stimulate larval growth in length. Nevertheless, numerous investigations have revealed that continuous light interrupts circadian rhythm alternation, affects larval development and raises the prevalence of skeletal abnormalities.

Melatonin, the major output signal of the circadian system, is a crucial pineal neurohormone that stimulates cell proliferation and embryonic development in many teleosts and enhances osseointegration in mice and humans. We believe that inhibiting MEL by continuous light during early life alters larvae growth and development and increases the incidence of skeletal deformities, particularly those affecting the opercular complex.

To our knowledge, no study has been conducted on the effect of exogenous melatonin in gilthead seabream larval development. Therefore, our main purpose in the present research was to investigate the effect of orally supplemented melatonin on larval performance and skeletal deformities in farmed gilthead seabream under standard rearing conditions.

Melatonin increased the frequency of skeletal deformities, especially those of the operculum, for which we have recorded new typologies. The first signs of the opercular complex deformities were recorded before any sign of mineralization, proving that the abnormalities occur during the onset of the operculum complex bone series. Caudal fin complex was also sensitive to exogenous melatonin administration, and its abnormalities' incidence was increased dose-dependent. In light of our results and bibliographic data, we hypothesize that skeletal deformities detected in experimental groups' larvae can be induced by the increased PTHrP expression level induced by exogenous melatonin or by a loss of coordination between skeletal muscle and bone growth. Future research should extend and unmask the melatonin-pathways behind muscle and bone growth in gilthead seabream. This is the first study to report the effect of exogenous melatonin on bone deformities and growth of Sparus aurata larvae reared under ordinary hatchery conditions.

Table of Contents

Table of Figures

List of Tables

List of Abbreviations

Abbreviation	Definition
MEL	Melatonin
HPF	Hours after fertilization
DPH	Days post-hatching
RT-PCR	Real-Time Reverse Transcription–Polymerase Chain Reaction Assay
L	Length
W	Weight
LWR	Length-weight relationship
HUFA	Highly unsaturated fatty acids
RHT	Retino-hypothalamic tract
SCN	Suprachiasmatic nuclei of the hypothalamus
PVN	Hypothalamic paraventricular nuclei
SCG	superior cervical ganglion
AANAT	Arylalkylamine N-acetyltransferase
SEM	scanning electron microscopy
IGF-1	Insulin-like growth factor 1
PTHrP	parathyroid hormone-related protein-coding gene
bglap	bone gamma-carboxyglutamate protein-coding gene
mlc2	myosin light chain 2
ef1α	elongation factor 1 alpha
ANOVA	Analysis of Variance
SEM	Standard error of the mean
SD	standard deviation

Statement of Original Authorship

I confirm that this Ph.D. thesis has not been previously presented elsewhere to fulfill any other qualification. The thesis contains no material previously published or written by another author except where due reference is made.

Kamel Mhalhel

15/09/2022

Acknowledgments

First and foremost, I would like to express my sincere gratitude to my research Tutor, Assoc.Prof. Dr. Giuseppe Montalbano for your continuous encouragement, support, and guidance over these past three years. Without your assistance and dedicated involvement, this thesis would have never been accomplished.

My sincere thanks also go to the head of the laboratory, Prof. Antonino Germanà, and Prof. Francesco Abbate, who generously provided expertise and insightful comments.

Special thanks go to Prof. Rosaria Laura, Prof. Maria Levanti, Assoc. Prof. Dr. Germana Patrizia Germanà and Assoc. Prof. Dr. Maria Cristina Guerrera for their continual advice and guidance and for helping me mature into the scientist I am today.

I thank my fellow labmates for entertainment during the sleepless nights we were working together before deadlines, which kept my sanity over the last three years.

Importantly, I would like to express my gratitude to my amazing family, who have supported me throughout my studies. Thank you for always being there on the other end of the phone and for all your sacrifices, love, and well wishes. Special thanks go to my partner for being by my side in everything I do, and for your constant encouragement, without which this would not have been possible.

Chapter 1: Introduction

1.1 BACKGROUND

The gilthead seabream (*Sparus aurata*), one of the most important species in Mediterranean aquaculture, with an increasing status of exploitation in terms of production volume and aquafarming technologies, has become an important research topic over the years (FAO, 2022a; Lupatsch, 2004; Sola et al., 2007). A better knowledge of the molecular pathways behind their functional and biological characteristics has significantly improved the aquacultural aspects, namely their reproductive success, survival, and growth (Kır, 2020; Manchado et al., 2016; Papandroulakis et al., 2002; Sadek et al., 2004; Verhaegen et al., 2007). Like most teleosts, gilthead seabream exhibit indeterminate growth, with muscle mass increasing by hyperplasia and hypertrophy (Rowlerson et al., 1995), and the first commercial size of 300 to 500 g takes between 18 and 24 months, and the size of 400 to 600 g takes around 24 months depending on rearing conditions (European Food Safety Authority (EFSA), 2008).

Even though the gilthead seabream aquaculture industry has made remarkable progress, hatchery conditions are still far from ideal, resulting in frequent abnormalities at the beginning of intensive culture, entailing significant economic losses (Bardon et al., 2009; Beraldo & Canavese, 2011; Negrín-Báez et al., 2015; Ortiz-Delgado et al., 2014; Sfakianakis et al., 2013).

Skeletal deformities in gilthead seabream fry typically affect the cephalic region, namely the snout and the opercula, as well as the vertebral column and fins (Galeotti et al., 2000; Koumoundouros, Oran, et al., 1997; Mhalhel et al., 2020; Moretti et al., 1999; Ortiz-Delgado et al., 2014; Sfakianakis et al., 2013). Those deformities are induced during the embryonic and post-embryonic

periods of life, and their development is still not well understood (Berillis, 2017; Ortiz-Delgado et al., 2014). Among the cephalic malformations, opercular complex anomalies are the most common and evident external abnormality in reared gilthead sea bream, affecting up to 80% of the population (Andrades et al., 1996; Beraldo & Canavese, 2011; Galeotti et al., 2000; Koumoundouros, Oran, et al., 1997; Negrín-Báez et al., 2015; Verhaegen et al., 2007). Besides the impairment of the image and market value of the final product, opercular anomalies affect the breathing process during water intake and discharge, reduce resistance to environmental stress especially reduced oxygen levels, and indirectly predispose the fish to gill diseases and bacterial infections (Beraldo & Canavese, 2011; Galeotti et al., 2000; Thuong et al., 2017; Verhaegen et al., 2007). Fish development and growth, from newly hatched larvae into juveniles, is associated with several morphological and physiological changes controlled and coordinated by many endocrine factors. In fish, as in mammals, melatonin (MEL) is the crucial output signal of the circadian clock produced mainly in two phototransducing sites, the retina and pineal gland, and displays daily and seasonal secretion patterns with a peak level during the dark phase (Boeuf & Falcon, 2001; Falcón, Migaud, et al., 2010; Kalamarz et al., 2009; Sánchez-Vázquez et al., 2019). The involvement of MEL in Teleosts larval development and growth has been demonstrated by several in vivo and in vitro studies showing that MEL stimulates cell proliferation and embryonic development in a dose-dependent manner (Danilova et al., 2004; Falcón, Migaud, et al., 2010; Fjelldal et al., 2004; Maria et al., 2018; Sun et al., 2020; Zhu et al., 2020). In the zebrafish embryo, MEL could regulate cell proliferation rate and accelerate fish development through MT2 receptors (Danilova et al., 2004).

Additionally, during the early ontogenesis of gilthead seabream and haddock (*Melanogrammus aeglefinus*), MEL controls the development and

protection against free radicals (Downing & Litvak, 2002; Kalamarz et al., 2009). Moreover, a study conducted in 2004 reported that MEL has numerous functions related to vertebral bone growth in Atlantic salmon (Fjelldal et al., 2004). It promotes osteoblastic differentiation, improves osseointegration in mice, and stimulates osteoblastic specialization of MC3T3-E1 cells and human mesenchymal stem cells (MSC)/peripheral blood mononuclear cells by increasing the expression levels of osteogenic markers (Maria et al., 2018; Sun et al., 2020; Zhu et al., 2020). In gilthead seabream larvae, MEL production initiates immediately after hatching to reach maximum levels between 6 and 10 days post-hatching (DPH) (Kalamarz et al., 2009). At this time, the hormones implicated in growth, metabolism, and development, i.e., growth hormone and prolactin, are shallow (Herrero-Turrion et al., 2003; Herrero-Turrión et al., 2003), and the number of growth hormone cells and growth hormone expression levels do not increase until 30 DPH (Deane et al., 2003).

A high MEL production during the first days post-hatching in gilthead seabream larvae, when growth hormone and prolactin supplies are still insufficient, suggested a distinct role of MEL in early organogenesis, particularly in skeletogenesis, by stimulating cell proliferation and differentiation processes (Danilova et al., 2004; Kalamarz et al., 2009).

1.2 CONTEXT AND PURPOSES

The larval rearing of gilthead seabream in continuous light is a common practice in Mediterranean hatcheries. Indeed, continuous light speeds up the depletion of yolk sac reserves, improves the conversion rate, stimulates feeding behavior by around 40%, and promotes larval length growth (Villamizar et al., 2011). However, several studies have shown that continuous light interrupts the circadian rhythm alternation, increases the prevalence of skeletal deformities, and affects larval development (Villamizar et al., 2009). The circadian rhythm alternation has a key role in synchronizing daily

behavioral processes in fish (food intake, shoaling behavior, locomotor activity), oxygen consumption, thermoregulation, MEL synthesis, and growth (Falcón et al., 2007).

In light of the above-mentioned bibliographical data, we thought that inhibiting MEL by continuous light during early life alters larvae growth and development and increases the incidence of skeletal deformities, particularly those affecting the opercular. To our knowledge, no study has been conducted on the effect of exogenous MEL intake on early life performance and skeletal deformities of gilthead seabream skeletogenesis. Therefore, our main purpose in the present study was to radiate the knowledge on early-stage gilthead seabream development and evaluate the effect of orally supplemented MEL on larval performance and skeletal deformities (especially the opercular complex abnormalities). Thus, we have fixed the down mentioned specifics objectives:

1st Specific objective: Characterization of the growth pattern of gilthead seabream larvae under standard rearing conditions.

2nd Specific objective: Investigation of the mineralization pattern and the beginning of the process in gilthead seabream larvae.

3rd Specific objective: Characterization of operculum complex deformities: moments of the apparition, the different forms, and its evolution over time.

4th Specific objective: The evaluation of the incidence of opercular complex deformities.

5th specific objective: The evaluation of the exogenous melatonin effects on larval growth

6th specific objective: The evaluation of the effects of exogenous melatonin on bone deformities, especially those affecting the operculum complex.

Chapter 2: Literature Review

2.1 GILTHEAD SEABREAM: TAXONOMIC AND BIOLOGICAL FEATURES

The gilthead seabream (*Sparus aurata*, Linnaeus, 1758), known as orata, is the single species of the genus *Sparus* that has given the whole family of sparidae its name. It belongs to the superclass of Actinopterygii ray-finned fishes, to the class of Osteichthyes, and the order of Perciformes (perch-like) (Pavlidis & Mylonas, 2011).

Kingdom	Animalia
Phylum	Chordata
Subphylum	Vertebrata
Superclass	Gnathostomata
superclass	Osteichthyes -Teleostei
Order	Perciformes
Family	Sparidae
Genus	Sparus
Species	*Sparus aurata*

Gilthead sea bream are characterized by a silvery grey oval body, recalling the shape of the glittering metallic tip of a spear, hence the name of the genus "*Sparus*" (FAO, 2022b; Pavlidis & Mylonas, 2011). It has several distinguishable characteristics. It has a large black blotch at the origin of the lateral line extending on the upper margin of the opercle. The head profile is regularly curved with two small eyes separated by a golden frontal band, hence the name of the species that comes from the Latin "auratus", which means golden.

It has a dorsal fin with 13 to 14 soft rays and 11 spines, an anal fin with 11 or 12 soft rays and three spines, scaly cheeks, and a scaleless preopercle (FAO, 2022b).

In the wild, it inhabits either solitary or in a small shoal, seagrass beds, sandy bottoms, and the surf or breaker zone, often to depths of about 30 m, even though adults may occur at 150 m deep. It is a sedentary euryhaline and eurythermal fish that can tolerate a wide range of salinity and temperatures and thus frequents coastal waters and estuaries (Pavlidis & Mylonas, 2011; Sola et al., 2007). The gilthead seabream is an opportunistic feeder, adapting its diet to the food items available in the habitat (Pita et al., 2002). It has mainly a carnivore diet consisting of gastropods and bivalves (Pita et al., 2002).

It is known as a common subtropical fish of the warm coastal waters of the Mediterranean, Black Seas, and the Eastern Atlantic Ocean, distributed from 62°N-15°N, 17°W-43°E. However, recent increasing capture records in England and Ireland have proved the distribution of this species in the cold waters of the English Channel and the Celtic Sea (The European Commission, 2014).

2.2 LIFE CYCLE

The overall life cycle of gilthead sea bream has been reconstructed through in vivo observations. At 18.5°C, the first cleavage division occurs around 1:15 hours after fertilization (HPF) occurs. Later, several cleavages, occurring in different planes, upgrade the two cells zygote morphology to 4, 8, 16, 32 cells-stages and morula at 1:45h, 2h, 2:30h, 3h, 4:15 h after fertilization, respectively. Then, cleavages continue, the blastodisc begins to look ball-like, and the high blastula stage is reached at 6:00 HPF. The epiboly continues, and the involution defines the initiation of gastrulation at 10:00 HPF. The gastrula undergoes a variety of morphometric movements, and from 18:00 h after the fertilization, the embryo started to become denser, and the first 5-6 couples of

somits and kupffer apparatus were observed two hours later. The appearance of the first pigmentation was recorded at 21:00 HPF (Kamacı et al., 2005). Two days after fertilization, zygotes hatch in the open sea from October to December in the Mediterranean, and the larvae released measure more or less 3 mm in length (Figure 1) (Desoutter et al., 1990; Kamacı et al., 2005). The planktonic larval stage lasts around 50 days at 17-18° C (Sola et al., 2007).

At hatching, the yolk-sac larvae (21 somites) were intermittent swimmers with a prominent head and a large yolk sac. Larvae of 15–18 days of age had the yolk-sac content completely resorbed and started to develop a functional gut with its related glands: the opening of the mouth, the beginning of external feeding, and the digestive functionality. At this stage, the larva could perform more regular searching-for-food swimming based on undulatory movements of the body. The axial muscle progressively acquired its definitive complicated anatomical pattern (Patruno et al., 1998; Yúfera et al., 2012). At the pre-metamorphic stage, larvae aged 30–45 days (about 5.5–8 mm in length, 25 definitive somites) showed a pronounced development at the origin of the classic vertebrate bauplan and the intestine maturation. Post-larvae aged 60–90 days represented true juveniles. The fry (about 14–20 mm in length) was characterized by the loss of the typical larval features and the development of gastric functionality (Patruno et al., 1998; Yúfera et al., 2012). Scales and rayed fins showed their definitive anatomical organization. Locomotion at this age was mainly based on the propeller push of the caudal region, and swimming performances improved significantly (Patruno et al., 1998). Fry of 150 days (about 28 mm in length) showed a general anatomy and swimming behavior comparable to those of adult fish (Figure 1) (Patruno et al., 1998).

The sea bream is a protandrous hermaphrodite. They mature as functional males in the first two years, and when they reach over 30 cm in length, they turn into females (Chaoui et al., 2006; Mehanna, 2007). Females

with asynchronous ovarian development are batch spawners and can lay between 20,000 and 80,000 eggs per spawning period of twenty-four hours over up to 3 months, and the normal fertilization ratio is 90 – 95 % (Sola et al., 2007).

During the male phase, the bisexual gonad has a ventral functional testicular, with asynchronous spermatogenesis and non-functional dorsal ovarian areas (Zohar et al., 1978). Considering the genetic identity between males and females, morphological and behavioral differences and sexual dimorphisms were explained by a sex-biased expression where genes are transcribed more or less in one sex than another (Pauletto et al., 2018; Tsakogiannis et al., 2019).

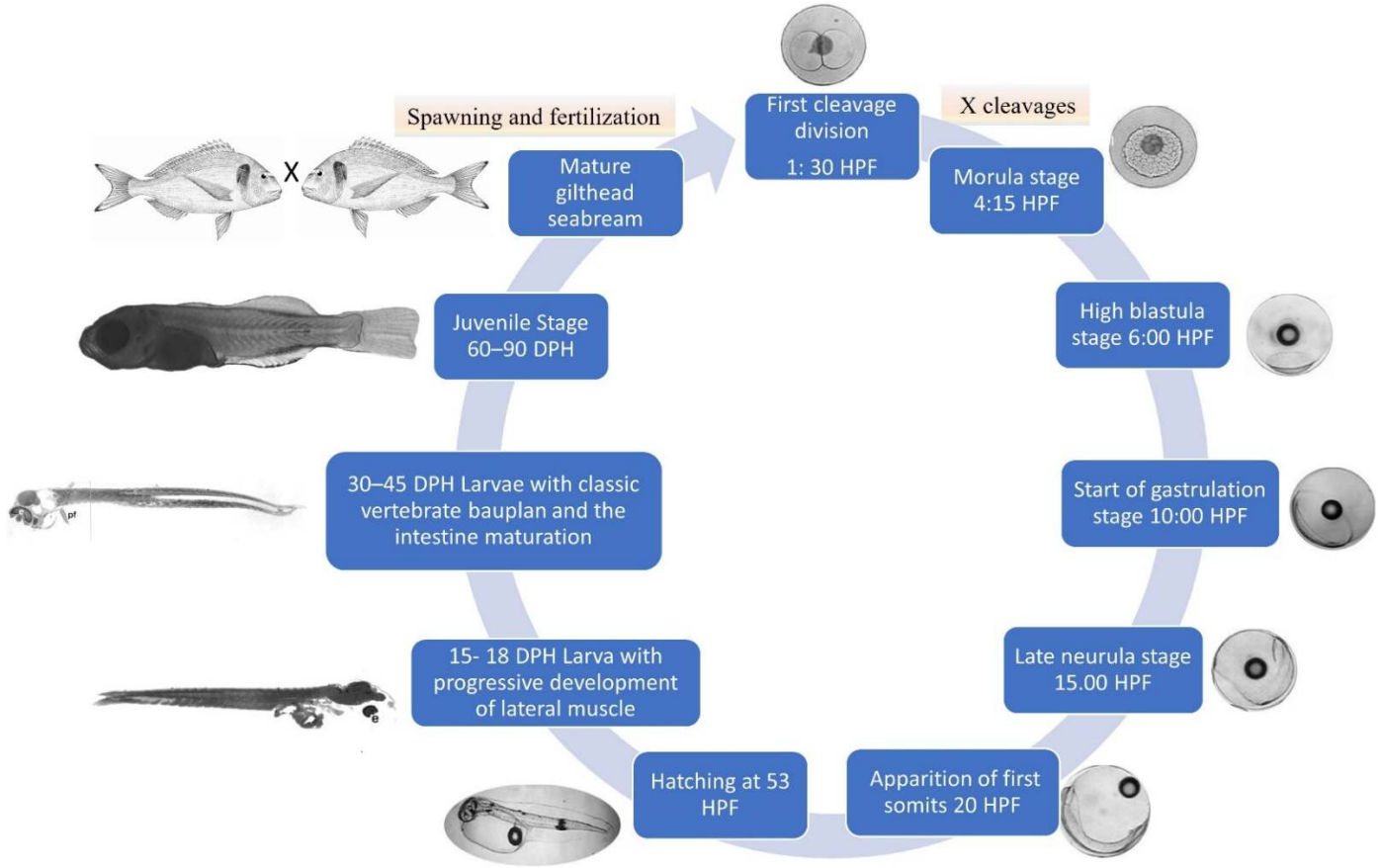

Figure 1. A reconstruction of gilthead seabream life cycle. Several cleavages in different planes upgrade the zygote morphology into a morula, and high blastula stage, at 4:15 h, and 6 HPF, respectively. The epiboly continues, and the involution defines the gastrula (10 HPF), which undergoes a variety of morphometric movements at the origin of a dense larva. Two days after fertilization, zygotes hatch, and larvae develop a functional gut and the classic vertebrate bauplan (15-45DPH) progressively. Planktonic larvae lose their typical features, and a pronounced development is at the origin of a true juvenile (60–90 DPH). They mature as functional males in the first two years, and when they reach over 30 cm in length, they turn into females. This figure was made using material from (Colloca & Cerasi, 2022; Kamacı et al., 2005; Patruno et al., 1998).

2.3 GROWTH CHARACTERISTICS

Growth is an integrated physiological process converting ingested energy to biomass. The efficacy of this conversion is regulated by the genetic growth potential of fish and various abiotic factors such as food disponibility and quality, temperature, photoperiod, and salinity (Debes et al., 2020).

Like most teleosts, Gilthead sea bream exhibits indeterminate growth, with muscle mass increasing by hyperplasia and hypertrophy throughout their lifespan (Rowlerson et al., 1995). It is a long-lived species, with a maximum reported growth of 57.5 cm (2500 g) on 12 years old fish in the Mediterranean and 61.4 cm (3080.6 g) on 14 years old Black Sea fish (Aydin, 2018; Kraljević & Dulčić, 1997). In aquaculture, producing commercial-size fish of 300 to 500 g takes between 18 and 24 months, depending on rearing conditions.

Gilthead sea bream is ectotherms. Thus, water temperature greatly influences their physiology and consequently their growth rate (Caterina et al., 2014). Although it is a eurythermal fish tolerating a wide range of temperatures, the optimal growth rate is observed between 25 and 30 °C (Kır, 2020).

The photoperiod, as well, is one of the directive factors on growth since it provides the fish with a signal that stimulates the endocrine system, namely growth hormone levels (Björnsson et al., 2000; Ginés et al., 2004). Several marine species react to long photoperiod growth-stimulating light treatments, which either directly improve their food intake and feed conversion efficiency, or suppress sexual maturation, thus enabling the redirection of energy from gonadal to muscle tissue and fat in the abdominal cavity (Ginés et al., 2004). Gilthead sea bream was one of the species where photoperiod's positive effects on larvae cultivation were demonstrated by enhancing prey detection (Vardar & Yildirim, 2012). In young and adult specimens, long and constant

photoperiods and permanent light have enhanced sea bream growth efficiency by delaying sexual maturity (Vardar & Yildirim, 2012).

Gilthead sea bream is a euryhaline species and thus can efficiently face variations in environmental salinity, which seems to have a minor effect on growth, at least in the adult stage (Zarantoniello et al., 2021). On gilthead sea bream larvae, however, decreasing the daily dilution rate of water salinity induced a significant increase in the average daily gain (mg/fish/day), specific growth rate (SGR), protein, fat, and energy gain (Mabrouk & Nour, 2011).

In addition to physico-chemical parameters of the aquatic environment, the growth is affected by many other factors, including the genetic component, food availability, and dietary quality (Ginés et al., 2004; Torno et al., 2019).

The optimal dietary protein requirements are known to be affected by several factors, including fish size, the quota of non-protein energy in the diet, and the protein source quality (Sankian et al., 2017). As insufficient non-protein energy is available in the diet, part of the dietary protein will be catabolized to supply energy. For this reason, dietary supplementation of energy-yielding nutrients, mainly lipids, was considered an optimal solution to improve the efficiency of protein utilization by fish. However, the supply of dietary lipids more than the requirement can limit feed consumption, thereby reducing the intake of the required amount of protein and other essential nutrients (Sankian et al., 2017).

For maximum growth, gilthead seabream needs a balanced diet made of 40-46% protein and 12 to 24% lipid, which would reduce the use of protein for energy production, leading to a protein-sparing effect (Caballero et al., 1999; Mongile et al., 2014).

Awareness of the nutritional importance of vitamins, specifically vitamins C and E, has grown progressively over the last decades. A study on gilthead seabream suggests that increasing dietary vitamin E levels associated

with medium HUFA enhanced larval growth performance in terms of total length. This finding indicates the importance of dietary vitamin E for larval growth and its interrelation with dietary HUFA (Atalah et al., 2012).

The length (L)-weight (W) relationship (LWR) expressed by the equation $W = aL^b$ estimated using the natural logarithmic equivalent log W = b logL + loga, where a = the intercept and b = the slope; reveals the extent to which the two growth variables are related to each other (Nie et al., 2013; Wang et al., 2012). It is useful to estimate indirect growth, biomass, fatness, body condition, gonad development, and ontogenetic changes of fish, helping to understand the developmental variation during their life cycle (De Guzman & Geronimo R, 2020). It has important implications for fishery management and aquaculture practice and between region comparisons of life histories of a specific species (Guo et al., 2014; Li et al., 2016).

Fish may attain an isometric growth (b = 3) which means that the body shape does not change as an organism grows. Negative allometric growth (b < 3) means that a fish becomes thinner as its weight increases; while positive allometric growth (b > 3) means that its body becomes relatively broader as the length of the fish increases (De Guzman & Geronimo R, 2020; Riedel et al., 2007).

Another index calculated from the relationship between the weight of a fish and its length, the condition factor (CF), which is extensively used in monitoring growth and determining the well-being status of the fish (Ndiaye et al., 2015). It assumes that heavier fish of a given length are in better condition and estimated from the relationship: K = 100 w/Lb, where W is the weight of the fish in grams, L is the total length of the fish in centimeters, and b is the value obtained from the length-eight equation formula (Daniel, 1984). The CF is affected by age, sexual maturity, season, and nutritional conditions. It is used in comparing two or more co-specific populations living in similar or

different rearing conditions, determining the period of gonadal maturation, and observing the feeding activity or population changes, consequently to modifications in food resources (Ndiaye et al., 2015). Morphometric analyses, such as weight and length analyses, and their mathematical relationship are usually applied, considering the economic aspect of costs and time.

Many studies have investigated the relationship between morphometric indices and physiological status for adult gilthead seabream and examined whether the use of feeds with different diets or different additives affects the length-weight relationship (Aysun et al., 2018).

Length-weight relationship with respect to feed with different protein levels (38%, 42% and 45%) were estimated to be $W= 0.051*TL^{2.63}$, $W=0.046*TL^{2.67}$ and $W=0.046*TL^{2.68}$ respectively. These values were in favor of higher growth in length than in weight for the three experimental groups (Aysun et al., 2018). Those results concord with the result reported on the Aegean Sea gilthead seabream populations during winter months, where the b values ranged from 2.736 to 2.737 (Akyol & Gamsiz, 2011; Tevfik et al., 2009), compared to 2.83 to 2.98 in the Mediterranean Sea (Cicek et al., 2006; Sangun et al., 2007). The reason behind the negative allometric growth reported by the first study (Aysun et al., 2018) can be explained by the gonadal development during which fish need to reach the length of sexual development, while that of Aegean Sea gilthead seabream was justified by the fish caught in winter when they still in spawning period (Akyol & Gamsiz, 2011; Aysun et al., 2018; Cicek et al., 2006; Sangun et al., 2007; Tevfik et al., 2009). Thus, the differences in the b value can be the result of various factors such as the length of the fish at initial maturity, age, gender, water temperature, and amount of feed.

Larvae grow from 3 mm to 9 mm in length in about 30 days (FAO, 2022b). During the larval stage, the feeds distributed are extremely small particles or live organisms from both rotifers and artemia. Studies have proved

that values of growth performance of gilthead seabream larvae were significantly increased by increasing the levels of live food (Eid et al., 2018). The preferences for food particles are related to the mouth opening ranging between 50 – 250 μm for larvae of 8 – 10 mm, 180 – 400 μm for larvae of 20 mm, and 315 – 600 μm for juveniles of 25 mm (FAO, 2022b).

2.4 POPULATION GENETICS

The gilthead seabream represents an important economic resource for Mediterranean aquaculture. Given its wide geographic distribution and economic importance, studies carried out on the genetic composition of natural populations, and the possible existence of panmictic or subdivided populations have been largely studied. Those studies have revealed a heterogeneous degree of genetic differentiation among gilthead seabream populations along the Atlantic and Mediterranean coasts through allozymes and microsatellites (Alarcón et al., 2004; Loukovitis et al., 2012; Rossi et al., 2006). Marker analyses identified a subdivision into three genetic clusters: East, West Mediterranean, and Atlantic. The first mentioned group could be further subdivided into an Ionian/Adriatic and an Aegean group using the outlier markers (Gkagkavouzis et al., 2019; Maroso et al., 2021; Rossi et al., 2006). Additionally, it was demonstrated that the intentional release of fry of unknown origin in restocking programs in non-confined coastal lagoons, or the accidental escape of fish from farms, have contributed to a mix of all gilthead sea bream genetic stocks (Sola et al., 2007). These results provide a baseline for future reference in any management program of both wild and farmed populations of gilthead seabream, a first step toward the study of the potential genetic impact of the sea bream aquaculture industry on wild populations (Gkagkavouzis et al., 2019; Maroso et al., 2021).

2.5 BREEDING AND CULTURE PRACTICES

2.5.1 History

The early culturing of gilthead seabream relied on the capture of wild juveniles that are the result of natural spawning in the wild, using valli and fish barriers taking benefit of the natural trophic migration of juveniles from the sea into coastal lagoons (Moretti et al., 1999). The pressures of the valli capture dramatically reduced the wild stocks' resources, limiting the expansion and even the continuation of the activity itself, creating the need to develop intensive production practices (Moretti et al., 1999). Large-scale production of fry was achieved in the early 1980's borrowing technology previously developed for the cage rearing of salmonids in northern Europe (Laird, 2001), and by the 1990's, the intensive production of juveniles and methods to produce fish to market size in cages or ponds were optimized (Moretti et al., 1999). The accumulation of knowledge on reproduction techniques, generating a reliable and programmable supply of fry, and advancements in the larval nutritional and environmental requirements have allowed the inflation of the scale of gilthead sea bream production, one of the major products of Marine fish farming (Laird, 2001; Moretti et al., 1999).

2.5.2 Production and trade

During the last decade, the fisheries and aquaculture sectors have been increasingly recognized for their essential contribution on fulfilling the demand for safe and healthy food for a world population that will reach nearly 10 billion by 2050 (FAO, 2022a). Gilthead sea bream is one of the most important reared species in worldwide aquaculture, especially in the Mediterranean Sea, with an increasing status of exploitation in terms of production volume and culture technologies. Gilthead seabream intensive production in the Mediterranean began in the early 1980s in marine cages and recirculating aquaculture systems. In the late eighteen' this species' production

was 1800 tonnes (Tn), and in teen years only (1997), it reached 45 000 Tn (Laird, 2001). In 2020, its production was estimated at 258,754 Tn, classifying our species 33rd among the most reared fish (FAO, 2022a; NFISS, 2022).

The main six producers worldwide are Turkey, Greece, Egypt, Tunisia, Spain, and Italy with 38.54%, 21,43%, 13,87%, 6,96%, 4,82%, and 2,84%, respectively, of the gilthead sea bream world production (FAO, 2022a). Since 2000, the 50% increase in UE production was promoted mainly by a six-times multiplied production in Croatia and two times in Cyprus. In 2019, the EU27 produced 93,639 Tn, which represented 36.19% of the world's production (NFISS, 2022).

Greece and Turkey are the largest exporters of gilthead seabream in the world with 52,879 Tn and 52,516 Tn, respectively, while Italy is the largest importer with 34,912 Tn, followed by Portugal with 13,351 Tn (NFISS, 2022).

The rapid growth of sea bream farming has been directly associated with the robustness and plasticity of this species, in addition to the reliable supply of high-quality juveniles spawned under controlled conditions in hatcheries (Laird, 2001; Manchado et al., 2016; Sola et al., 2007).

Several studies have indicated that there is a large economic potential for gilthead production, and its worldwide 130,042 Tn export was evaluated at 653 million USD, while the 100,584 Tn import in 2018 was evaluated at almost 532 million USD (NFISS, 2022).

2.5.3 The production cycle of gilthead seabream

The production cycle of gilthead seabream in intensive aquaculture begins with collecting good-quality fish eggs from the mass spawning activity of the broodstock. Selection criteria to identify adult fish as suitable breeders include normal body shape and color, absence of skeletal deformities, overall health status, normal behavior such as a quick response to food distribution, fast swimming, the largest size within its age group, the best growth and food

conversion rate within its age group, as well as newly estimated genetic parameters (Manchado et al., 2016; Moretti et al., 1999; Thorland et al., 2007). The genetic approach aims to identify genes whose expression is associated with disease and stress resistance. Breeders of various age groups, from one-year-old males to five-year-old females, may be conditioned by environmental manipulation (photoperiod and temperature) in order to induce sexual maturation (Colloca & Cerasi, 2022). The optimal sex ratio in the spawning tanks is kept at two males per female.

Males are left to release sperm spontaneously or on stripping. Females maturation stage has to be confirmed by extracting oocytes from the ovary, and only females with oocytes in the late vitellogenic stage (diameter larger than 500 μm) are selected (Moretti et al., 1999). Females can be left to release eggs by natural spawning or inducing it by hormonal treatment (5-20 mg/kg GnRHa(1) (D-Ala6; Pro9Net-mGnRH), at 15-17°C (Colloca & Cerasi, 2022; Moretti et al., 1999).

In the gilthead sea bream, as in other Sparidae, the buoyancy of spawned eggs is one parameter used in hatcheries to evaluate the potential of a batch of eggs to produce viable embryos and hatched larvae. This relates to the fact that proper hydration of the egg during oocyte maturation and immediately after spawning is essential for its further development and survival (Cerdà et al., 2007; Mylonas et al., 2011). Loose of eggs buoyancy was explained by a defect in their vitelline envelope components, or a differential concentration of cathepsin D and L, proteolytic enzymes involved in processing yolk proteins, and the increase of the osmotic pressure necessary for egg hydration; which induced an excessive hydration (Carnevali et al., 2001; Mylonas et al., 2011).

The eggs are collected by a simple screen within the outflow system of the broodstock tank after have been skimming the surface of the collecting

tank to remove only the floating eggs, and placed into conical incubating tanks in the dark for 36-48 hours at 18-22°C (Moretti et al., 1999).

Briefly before the estimated hatching time, water renovation should be increased to two complete exchanges per hour, after which environmental parameters should be reset according to the indications contained in table 1 (Moretti et al., 1999).

Table 1: Main Environmental parameters variation

	Incubation	Hatching	Larval stage	Fry stage
Water temperature (°C)	15-17	15-17	15-20	20
Salinity (ppt)	35-38	35-38	35	30
Photoperiod (h)	-	16:8	16:8	14:10
Water renewal (time/day)	12	12	8-12	18

The hatched larvae are transferred to a rearing tank of an individual capacity of 6-10 m^3, where they show a pronounced tendency to sink, conserving a uniform dispersion in the water body (Moretti et al., 1999). Directly after hatching, the digestive tract is still incomplete, the mouth is still closed, and the eyes are not yet pigmented. During this period, the larvae survive on the reserves of their yolk sac. Once the visual and digestive organs are fully developed, they involve progressively active movements characterizing the first-feeding predatory position (Moretti et al., 1999).

Thus, larvae can start feeding on live prey from the third to the fourth day of hatching, beginning with Branchionus spp. (Rotifers), followed by Artemia (Brine shrimp) (Moretti et al., 1999). In addition, during the first 25 days after hatching, microalgae are added to the rearing tanks ('green water' method), where they work both as immunological stimuli and as a conditioner of water quality (Moretti et al., 1999; Papandroulakis et al., 2002). Feeding on live microorganisms lasts between 40 and 50 days. During the first seven days, larvae receive a daily amount of 20 million rotifers per tank and 40 liters (12x106 cell/ml) of mature algal culture; from 8 to 12 days, the amount of

rotifers is increased by 20% and by 40% from day 13 to 16. At 17 DPH, rotifer provided are increased to 60%, and microalgal supplements are decreased to 50% to which 0.1 to 0.5 million Artemia AF are added to the larvae tank (Moretti et al., 1999). The high prey density increases the chance for the fish to approach and gulp some microorganisms, significantly improving their survival possibilities (Figure 2).

From day 20, algae and rotifers quantities are reduced to 10 liters and 20 million, respectively, in favor of an increased amount of artemia AF (0.5-1 million) and 0.3-0.6 million artificially enriched artemia metanauplii and a small amount of inert feed adapting the growing larva to the new food (Moretti et al., 1999). From day 24 to day 27, algae are progressively eliminated, rotifers decrease to 10 million, artemia AF increases to 250-500% (1.5 million) and large size artemia EG or RH to 3 million. Artificial feed is also increased progressively to accustom fish to the new flavor. From day 28, algae, rotifers and artemia AF nauplii supply is suspended while artemia EG or RH (10 million) and inert feed (15-20 g) are fed to fish. From day 34 to day 39, fish are given more EG or RH artemia (12 million) and 20 g of medium size (80-200 μm), plus 10 g of the larger 150-300 μm size inert food. From day 40 to day 43, when metamorphosis from larval to juvenile shape (fry) has started, EG or RH artemia and 150-300 μm inert feed supply, which fit better the larval requirements in terms of composition, size, buoyancy, and flavor, are increased up to 16 million and 30 g respectively. The feed should be distributed three times per day, starting as soon as the lights have been switched with a lapse time of 6 hours, until four hours before the artificial sunset. From this point, the fingerlings or juveniles of 2-3 grams assuming the adult aspect, are ready to be moved to the weaning sector (Moretti et al., 1999; Webster & Lim, 2002). The weaning stage represents a true intensive rearing system where the biomass of juveniles can reach up to 20 kg/m^3. Feeding

procedures and environmental parameters in this critical step are marked by the end of the live feed supply and the automatic distribution of dry feed. The environmental parameters in the weaning section are based on the protocol detailed in Table 1. The feeding protocol is based on the use of dry feeds while moist food, freshly prepared and totally consumed within the same day, represents a resource to supply additional nutritional integrators and drugs. Live feed supply end when juveniles reach an age of sixty days, after which they are fed exclusively with dry compounded feed (Figure 2). When a size of 2 to 5 g is reached, weaned fry leave the hatchery to be marketed in the fattening facilities, either pre-growing tanks or floating cages (Moretti et al., 1999).

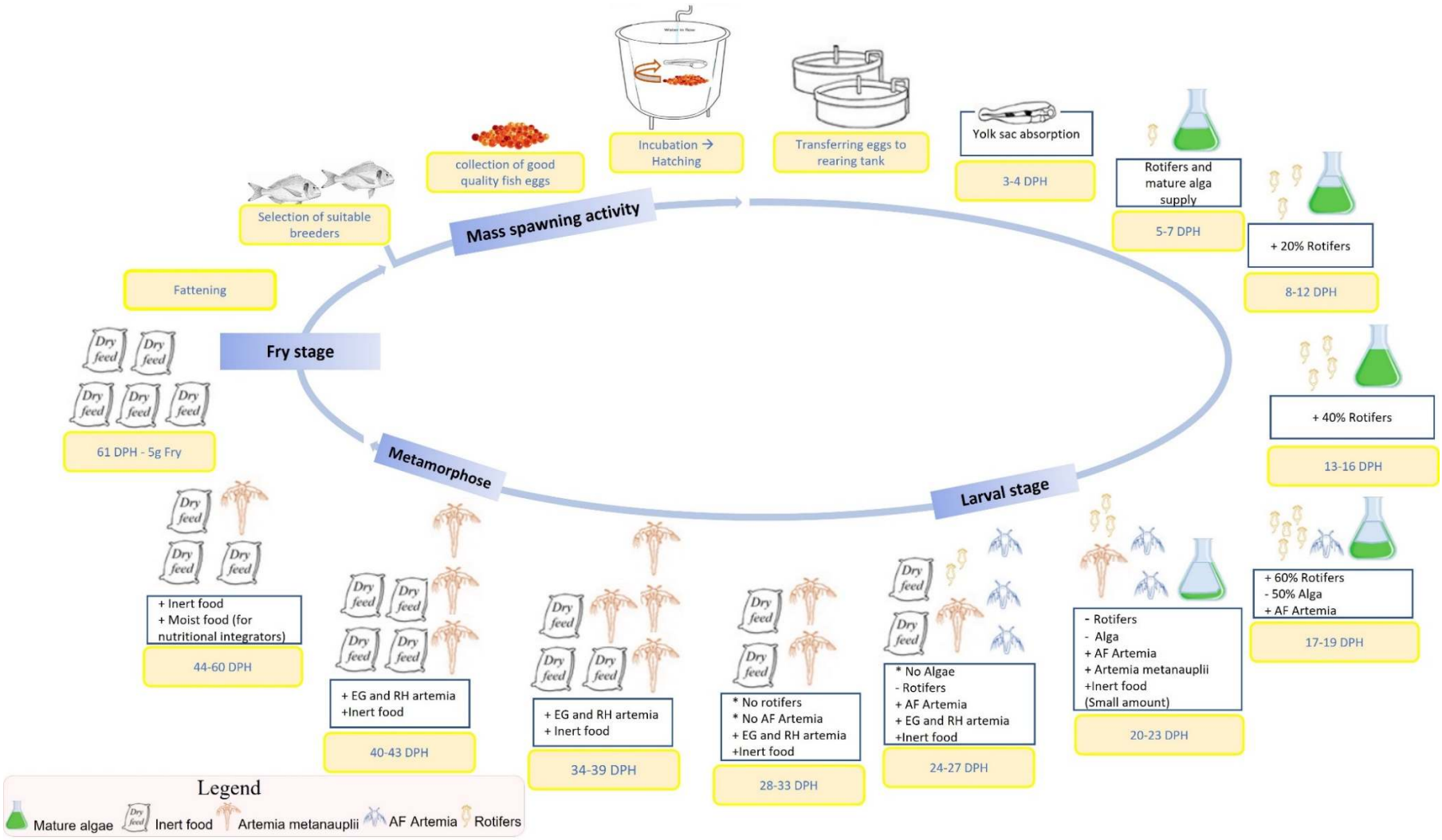

Figure 2. The production cycle of gilthead seabream

2.6 FISH SKELETOGENESIS

Vertebrate skeletogenesis involves three main cell types: chondrocytes, osteoblasts, and osteoclasts (Shahar & Dean, 2013). The first two cell types secrete the extracellular matrix proteins of the cartilage and bone, respectively. In contrast, the third type produces matrix metalloproteinases, cathepsins, and tartrate-resistant acid phosphatase (TRAP), providing an acidic environment in which the mineralized matrix is broken down (Ortiz-Delgado et al., 2014; Ytteborg et al., 2010). In addition, a fourth type of cell known as osteocytes is involved in maintaining bone matrix, regulating bone formation and resorption, and acting as mechanical load sensors. Contrarily to fish with cellular bone, teleosts have derived skeletons composed only of acellular bone, a tissue without osteocytes in the mineralized matrix. The lack of osteocytes in acellular bone implies that bone remodeling is covered by other cell types (Boglione, Gisbert, et al., 2013, p. 2). Other than different types of cells, 65% of the dry mass of bone is made of hydroxyapatite salts, and the remaining part is a collagen fiber matrix (Mahamid et al., 2008). Osteogenesis is ensured by a complex set of regulated molecular pathways involving signaling molecules, transcription factors, and extracellular matrix (ECM) constituents, among which alkaline phosphatase (ALP) or non-collagenous proteins, namely the matrix Gla protein (MGP) or osteocalcin (OC) (Boglione, Gisbert, et al., 2013). Thus, the perturbation of those factors implicated in the control of bone development and homeostasis, as well as the incapacity of the self-regulating process to compensate the stressful environmental conditions, induce the disruption of skeletogenesis and leads to the appearance of skeletal deformities (Boglione, Gisbert, et al., 2013; Ortiz-Delgado et al., 2014).

Several studies have described skeletogenesis and the histological organization of skeletal tissues in gilthead sea bream as well as the different typologies of skeletal deformities in order to investigate the effects of different

biotic and abiotic factors on the development of bone and the appearance of skeletal anomalies (Ortiz-Delgado et al., 2014).

2.6.1 Bone deformities

In the last two decades, the gilthead seabream aquaculture industry has experienced a rapid development with impressive progress in rearing techniques, disease control, nutrition, and industrial hatcheries knowledge. As a maximal yield in growth success may come into reach, several problems arise with respect to the overall quality of the larvae and subsequent juvenile fish. The quality of fish–depends on Morpho-anatomic and organoleptic characteristics that should be as similar as possible to that of wild fish, which is the quality reference by the consumer (Ortiz-Delgado et al., 2014). Various morphological abnormalities induced during the embryonic and post-embryonic periods of life, hindering the efficiency of the production cycle, have been reported in many studies (Al-Harbi, 2001; Beraldo & Canavese, 2011; Ortiz-Delgado et al., 2014; Verhaegen et al., 2007). These deformities, affecting as much as 80% of the fingerling production, cause an enormous economic slump in the industry by the primarily affection on the survival rates, growth, biological performance, the quality of the reared fish, the consumers' overall perception of fish and thus the cost-efficiency of marine fish aquaculture (Galeotti et al., 2000; Lorenzo-Felipe et al., 2021). A significantly higher prevalence of anatomical abnormalities may be observed in gilthead seabream produced in intensive aquaculture than in wild-caught animals (Ortiz-Delgado et al., 2014).

Although the improvement of rearing techniques, hatchery conditions in aquaculture farms are still far from ideal, this is why the most frequent abnormalities are recorded at the beginning of gilthead sea bream intensive culture, during embryonic and larval periods long before osteological

deformities are externally visible (Boglione, Gavaia, et al., 2013; Koumoundouros, Oran, et al., 1997; Ortiz-Delgado et al., 2014).

Skeletal deformities will fully develop to be visually identified only when fish are over 0.5 g in size and batches affected have to be screened and animals that carry the deformities must be detected and eliminated immediately since they will compete for food and space with healthy fish (Moretti et al., 1999).

Skeletal deformities in gilthead seabream fry typically affect the cephalic region (snout and opercula), showing a deformed upper and lower jaw in a variety of shapes as well as operculum complex deformities affecting its bone serie, leaving part of the gills exposed; the vertebral column in the form of kyphosis, lordosis or a mix of them, and fins especially the caudal fin deformities and saddle-back syndrome (Galeotti et al., 2000; Koumoundouros, Oran, et al., 1997; Mhalhel et al., 2020; Moretti et al., 1999; Ortiz-Delgado et al., 2014; Sfakianakis et al., 2013).

The opercular complex deformities

The operculum is a hard, plate-like, bony flap, made of opercles, subopercles, and interopercles, overlie an opercular membrane forming together a protective wall for the orobranchial chamber that covers the gills. This structure is known as well as gill cover or bony operculum. Below the opercular series, the branchiostegals are arranged in series with the sub- and interopercles and are attached proximally to the ventral face of the hyoid bar. The branchiostegal rays and membranes play only a passive role in the abduction and adduction of the branchial cavity and appear to serve primarily as a ventral sealing valve (Figure 3) (Huysseune, 2000).

Among cephalic malformations, anomalies of the opercular complex are the most common and evident external abnormality in different fish species, especially in reared gilthead sea bream, affecting up to 80% of the population

(Andrades et al., 1996, 1996; Beraldo & Canavese, 2011; Galeotti et al., 2000; Koumoundouros, Oran, et al., 1997).

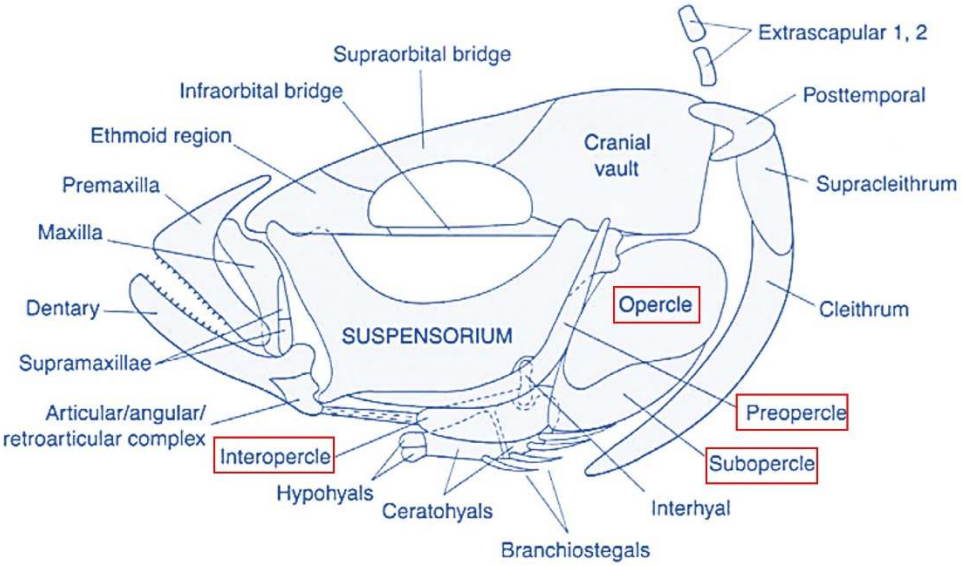

Figure 3. The teleostean operculum complex organization. Schematic representation adapted from (Huysseune, 2000)

This malformation affecting the bone series of operculum complex and the branchiostegal membrane consists of a more or less sharp inward folding (Figure 4.a) or shortening (Figure 4.b) of the structure, often associated with different degrees of malformation of the surrounding cranial region and exposure of the gills (Koumoundouros, Oran, et al., 1997; Verhaegen et al., 2007). This deformity may affect one or both operculum; however, the prevalence of those monoliteral is higher than the bilateral ones. The moment of apparition has not been precisely detected but is generally thought to be during the weaning and/or the pregrowing phase (Koumoundouros, Oran, et al., 1997; Verhaegen et al., 2007). Still, its premonitory symptom and morphoanatomical description remain incomplete. Although the image and market value of the final product are impaired, opercular anomalies affect the breathing process during water intake and discharge, reduce resistance to environmental stress especially reduced oxygen levels, and indirectly

predispose the fish to gill diseases and bacterial infections (Beraldo & Canavese, 2011; Galeotti et al., 2000; Verhaegen et al., 2007).

Over the years, biotic, abiotic, physiological, xenobiotic, nutritional, and rearing factors deterministic causes have been incriminated (Beraldo et al., 2003; Koumoundouros, Oran, et al., 1997). However, etiological knowledge is still insufficient for the elaboration of a cartesian experimental hypothesis concerning predisposing causes of the apparition.

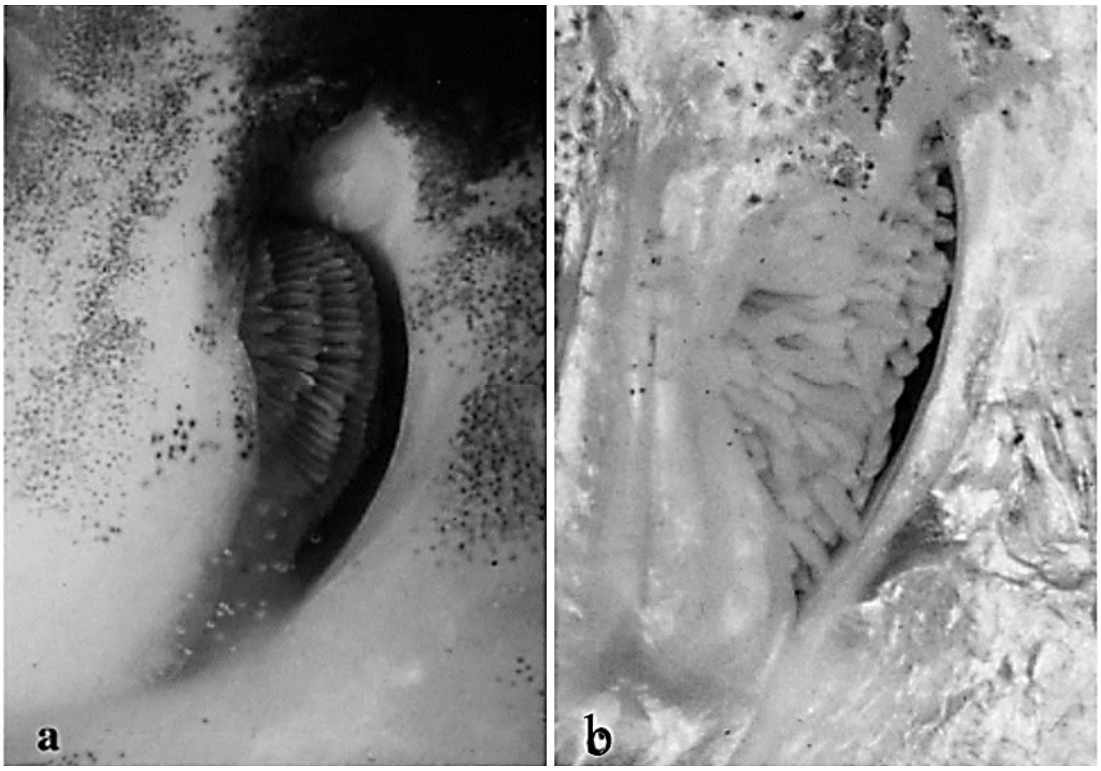

Figure 4. Stereomicrograph of two different forms of operculum complex deformities. (a) a folded into the gill chamber operculum, (b) a partial lack of the operculum. Adapted from Beraldo et al., 2003 (Beraldo et al., 2003)

Other cranial deformities

According to previous studies, about 35-40 % of produced gilthead seabream had head deformities (Mhalhel et al., 2020; Verhaegen et al., 2007). Various head deformations were associated with deoperculation, including a forward shift of the caudal margin of the opercular and subopercular, and the upward shift of the interopercle, the infraorbital, and shortening of the neurocranium and preorbital region (Verhaegen et al., 2007).

Additionally, jaw abnormalities have been frequently reported to develop in reared finfish, and gilthead seabream is no exception. Those abnormalities have several different types, including size reduction and deformity of the maxillaries and premaxillaries (Figure 5). Different jaw skeletal elements, including Meckel's cartilage, dentaries, articulars, pre-maxillaries, maxillaries, ethmoid, vomer, and palatine, are involved in the abnormal phenotypes generating a very complex anatomy of abnormalities (Boglione, Gavaia, et al., 2013; Faustino & Power, 2001; Fragkoulis et al., 2018). Fish with head deformity swam normally; however, growth may be affected as in all other forms of abnormalities (Boglione, Gavaia, et al., 2013; Fragkoulis et al., 2018).

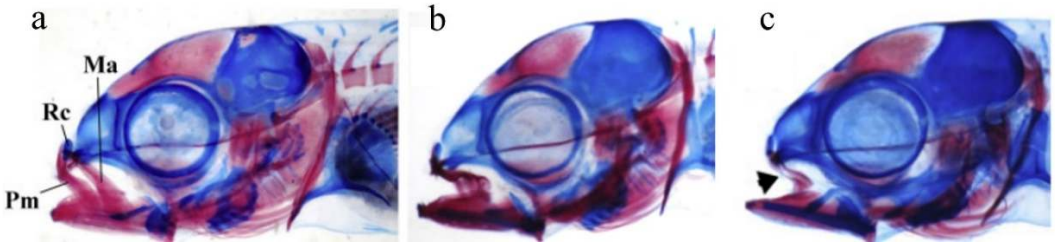

Figure 5. Stereomicrograph of different abnormality types of the maxillaries and premaxillaries in gilthead seabream. (a) normal anatomy of maxillaries (Ma), premaxilaries (PM), and rostral cartilage (Rc), in a seabream larva (9.5 mm TL), (b) size reduction of the premaxillaries; (c) narrowing of maxillaries (arrow) and complete absence of the premaxillaries. Adapted from Fragkoulis et al., 2018 (Fragkoulis et al., 2018).

Spinal deformity

In gilthead seabream production industry, vertebral deformities are frequent abnormalities affecting between 27% and 50.3% in seabream larvae, 17.2% at post larvae, and 5% incidence in adults (Loizides et al., 2014; Ruiz, 2000). Three main types of deformities exist, differentiated by the direction of their curvature. Scoliosis is defined as an aberrant lateral curvature of the vertebral column, detected either by dorsal or ventral examination (Figure 6.a, Figure 6.b). Lordosis, however, is an abnormal ventral curvature of the vertebral column accompanied by abnormal calcification of the afflicted

vertebrae compared to the normal anatomy of the vertebral column (Figure 6.a, Figure 6.c), and finally, kyphosis is a dorsal curvature (Kranenbarg et al., 2005; Ruiz, 2000). Axis deformations are considered among the predominant types of spinal deformities besides the compression and fusion of vertebral bodies and some phenotypes of lack or extra-formation of the different vertebral elements (Koumoundouros, 2010; Loizides et al., 2014; Roo et al., 2005). The spinal column deformities vary with the degree of deformity and in the number of flexions of the vertebral column, resulting in a continuous distribution of the external morphology ranging from insignificant to severe body-shape alterations (Fragkoulis et al., 2019). Different studies recorded thirty-nine types of skeletal deformities attributed to dislocation, fusion, shortening, or deformation of the implicated vertebrae (Koumoundouros, 2010; Ruiz, 2000). These basic deformities have been reported to develop solitary or in various combinations of the different types, e.g., lordosis and kyphosis in the saddleback syndrome (Kranenbarg et al., 2005) or the consecutive repetition of lordosis/scoliosis/kyphosis (LSK) from head to tail, was reported in some studies on gilthead seabream (Negrín-Báez et al., 2015; Ruiz, 2000). They first appeared at the larval stage and have been correlated with the absence of a functional swimbladder, which has been reported to be partly or totally corrected following late inflation of the swimbladder, or to other biotic and abiotic factors (Berillis, 2015).

Fish with spinal deformities either swim upside down or sideward, and the growth was slow compared to normal fish (Al-Harbi, 2001).

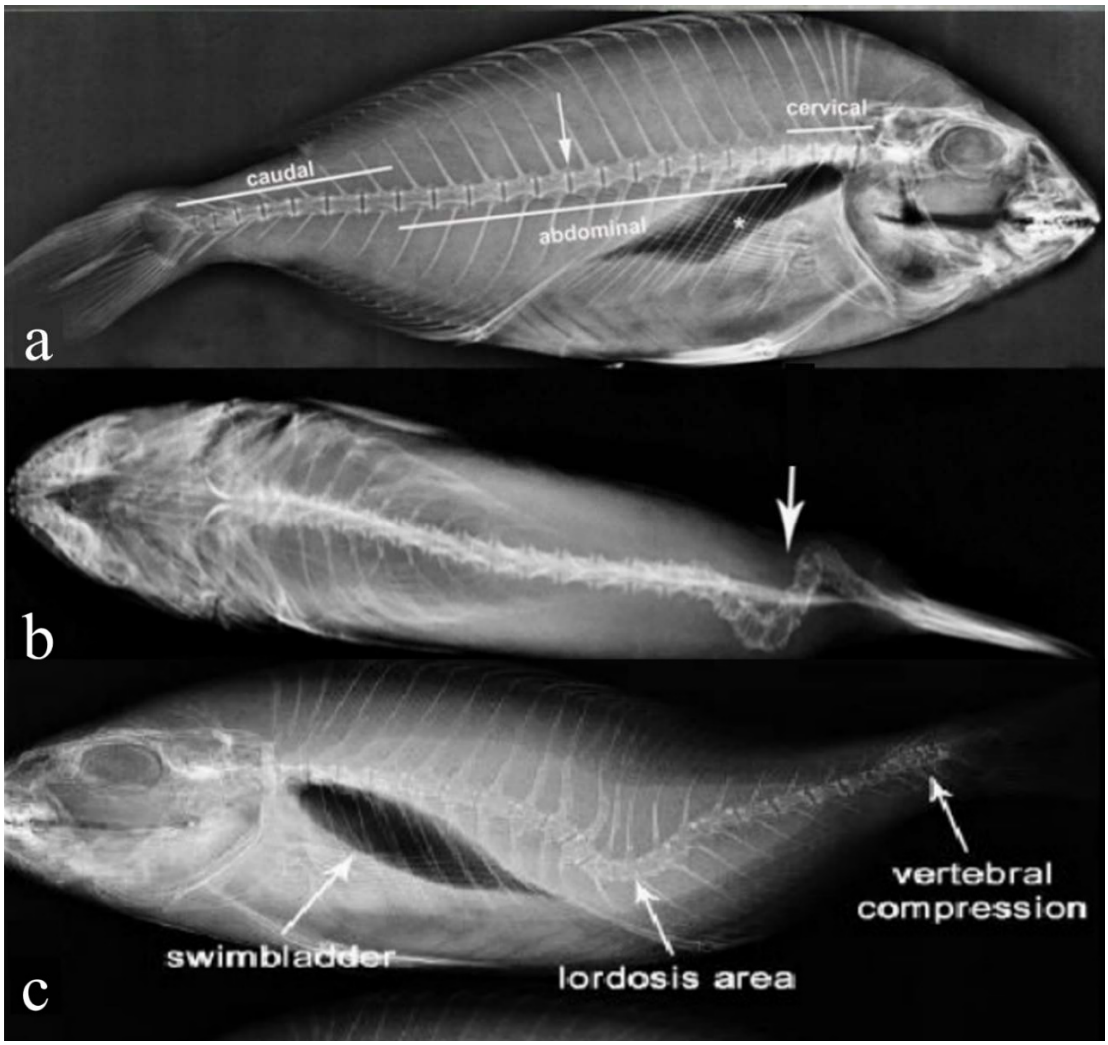

Figure 6. X-ray of gilthead seabream with different forms of spinal deformities. (a) normal anatomy of cervical, abdominal and caudal regions of the vertebral column, Inter-vertebrae space is highlighted with an arrow, and swim bladder is indicated with a star; (b) apical X-ray of seabream caudal region with scoliosis (highlighted with arrows); (c) X-ray of seabream with coexisting two main deformities of the vertebral column lordosis and vertebral compression. (a) and (b) are adapted from Boursiaki et al., 2019 (Boursiaki et al., 2019), while (c) is adapted from Berellis et al., 2015 (Berillis, 2015).

Caudal fin deformity

Caudal fin abnormalities have been reported to develop in reared fish, and their prevalence in gilthead seabream production ranged between 25-65% (Fernández et al., 2008; Koumoundouros, Gagliardi, et al., 1997). Severity degrees show a wild variety of phenotypes, ranging from the lack of rays to the lateral twisting of the whole caudal complex (Figure 7.a) or the duplication of the caudal fin (Figure 7.c), beside extra-numerous fusions, deformities, and displacements of the elements (Fragkoulis et al., 2020; Koumoundouros, 2010;

Koumoundouros, Gagliardi, et al., 1997). All the elements of the caudal region (neural arch, epurals, hypurals and parahypurals, and the uroneural and vertebra centra) are implicated in abnormalities (Koumoundouros, Gagliardi, et al., 1997).

The incomplete development of both dorsal and anal fins was reported to be one of the most severe deformities (Saddleback syndrome) in gilthead seabream and other fish species (Figure 7.b, Figure 7.d) (Koumoundouros, 2010). Those deformities were highly correlated to posterior notochord deformities, mainly the lack of upper lepidotrichia and dermatotrichia at the pre-flexion phase (Koumoundouros, 2010).

Existing literature on the causative factors of these abnormalities mostly focuses on the effects of the rearing environment, including temperature, nutrition, dietary levels of vitamin A, and the genetic basis (Fernández et al., 2008; Fragkoulis et al., 2020; Koumoundouros, 2010).

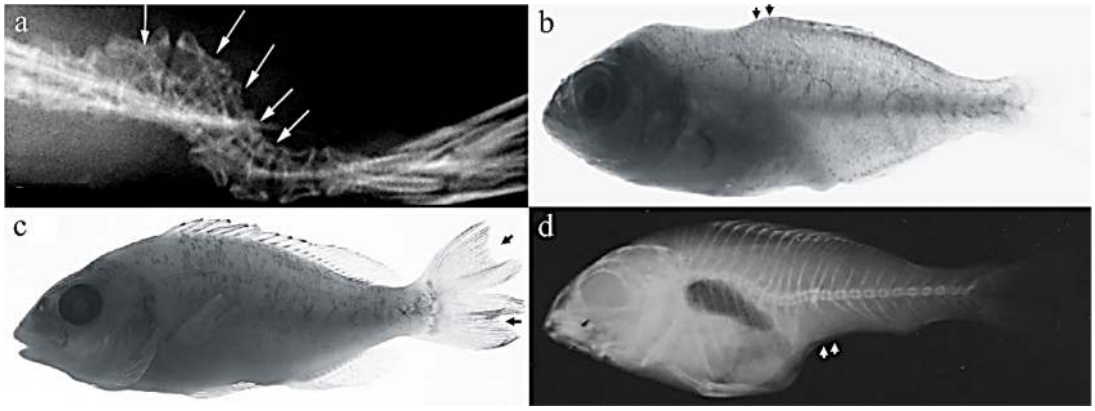

Figure 7. Caudal-fin deformities in gilthead seabream. (a) lateral twisting of the whole caudal complex, (b) Incomplete formation of dorsal fin in juvenile S. aurata, (c) duplication of caudal fin, and (d) complete lack of anal fin in juvenile S. aurata.

Body shape deformities

The body shape is the main quality trait of reared fish, especially those sold as a whole, like gilthead seabream. Several studies proved that shape deviations from the typical pattern are usually affected by all the previously detailed skeletal abnormalities (Fragkoulis et al., 2021; Koumoundouros,

2010). However, the shape differentiations are very common even in subjects without skeleton deformities, as a direct result of the different rearing conditions and the genotype (Fragkoulis et al., 2021; Koumoundouros, 2010). In fact, canonical variate analysis revealed that both rearing methodologies and the origin of fish as wild or reared significantly affect the body shape of seabream during the on-growing phase (Fragkoulis et al., 2017).

2.6.2 Cause of deformities

Deformities are one of the most recurrent biological problems affecting finfish aquaculture, defined as the common abnormal transformations of normal skeletal structures into abnormal structures different from the normal prototype in both wild and cultured fish populations; however, their frequencies are greater in hatchery populations (Koumoundouros, 2010; Ortiz-Delgado et al., 2014). The high incidence of skeletal deformities found in farmed fish can be explained by the maximized fish survival due to the absence of predators and the high availability of food. Technical errors or knowledge gaps in some critical segments of the rearing process on producing high-quality and healthy fry were also suspected (Boglione, Gavaia, et al., 2013; Boglione, Gisbert, et al., 2013; Koumoundouros, Gagliardi, et al., 1997). Available evidence suggests that those abnormalities appear in the early stages of development during the embryonic and larval stages of life, long before they can be externally visible (Al-Harbi, 2001). However, the etiology of these syndromes is not yet well understood. (Al-Harbi, 2001)

Osteogenesis is ensured by a complex set of regulated molecular pathways involving signaling molecules, transcription factors, and extracellular matrix (ECM) constituents, among which alkaline phosphatase (ALP) or non-collagenous proteins such as the matrix Gla protein (MGP) or osteocalcin (OC) (Boglione, Gisbert, et al., 2013). Thus, the perturbation of those factors implicated in the control of bone development and homeostasis,

as well as the incapacity of the self-regulating process to compensate stressful environmental conditions, induce the disruption of skeletogenesis and leads to the appearance of skeletal deformities (Boglione, Gisbert, et al., 2013; Ortiz-Delgado et al., 2014).

Different studies suggest that unfavorable environmental biotic, abiotic disturbances, nutritional imbalances, presence of xenobiotic substances and/or genetic disorders, and unsuitable rearing conditions are the most probable causative agents of deformities in reared fish, to which we can add traumatic injury and parasites infections (Al-Harbi, 2001; Boglione, Gisbert, et al., 2013; Moretti et al., 1999; Ortiz-Delgado et al., 2014).

Even though several studies have listed the different abnormalities affecting the skeletal structures in cultured seabream and have reported the effects of some rearing conditions (temperature, light) or substances (Vitamins) on the prevalence of bone abnormalities. However, etiological knowledge is still insufficient for elaborating cartesian experimental hypotheses concerning predisposing causes of the apparition and the underlying processes behind abnormalities since this is considered a multifactorial problem (Faustino & Power, 2001; Ortiz-Delgado et al., 2014).

2.6.3 Perspective for Investigating Bone Defects

In order to improve cost-efficiency for farmed gilthead sea bream, fast and early recognition of developing abnormalities is of great importance for fish farmers since abnormal subjects, with adversely affected growth rates and reduced survival rates, will compete for food and space with healthy fish (Noble et al., 2012). A careful examination should be done on both sides of each fish. When the percentage of deformities in a given fish population exceeds the quality standards, the deformed animals should be sorted out. The only effective technique to remove such fry is to sort them by hand (Moretti et al., 1999).

For this reason, various procedures have been applied as simple and rapid diagnostic tools for studying skeletal deformities, abnormal growth in different skeletal structures, as well as the unusual swimming behavior revealing abnormal development in fish. The visual examinations, including the analysis of geometric morphometrics, stereoscopic observations, double staining, computer tomography, and soft X-rays, allow the description of shape variation in growing and transforming fishes and the effect of rearing conditions on the body shape (Moretti et al., 1999; Ortiz-Delgado et al., 2014). The histological procedures are considered another valuable tool for providing basic knowledge on bone formation and the structural changes occurring in deformed skeletal structures (Ortiz-Delgado et al., 2014).

All the above-mentioned analyses of the morphology of different fish tanks allowed quantitatively and qualitatively analysis of the nature of osteological aberrations in fish and the different degrees of shape changes in the external morphology.

2.7 PHOTOTRANSDUCTION AND MELATONIN RHYTHMS

In fish, larval development, oxygen consumption, thermoregulation, food intake, and shoaling behavior are among several functions that display daily rhythms. Horizontal migration, growth, immune response, and reproduction are the main functions that exhibit annual rhythms. These daily and annual rhythms can be a passive response to the variations in photoperiod and temperature, or driven by internal clocks, under constant conditions, that free-run with a period close to 24 h (circadian rhythms) or one year (circannual rhythms). Organisms with such time measurement systems can anticipate environmental changes so that the right event occurs at the right time (Falcón, Besseau, et al., 2010; Falcón, Migaud, et al., 2010).

The circadian system involves three basic components by which light enters the organism and is translated into a scheduled nervous or hormonal

physiological signal. The system is made of a photodetector synchronizing the autonomous activity of the endogenous clock machinery by the light perceived; in turn, the clocks induce synthesizing machinery and drive the production of the output signals (Falcón, Gothilf, et al., 2003; Falcón, Migaud, et al., 2010).

MEL is one major component of the circadian system, which conveys rhythmic information to the organism. It is made in two phototransducing sites, the retina and pineal gland, as well as a number of tissues, including the Harderian gland, gastrointestinal tract, reproductive organs, skin, platelets, and several brain regions (Jimenez-Jorge et al., 2005). Still, the major source of MEL is the pineal gland or epiphysis cerebri, which develops as an evagination of the top of the diencephalon, located at the surface of the brain. The semi-transparent skull bone above the pineal gland is thinner, and the skin is less pigmented, forming a pineal window (Figure 8.a) (Acharyya et al., 2021; Falcón et al., 2020). In the teleost fish, the epiphysis is made of three distinct structures: (1) an elongated and a flattened vesicular body located close to the cranium known as the "end vesicle" (2) a structural connection that connects the "end vesicle" to the brain known as the "pineal stalk" and finally (3) a saccular structure, which encircles the "pineal stalk" at the cerebral end called the "Dorsal sac" (Figure 8.b) (Dey et al., 2003).

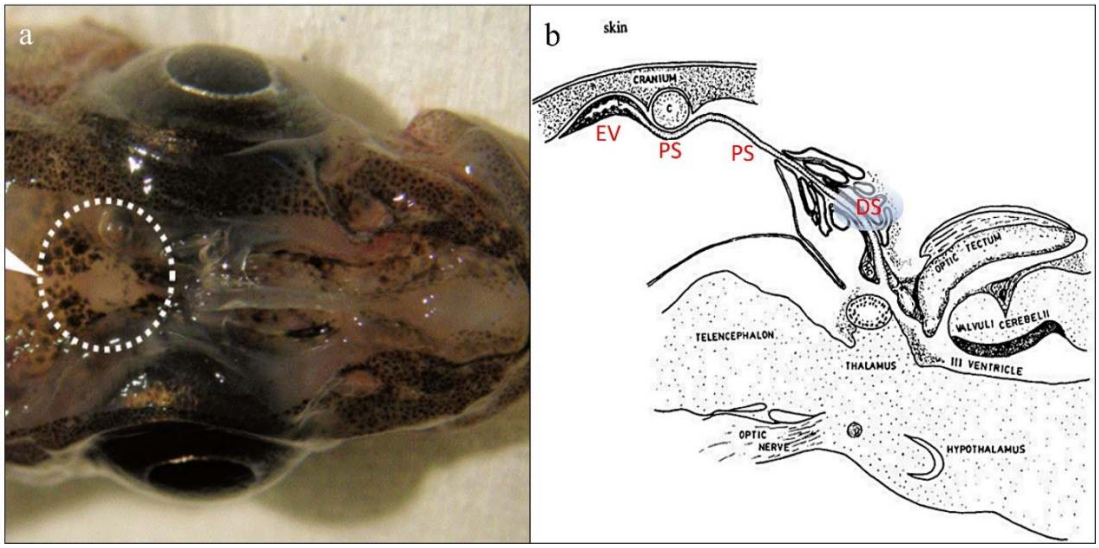

Figure 8. A dorsal view of a fish head showing the depigmented area around the pineal window (White broken line circle). (b) schematic illustration of the three constituent parts of the pineal gland. EV, end vesicle; PS, pineal stalk; DS, dorsal sac; C, cartilage. The figure is adapted from (Dey et al., 2003; Falcón et al., 2011).

The pineal-derived MEL commands the daily rhythm in circulating MEL and provides a hormonal signal transducing light and dark information to the organism. This signal plays a role in synchronizing and controlling several physiological and behavioral rhythms (Falcón, Gothilf, et al., 2003; Zachmann et al., 1992). Retinal MEL, however, is metabolized in the eye. It has a local paracrine function related to photic adaptation and does not contribute to its blood levels (Cahill & Besharse, 1995; Falcón, Gothilf, et al., 2003; Masayuki ligo et al., 1997). The daily pattern of MEL secretion is much conserved among vertebrates, emphasizing this neurohormone's crucial role in this subphylum taxa. However, the arrangement of the circadian system that controls MEL rhythm has changed dramatically during evolution.

In mammals, the photic signal is perceived through the eyes and transmitted, through a retino-hypothalamic tract (RHT), to reach the suprachiasmatic nuclei of the hypothalamus (SCN) clocks. The SCN clocks, in turn, induced the cyclical MEL secretion through a multisynaptic pathway (hypothalamic paraventricular nuclei [PVN] -> preganglionic neurons of the sympathetic nervous system -> superior cervical ganglion [SCG]). Melatonin

feeds back to the *pars tuberalis* of the pituitary and other brain areas modulating seasonal neuroendocrine functions (Figure 9.a)(Falcón, Migaud, et al., 2010; Simonneaux & Ribelayga, 2003).

In fish, MEL rhythm generating systems is organized as a network of more or less tightly independent and interconnected light-sensitive oscillatory circadian units located mainly within individual photoreceptor cells in the retina, the pineal gland, and, perhaps, in the brain (Figure 9.b) (Falcón et al., 2007; Falcón, Migaud, et al., 2010). In contrast to that of mammals, fish pineal photoreceptors cells contain the entire machinery of the light-entrained circadian system: photoreceptor unit, clock machinery, and MEL production system covering both sensory and secretory functions (Bolliet et al., 1996; Falcón et al., 2007). In fact, MEL synthesis in most teleost species continues to follow a circadian pattern in pineal explants, and its rhythm adjusts to a 24-h cycle when exposed to a fluctuating light environment reflecting the clock (Bolliet et al., 1996; Falcón, Gothilf, et al., 2003; Sánchez-Vázquez et al., 2019). The pineal epithelium photoreceptor cells, resembling structurally and functionally the retinal cones, depolarize in the dark and elaborate an electrical message at the origin of an excitatory neurotransmitter (Sánchez-Vázquez et al., 2019). Meanwhile, light brings the photoreceptor cells to hyperpolarization and inhibits the discharge of the pineal neuronal units (Ekström & Meissl, 1988). Additionally, those photoreceptor cells contain the amino acid (tryptophan), enzymes, and all the indole compounds (serotonin, N-acetylserotonin, MEL) needs to produce MEL (Falcón, Migaud, et al., 2010; Sánchez-Vázquez et al., 2019).

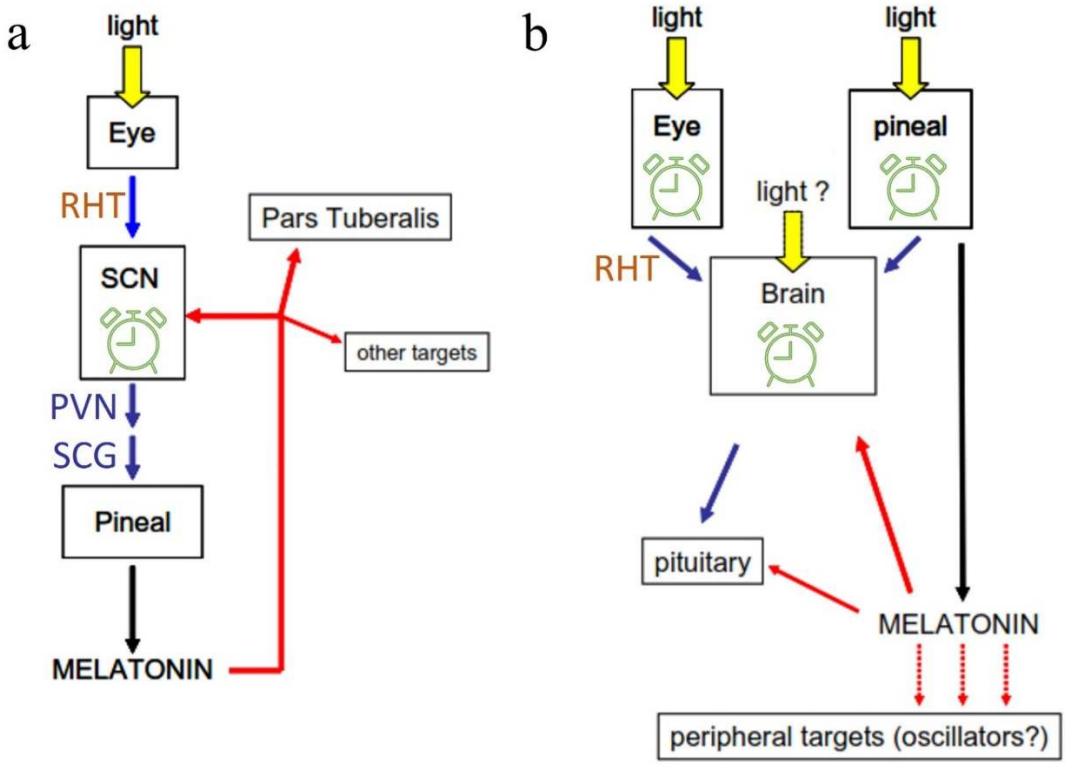

Figure 9. Schematic representation of mammals (a) and fish (b) photoperiodic and circadian control of MEL secretion. The green alarm clock represents the endogenous clocks, PVN = paraventricular nucleus, RHT = retino-hypothalamic tract; SCG = superior cervical ganglion, and SCN = suprachiasmatic nucleus the feedback. The schematic representation is adapted from (Falcón et al., 2011).

2.7.1 Melatonin Biosynthesis Pathway

Melatonin is primarily produced within the pinealocytes of the pineal gland in a rhythmic manner, having extreme light sensitivity in its biosynthesis. Further studies revealed that this indole is also synthesized in several extra-pineal tissues, namely the retina, gut, and harderian gland. Thus, the distribution of MEL is ubiquitous (Acharyya et al., 2021).

The MEL biosynthesis from the precursor molecule L-tryptophan (L-Trp) is conducted in a four-step pathway in the different production sites. The tryptophan pathway starts with the entry of L-Trp into the site of synthesis from the bloodstream and its hydroxylation to 5-hydroxy-tryptophan (5-HTP) catalyzed by the tryptophan hydroxylase (TPoH). The resulting 5-hydroxytryptophan is then decarboxylated by the aromatic amino-

acid decarboxylase (AAAD) to produce serotonin (5-hydroxytryptamine). The aforenamed is converted to n-acetylserotonin under the action of arylalkylamine n-acetyltransferase (AANAT). The n-acetylserotonin, in turn, is then o-methylated by the action of the hydroxyindole-o-methyltransferase (HioMT) to produce the N-acetyl-5- methoxytryptamine or MEL (Figure 10) (Acharyya et al., 2021; Falcón et al., 2011).

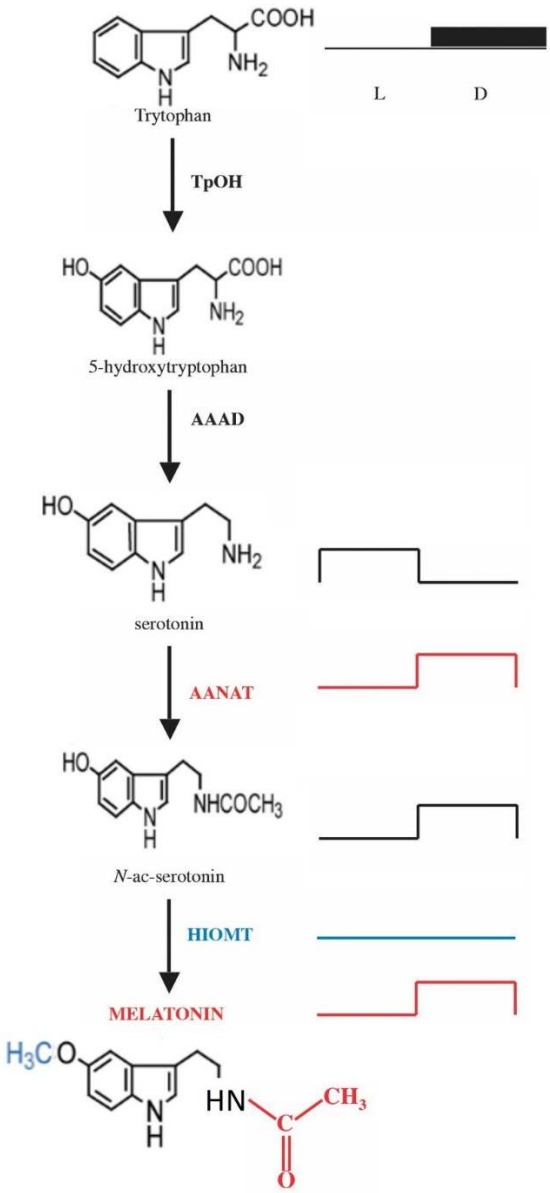

Figure 10. Melatonin biosynthesis pathway in the pineal. The daily rhythms of the different cofactors or enzymes are designated in the right column. TpOH: tryptophane hydroxylase, AAAD: aromatic aminoacid decarboxylase; AANAT: arylalkylamine n-acetyltransferase; HIOMT: hydroxyindole-o-methyltransferase; D: dark (black box) and L: light. Schematic representation adapted from (Falcón et al., 2011).

Melatonin production is shown to be driven by similar changes in the activity of the arylalkylamine N-acetyltransferase (AANAT), which controls the rate at which serotonin is converted to N-acetylserotonin (Falcón, Migaud, et al., 2010). Unlike all other vertebrates, teleost fish possess at least two forms of aanaT genes, AANAT1, and AANAT2, most likely resulting from a genome duplication (Falcón et al., 2001; Falcón, Migaud, et al., 2010; Jaillon et al., 2004). The two aanat genes display a tissue-specific distribution. AANAT1 is expressed brain and retina, while AANAT2 is specific to the pineal organ (Falcón et al., 2001; Falcón, Migaud, et al., 2010).

In seabream, like in other fish species, the rhythmic changes in AANAT2 activity drive the rhythm in MEL production. The translation of endogenously driven changes in AANAT2 mRNA into changes in AANAT2 activity is influenced by an exogenous signal –light. Light can adjust and resets the endogenous circadian clock gradually and, consequently, the rhythm in AANAT2 mRNA and activity, or suppress AANAT2 activity, independently of the clock. Light drastically inhibits pineal MEL production at molecular levels by inducing direct proteolysis of the AANAT protein through proteasomal proteolysis. AANAT2 pathway may also be regulated by the cAMP-dependent pathway protecting AANAT2 from degradation, phosphorylating the AANAT through highly conserved N- and C-terminal cAMP-dependent protein kinase phosphorylation sites, and inhibiting the proteasomal proteolysis (Acharyya et al., 2021; Bairwa et al., 2013; Falcón, 1999; Zilberman-Peled et al., 2007).

2.7.2 Melatonin in the Regulation of Fish development

Fish development and growth, from newly hatched larvae into juveniles, is associated with several morphological and physiological changes controlled and coordinated by many endocrine factors. Melatonin seems to be one of the key hormones in the development of teleosts (Boeuf & Falcon, 2001; Falcón,

Migaud, et al., 2010; Kalamarz et al., 2009). Indeed, many in vitro studies proved the MEL action on cell proliferation rate and on the growth and development processes of fish embryo cells, alone or with growth factors (Kalamarz et al., 2009; Roth et al., 1999). Additionally, in the zebrafish embryo, MEL was able to regulate cell proliferation rate and accelerate fish development through MT2 receptors (Danilova et al., 2004). During the early ontogenesis of gilthead seabream and haddock (Melanogrammus aeglefinus), MEL controls the development and protection against free radicals (Downing & Litvak, 2002; Kalamarz et al., 2009).

The lipophylic character and small size of MEL permit penetration and action in many peripheral tissues to synchronize and integrate growth and development functions (Falcón et al., 2007; Falcón, Migaud, et al., 2010; Kazemi et al., 2020).

Several studies on vertebrates have highlighted a relationship between MEL and Thyroxine (T4) (Taheri et al., 2019; Wright et al., 2000). Thyroxine (T4) is a crucial hormone in the development and metamorphosis of fish, especially at the initial period of ontogenesis and larva–juvenile transition (Campinho, 2019; YAMANO, 2005).

Additionally, in a study published in 2003, in vitro culture of trout hypophysis with a physiologically relevant concentration of MEL increased the release of growth hormone and sustainably inhibited prolactin release (Falcón, Besseau, et al., 2003).

In goldfish (Carassius auratus), intraperitoneal MEL administration (25 and 50 μg/fish) has accelerated postexposure growth and weight (De Vlaming, 1980). In the same way, different MEL concentrations (0.04 and 0.2 g/kg food) mixed with the commercial food paste and applied as rainbow trout feed have increased fish growth parameters, namely the food intake capacity, and reduced the stress markers in a dose-dependent manner (Conde-Sieira et al.,

2014). In another experiment, 0.1, 0.5, and 2.5 mg/kg body weight MEL supplied to finfish European sea bass (Dicentrarchus labrax) were able to modulate the pattern of macronutrient selection significantly (Acharyya et al., 2021; Rubio et al., 2004).

Chapter 3: Materials and Methods

3.1 LARVAL REARING

The experiment was conducted on gilthead seabream during the early stages of development (from 13 to 83 DPH), at the AQUACULTURE TUNISIENNE, a Sousse-based hatchery (Tunisia), according to the principles outlined in the Declaration of Helsinki, the directive 2010/63/EU of the European Parliament and of the Council of 22 September 2010 on the protection of animals used for scientific purposes (European Union, 2010), to the Guidelines on the Handling and Training of Laboratory Animals by the Universities Federation for Animal Welfare, and was approved by the local ethics committee. The production cycle started with collecting good-quality fish eggs coming from pre-selected breeders. Eggs are incubated in conical tanks of an individual capacity of 2.5 m^3 in the dark for 36-48 hours at 18-22°C. After hatching, gilthead seabream larvae were transferred to cylindroconical rearing tanks and raised under standard hatchery conditions (initial density of 120 larvae/L). Daily water renewal in the rearing tank was 3–15%/h, the temperature was 20–21 °C, and the light intensity was 150 lux, with gentle and continuous aeration. During the first 2-3 days, larvae survive on the reserves of their yolk sac. From 3 to 25 DPH, Rotifers *Brachionus picatilis* pre-enriched with green algae were added to tanks daily as an early live food. Artemia salina nauplii were introduced from 26 to 38 DPH, progressively increasing the amount added and compensating the reduction in the amount of rotifers. One day before being fed to the larvae, rotifers, and metanauplii were enriched with phytoproteins and highly unsaturated fatty acids using an encapsulated fish oil-based emulsion called Red Pepper© (Bern Aqua, Olen, Belgium) for at least 6 and 12h, respectively for rotifers and artemia. At 38 days, larvae were

weaned progressively, reducing the quantity of Artemia and increasing the dry pellets introduced amount.

3.2 EXPERIMENTAL DESIGN

The investigations were carried out on 2400 gilthead seabream larvae, which were randomly distributed into three groups of 800 larvae placed under ordinary hatchery conditions: two experimental groups (MEL1) and (MEL2) and a control group (Ctrl). In order to evaluate the effect of exogenous MEL supplementation on skeletal deformities and larval performance, the exogenous supply of MEL was ensured from the 3rd to 38 DPH via rotifers and/or nauplii of Artemia. Rotifers and Artemia were enriched with 0.04 g/kg (MEL1) or 0.2 g/kg (MEL2) of neurohormone (Cat.# M5250, Sigma-Aldrich, St. Louis, USA) added to fish oil-based emulsion called Red Pepper© (Bern Aqua, Olen, Belgium). The lipophilic nature of MEL helps its solubility in this lipid emulsion. The choice of the MEL1 and MEL2 concentrations was made considering the range of previously tested doses with clear responsiveness in other species of teleost (Amano et al., 2004; Conde-Sieira et al., 2014; López-Olmeda et al., 2006). Sampling was performed every ten days between 13 and 83 DPH from the three fish groups (MEL1, MEL2, and Ctrl), and larvae were sacrificed with an overdose of tricaine methane sulfonate (MS222); 1000–10,000 mg L^{-1}. The experiment was performed in triplicate.

3.3 SAMPLING

Sampling was performed every ten days from 13 to 83 DPH. One hundred larvae per experimental group were collected to record growth rates (the total length and weight) and analyze opercular complex abnormalities by stereomicroscopy. In tiny larvae of 13–53 DPH, opercular complex deformities were investigated by means of scanning electron microscopy (SEM). Thirty larvae from those already investigated for operculum complex anomalies

were stained with alcian blue and alizarin red acid-free staining solution. For gene expression analyses, 5 to 20 individuals per tank, depending on fish size, were collected for total RNA extraction and the evaluation of the expression levels of genes implicated in muscle and bone growth.

3.4 MORPHOLOGICAL STUDIES

For each fish, the total length was measured using a digital camera Leica IC80 HD (Leica, Milan, Italy) mounted on a stereo-microscope (Leica, Milan, Italy), and weight was determined with the KERN 770 analytical scale (KERN & Sohn, Balingen, Germany). Additionally, the study of external body shape and operculum complex anomalies was performed using Leica M205C stereomicroscope observations (Leica, Milan, Italy) or scanning electron microscope Zeiss EVO LS 10 (Carl Zeiss NTS, Oberkochen, Germany) magnification for the tiny larvae (larvae of 13-53 DPH: 15 larvae).

3.5 SCANNING ELECTRON MICROSCOPY

After fixation in 2.5% glutaraldehyde in Sörensen phosphate buffer 0.1 M, samples were rinsed several times in the same buffer and in a asecond time dehydrated with a graded alcohols series. After dehydration, specimens were critical-point dried using a Balzers CPD 030 (BAL-TEC AG, Balzers, Liechtenstein). Before observation, 3 nm gold sputter was coated with using the SCD 050 sample coater (BAL-TEC AG, Balzers, Liechtenstein). The examination and photography were made under a Zeiss EVO LS 10 (Carl Zeiss NTS, Oberkochen, Germany).

3.6 ACID-FREE DOUBLE STAINING

The double staining procedure was performed using an adjusted protocol of Walker and Kimmel (Walker & Kimmel, 2007). An acid-free double staining solution was prepared by mixing a cartilage and bone staining solutions. The cartilage staining solution was made by adding together 0.2%

alcian blue 8 GX C.I. 74,240 (Sigma, St. Louis, MO, USA, Cat.#33864-99-2) in 70% ethanol, and 100 mM $MgCl_2$ (for mucosubstances differentiation). The second part for bone staining was made of 0.5% alizarin red S C.I. 58005 (Sigma, St. Louis, MO, USA, Cat.#130-22-3). The final acid-free staining solution was prepared by adding 100 μL of the second to 10 mL of the first solution. After fixation in 4% paraphormaldehyde in phosphate buffered saline (PBS) for two h, larvae of 23, 33, 43, and 53 DPH were washed and dehydrated, at room temperature, in ethanol 50% for 10 min. once removed from the ethanol, specimens were rocked in acid-free double stain solution at room temperature overnight in order to incorporate the stain adequately. The next day, specimens were bleached for 20 min using a bleach solution made of 1.5% H_2O_2 and 1% KOH at room temperature. Once bleached, specimens were transferred in two clearing solutions overnight each time. The first clearing solution consisted of 20% glycerol and 0.25% KOH while the replacement solution was 50% glycerol and 0.25% KOH. Larvae were investigated for ossification patterns and bone deformities and photographed with M205C stereomicroscope (Leica, Milan, Italy) in the same solution.

3.7 INSULIN-LIKE GROWTH FACTOR 1 QUANTIFICATION

The insulin-like growth factor 1 (IGF-1) quantification was performed using tissue homogenates (25% *w*/*v*) made from pools of 40–55 larvae in each experimental group and at each sampling time. The tissue homogenates were made in 0.05 mol/L phosphate buffered saline pH 7.4, using a knife homogenizer (Polytron) at 4 °C. Homogenates were centrifuged at 16,000× g for 20 min at 4°C and the recuperated supernatant was used for analyzes.

The quantitative measurement of IGF-1 in larvae was performed using Fish insulin-like growth factors 1 (IGF-1) ELISA Kit Fish (Cusabio Biotech, Wuhan, China, Cat.# CSB-E12122Fh) according to the manufacturer's instructions. The assay uses the competitive inhibition enzyme immunoassay

method. The microtiter plate furnished in the kit was pre-coated with goat-anti-rabbit antibody. The provided standards as well as our samples, were pipetted to the appropriate microtiter plate wells with an antibody specific for IGF-1- and horseradish peroxidase (HRP)-conjugated IGF-1. The competitive inhibition reaction is initiated among unlabeled IGF-1 and HRP-labeled IGF-1 with the antibody. Later we added the substrate solutions to wells, and after 15 min incubation in the dark and at 37°C, the colorimetric reaction was deferentially developed, and it was negatively correlated to the amount of IGF-1 in the sample.

Immediately after the incubation, color development was stopped, and the optical density of each well was measured within 10 min utilizing a microplate reader set to 450 nm.

3.8 GENE EXPRESSION ANALYSES

Bone and skeletal muscle-specific gene expression levels were investigated in compliance with the minimum information for publication of quantitative real-time PCR experiments guidelines (Bustin et al., 2009). Total RNA was extracted from pools of muscle or bone tissues separated from 5 to 20 gilthead seabream larvae (per group and sampling time) using the TRIzol reagent (Invitrogen, Carlsbad, CA, USA). The RNA purity and concentration were determined using the NanoDrop® ND-1000 spectrophotometer (Thermo Fisher Scientific, Wilmington, USA). Two micrograms of total RNA were reverse transcribed using the High-Capacity cDNA Archive Kit (Applied Biosystems, Foster City, CA, USA). The mRNA levels of bone-specific genes: parathyroid hormone-related protein-coding gene (*PTHrP*) and bone gamma-carboxyglutamate protein-coding gene (*bglap*); as well as skeletal muscle specific gene: myosin light chain 2 (*mlc2*), were analyzed using the SYBR® Premix DimerEraser™ (TAKARA BIO INC, Otsu, Shinga, Japan, Cat. #RR091A). The primers were constructed using NCBI Primer-BLAST (Ye et al.,

2012) to bind gilthead seabream *PTHrP*, *bglap*, and *mlc2* transcript sequences. Table 2 lists the GenBank accession number and primer sequences. Reactions were performed in technical triplicate in order to check our satisfactory technical reproducibility, using a 7500 PCR real-time system (Applied Biosystems) pre-set with the flowing cycling parameters: 95 °C for 10 min, (40 cycles: 95 °C for 15 s, 58 °C for 30 s, 72 °C for 40 s), 95 °C for 15 s at the end of the amplification time. The results were computed using the $2^{-\Delta\Delta Ct}$ algorithm against the elongation factor 1 alpha (*ef1α*) and expressed as the n-fold difference compared to an arbitrary calibrator, chosen as a higher value than ΔΔCts.

Table 2. *bglap, PTHrP* and *mlc2* Primers for RT-PCR. F, Forward, R, reverse; Tm, annealing temperature.

Gene	Primer sequences (5′→3′)	Tm°C	Accession Number
bglap	F: AGT GAC AAC CCT GCT GAT GA R: TCC CTC AGT GTC CAT CAT GT	58	AF289506
PTHrP	F: CCC AGA GCC AAA CAT TCA GT R: CGG CCT AAC CTC ACC TTT TT	58	AF197904
mlc2	F: TGG CAT CAT CAG CAA GGA R: TTG AAA GCG CTC ACG ATG	54	AF150904

3.9 STATISTICS

Statical analyzes and graphs were conducted using IBM SPSS Statistics for Windows version 22 (IBM Corp, Armonk, NY, USA) and GraphPad Prism version 8.0.1 for Windows (GraphPad Software, San Diego, California, USA). Data normality was analyzed using the Shapiro–Wilk test, and homogeneity of variance was estimated using Levene's tests. Differences between measurements were analyzed using the Chi-Square test for incidence of bone deformities (Qualitative data), by Mann–the Whitney U Test for growth parameters (when the assumptions of normality and homogeneity of variance were violated), and Welch's ANOVA test for gene expression levels analysis (normally distributed data that violates the assumption of homogeneity of

variance). Values are expressed as mean ± Standard error of the mean (SEM) or mean± standard deviation (SD) considering the conditions reviewed by (Altman & Bland, 2005). The signification threshold was established as the p-value (P) < 0.05.

Chapter 4: Results

4.1 EFFECT OF EXOGENOUS MELATONIN ON GROWTH RATE

The investigation of the effects of the two concentrations of MEL on growth rate showed that, at the first sampling time point (13 DPH), there were no statistically significant differences between the two experimental groups (MEL1 and MEL2) and the control group (Ctrl) for both length and weight (Figure 10 and Figure 11). At 23 DPH, however, the highest length was recorded in the Ctrl group (0.614 ± 0.0155 cm), which was statistically different from that of MEL1 (Mann–Whitney U test, $p < 0.05$) (Figure 11). The growth in weight showed the same growth pattern in length, and statistical comparison has not revealed any significant difference between all three groups of larvae (Mann–Whitney U test, $p < 0.05$) (Figure 12). At 33 DPH, the MEL1 group registered the lowest weight value, while the Ctrl group showed the highest ponderal growth. The Mann–Whitney U test detected a significant difference between Ctrl and both treated groups for the weight ($p < 0.05$) (Figure 11). However, those differences were not significant for the growth in length (Figure 11). On larvae aged 43 DPH, the length showed a statistically significant difference only between Ctrl and MEL1 groups (Mann–Whitney U test, $p < 0.05$). MEL2 larvae displayed the highest growth in weight (0.0179 ± 0.001148 g), while MEL1 registered the lowest. The difference in weight means between the three groups was statistically significant at the 0.05 level (Mann–Whitney U test) (Figure 11). At 53 DPH, the larvae from the MEL2 group showed the highest length (2.17 ± 0.0163 cm), while the MEL1 group larvae showed the lowest growth in length among the three groups of larvae (Figure 10). At this age, the weight distribution between the three groups coincided well with the growth in length. The differences between the three groups for

both length and weight were statistically significant (Mann–Whitney U test, $p < 0.05$) (Figure 11 and Figure 12). Ten days later (63 DPH), the larval growth in MEL1 exceeded that in Ctrl but was lower than that of MEL2 for both length and weight. The differences between the three groups were significant based on Mann–Whitney U test and considering a p-value < 0.05. From 63 DPH, , the MEL1 length growth continued to increase and reached 4.06 ± 0.0224 cm at 73 DPH, while in the Ctrl and MEL2 groups, it did not exceed 3.380 ± 0.0197 cm and 3.295 ± 0.197 cm, respectively (Figure 11). The length crest in MEL1 went with a weight crest of 1.021 ± 0.0196 g, which was 44.47%, and 50.66% higher than that of the Ctrl group and MEL2 group, respectively (Mann–Whitney U test, $p < 0.05$). At the end of the experience (83 DPH), the both experimental groups showed almost an equal growth rate (4.48 cm / 1.323 g – 4.47 cm / 1.342 g) and were statistically 6.40% longer and 22.38% heavier than those of the Ctrl group (Mann–Whitney U test, $p < 0.05$) (11 and 12).

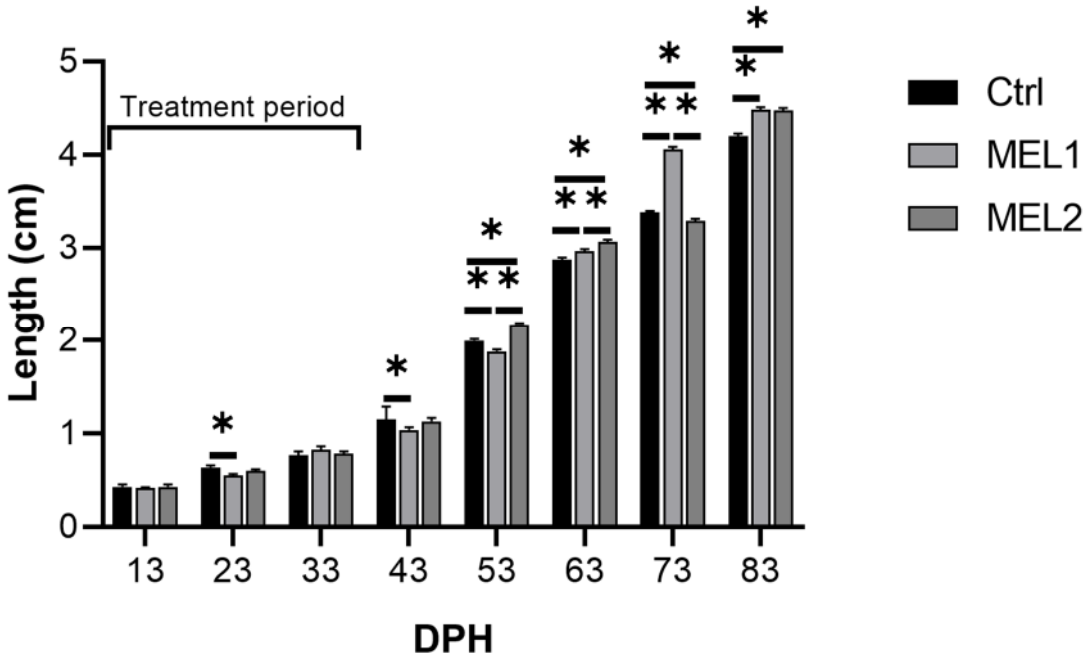

Figure 11. Total length variation in gilthead seabream larvae fed with rotifers and Artemia enriched with two MEL concentrations (MEL1 and MEL2). Data are expressed as mean ± SEM. Asterisks indicate significant differences between the two experimental groups and control group based on Mann–Whitney U test, $p < 0.05$).

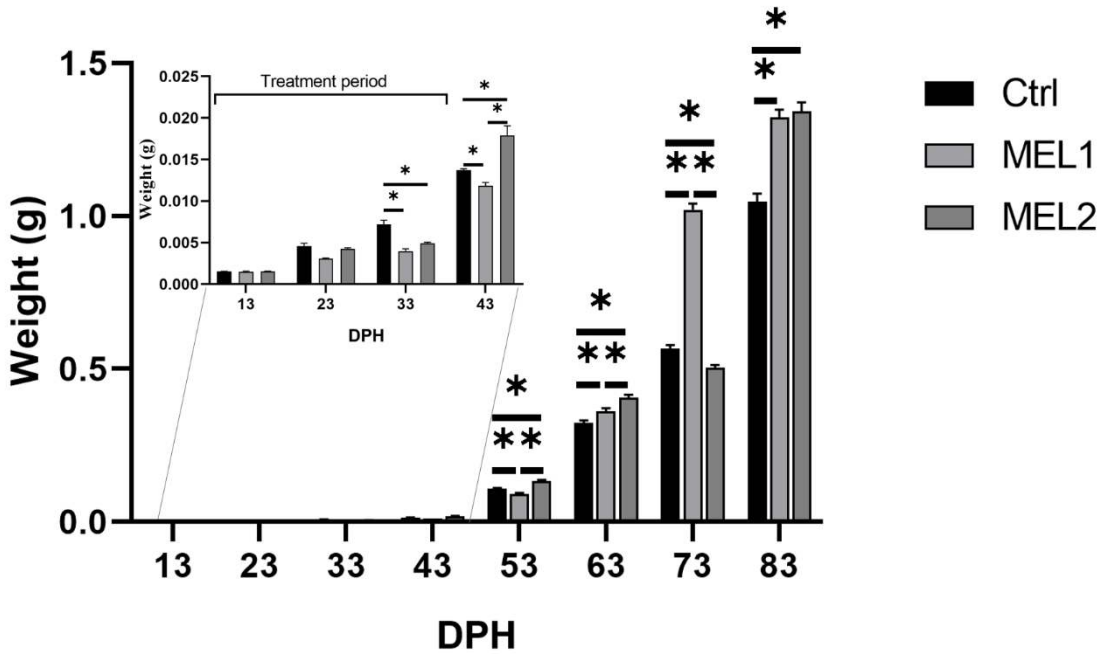

Figure 12. Weight variation in gilthead seabream larvae fed with rotifers and Artemia enriched with two MEL concentrations (MEL1 and MEL2). Data are expressed as mean ± SEM. Asterisks indicate significant differences between the two experimental groups and control group based on Mann–Whitney U test, $p < 0.05$.

In the three groups of larvae, we have calculated the length –weight relationship expressed by the equation $W = aL^{b,}$ which was logarithmically transformed to log W = b log L + log a. The regression equation for MEL1, MEL2, and Ctrl groups were log W = 1.087 logL−1.18, logW = 0.954 logL−0.992, and log W = 3.055 logL−4.383, respectively. In both experimental groups, the b values were $b_{MEL1} = 1.087$, and $b_{MEL2} = 0.954$ for MEL1 and MEL2 respectively. Thus, the b values inferior to three were in favor of a negative allometric growth pattern which means that larvae fed with the two MEL concentration gained less weight than the cube of its length, and they were slimmer with increasing length. Conversely, Ctrl group larvae, with a b value of 3.05, showed a positive allometric growth pattern, which means that while weight was still progressing, gains in length stopped.

4.2 EFFECT OF EXOGENOUS MELATONIN ADMINISTRATION ON INSULIN-LIKE GROWTH FACTOR 1 CONCENTRATION

The IGF-1 concentration on gilthead seabream larvae fed with a graded level of MEL is shown in Figure 13. The bell-shaped histogram manifested a baseline concentration at 23 DPH, which increased two-fold between 33 and 43 DPH, after which the growth hormone rate dropped to the baseline level announcing the end of metamorphosis (around 43 DPH). Before the end of the metamorphosis, at 23, 33, and 43 DPH, MEL2 larvae showed a higher concentration on IGF-1 than that of the Ctrl group. Still, that difference was statically significant only at 23 and 43 DPH (Mann–Whitney U test, $p < 0.05$). Moreover, MEL1 larvae showed a higher IGF-1 concentration than that of Ctrl group at 23 and the differences were not statically significant at 23, 33, and 43 DPH. After the late metamorphosis (43 DPH), there were no statistically significant differences between the IGF-1 levels of the three experimental groups (Mann–Whitney U test, $p < 0.05$).

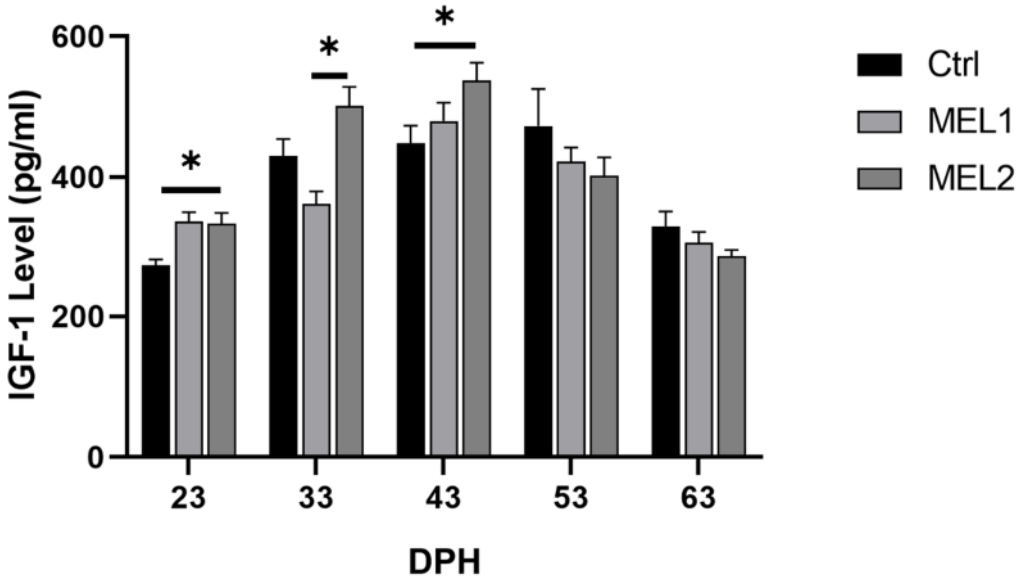

Figure 13. Insulin-like growth factor 1 (IGF-1) level of gilthead seabream larvae fed with rotifers and Artemia enriched with two MEL concentrations (MEL1 and MEL2). Data are expressed as mean ± SD. Asterisks indicate significant differences between the experimental groups and the control group (Mann–Whitney U test, $p < 0.05$).

4.3 EFFECTS OF EXOGENOUS MELATONIN IN THE OSSIFICATION PATTERN

The ossification state in farmed gilthead seabream larvae was investigated using acid-free double staining. Figure 14 shows the chronology of the ossification in the two experimental groups (MEL1 and MEL2) and the Ctrl group larvae. Until 33 DPH, the double staining revealed only cartilaginous structures such as epiphysial tectum, sclerotic, lamina precerebralis, rostral cartilage, premaxillary, maxillary, dentary, branchiostegal rays, cleithrum, coraco scapular cartilage in the cranial region (Figure 14.a, Figure 14.d, and Figure 14.g). Within the vertebral column, we identified 23 neural arches and three epurals beside three parapophyses, 13 hemal arches, and five hypural cartilages (Figure 14.a, Figure 14.d, and Figure 14.g). At 43 DPH, all cartilaginous structures earned volume, and the ossification was begun in the head region's dentary, maxillary, and opercular complex (Figure 14.b, Figure 14.e, Figure 14.h). Later, a saltatory ossification process was introduced on the vertebral column on centra 1 - 4, 8 - 10, and 14 - 19 (Figure 14.b, Figure 14.e, and Figure 14.h). The accomplishment of the ossification process occurred at 53 DPH when alizarin red staining had preeminency over the larva (Figure 14.c, Figure 14.f, Figure 14.i). Under the standard rearing conditions, the same ossification patterns were observed between the two experimental groups and the Ctrl group of larvae: a continuous process (from 43 to 53 DPH) with the same ossification rate (Figure 14).

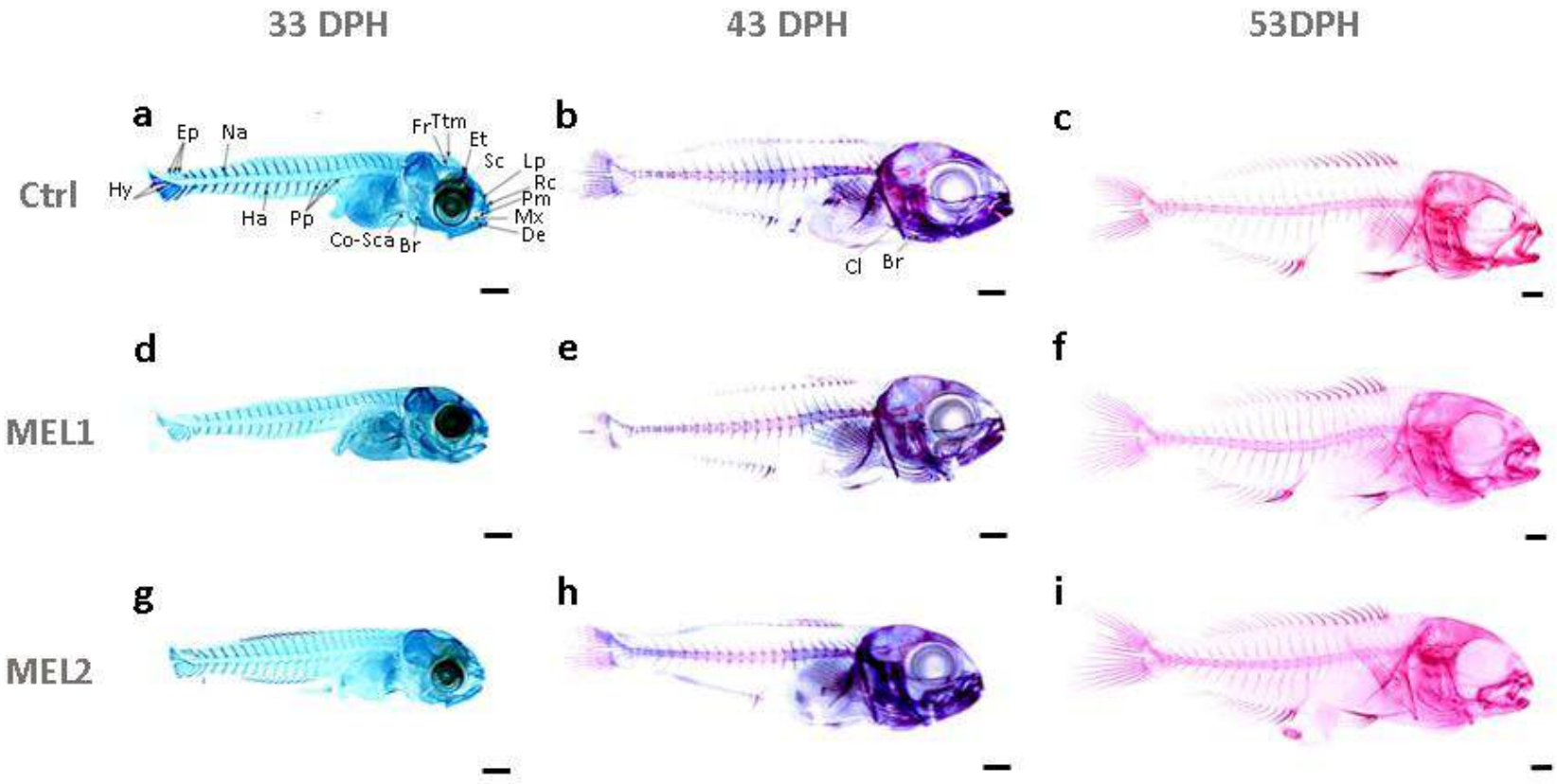

Figure 14. The ossification pattern of gilthead seabream larvae from the Ctrl: (a) at 33 DPH, (b) at 43 DPH, (c) at 53 DPH; from MEL1 group: (d) at 33 DPH, (e) at 43 DPH, (f) at 53 DPH; from MEL2 group: (g) at 33 DPH, (h) at 43 DPH, (i) at 53 DPH. Double stained larvae showed alician blue-stained cartilaginous structures and alizarin red-stained bony structures. Fr, frontal; Ttm, taenia tecti medialis; Et, epiphysial tectum; Sc, sclerotic; Lp, lamina precerebralis; Rc, rostral cartilage; Pm, premaxillary; Mx, maxillary; De, dentary; Br, branchiostegal rays; Cl, cleithrum; Co-Sca, coraco scapular cartilage; Pp, parapophyse; Ha, hemal arches; Hy, hypural; Ep, epural; Na, neural arches. Scale bar: 0.5 mm.

4.4 OPERCULAR COMPLEX DEFORMITIES

4.5 GROSS ANATOMY

Since 53 DPH, larvae were wholly ossified in Ctrl, MEL1, and MEL2, all types of operculum complex abnormalities at this stage were definitive. Figure 15 illustrates some forms of operculum complex deformities recorded in 53 DPH larvae from the three groups. Operculum anomalies were registered as various gill cover irregularities and different degrees of gill chamber exposure. Those abnormalities were generated by a reduction (Figure 15.a, Figure 15.e, and Figure 15.i), folding (Figure 15.d, Figure 15.h, Figure 15.l), or both reduction and folding (Figure 15.b, Figure 15.c, Figure 15.f, Figure 15.g, Figure 15.j, Figure 15.k) of one or more bones composing the opercular complex. The wide variability of abnormality typologies stated in this study, and their severity did not allow the definition of accurate, specific patterns of the operculum deformities. Furthermore, no type of abnormality was defined as group specific.

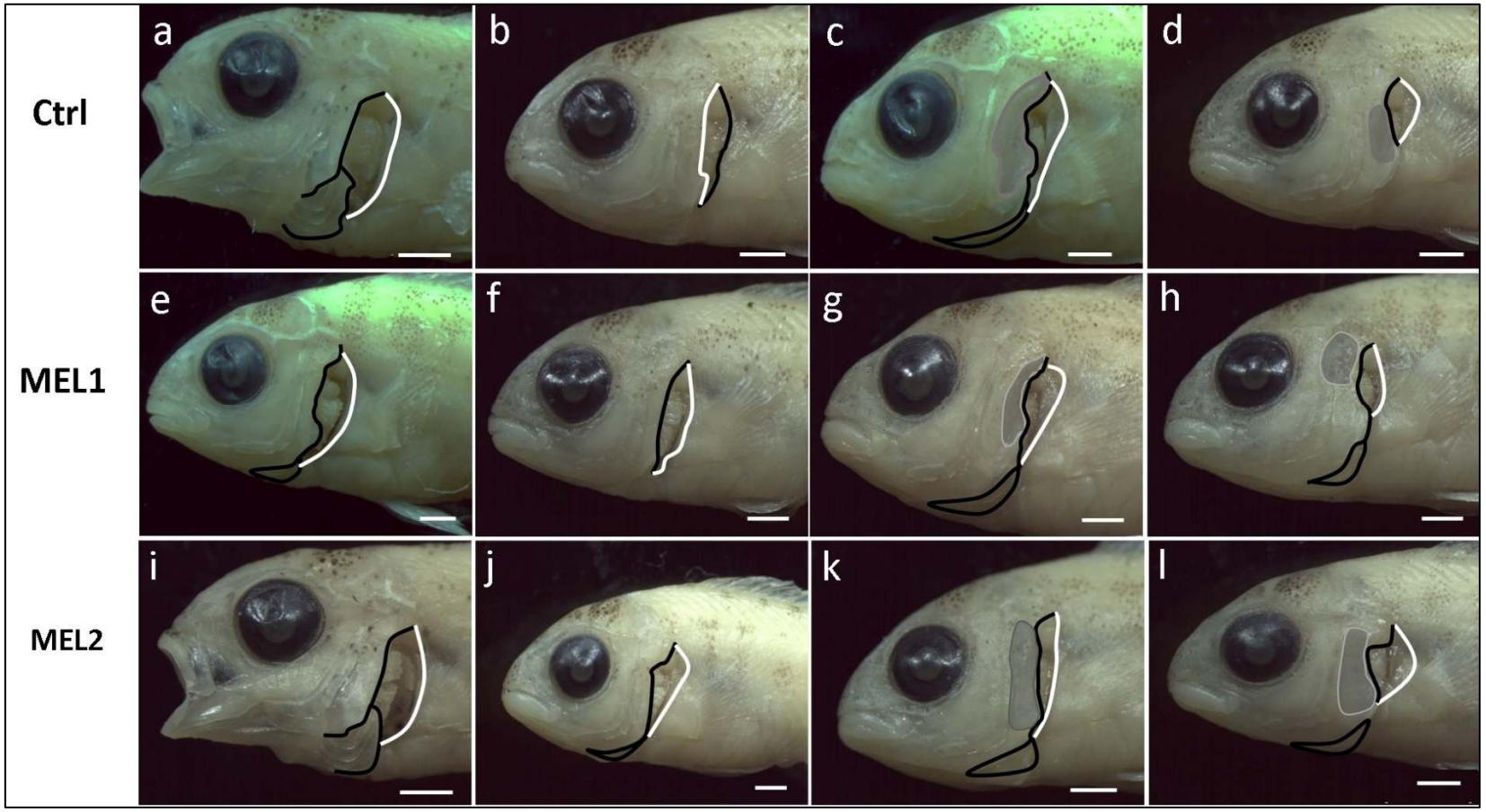

Figure 15. Different forms of opercular complex anomalies registered in gilthead seabream larvae of 53 DPH from (a–d) Ctrl, (e–h) MEL1, and (i–l) MEL2. (a,e,i) Severe reduction in gills cover (opercle, subopercle, and interopercle); (b,f,j) severe reduction in gills cover (opercle and subopercle); (c,g,k) folded opercle upper corner and reduced subopercle and opercle lower corner; (d,h,l) folded gills cover leading to gills exposition. Grey-shaded areas indicate folded bones. Black lines designate the loose edge of the operculum and branchiestegal rays, while the white lines define the standard limits of the branchial chamber. Scale bar: 1m

The incidence of opercular complex abnormalities and the nature of this disorder as being unilateral or bilateral in the three groups of gilthead seabream larvae are shown in Figure 16. The incidence of the opercular complex deformities in larvae fed the lower dose of MEL MEL1 was significantly higher than that observed in the control group at 53, 63, and 83 DPH (Chi-square test, $p < 0.05$). Still, at 73 DPH, this difference was not statistically significant (Chi-square test, $p < 0.05$). Regarding the incidence of operculum deformities between MEL2 and Ctrl group larvae, there were no significant statistical differences (Chi-square test, $p < 0.05$) at 53, 63, and 73 DPH, but there was at 83 DPH. In both experimental and control groups, the anomalies were mostly unilateral in 65.6 and 100% of the cases, and in some cases, they were bilateral.

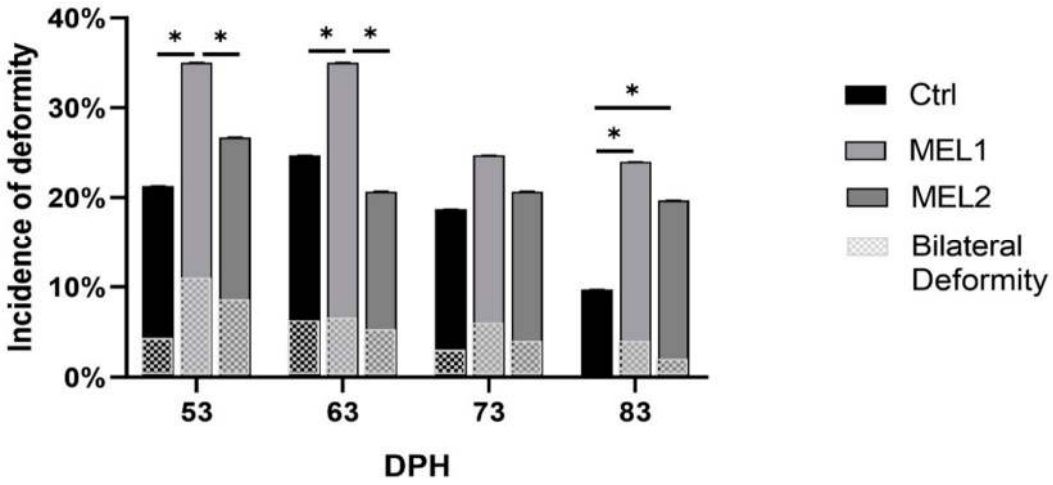

Figure 16. Incidence of opercular complex deformities on gilthead seabream larvae fed with rotifers and Artemia enriched with two concentrations of MEL (MEL1 and MEL2). Asterisks indicate significant differences between the three experimental groups of larvae (Chi-square test, $p < 0.05$).

4.6 OPERCULAR COMPLEX ABNORMALITIES UNDER SCANNING ELECTRON MICROSCOPE (SEM)

SEM observation provided a better perception and insight into the different forms of opercular complex abnormalities compared to stereomicroscope observation. The detected opercular complex anomalies involved the various opercular bones (opercle, subopercle, interopercle, and

preopercle) and branchiostegal membrane and rays. The protecting wall for the orobranchial chamber can be reduced on different levels, with references to a reduction or even lack of one of the various operculum bones (Figure 17.a, Figure 17.b). Other types of anomalies are attributed to the inside or outside folding of one or more opercular bones (Figure 17.c, Figure 17.d) or a combined shortened-folded operculum (Figure 17.g). Moreover, we have detected for the first-time new forms of operculum deformities, including wave-like (Figure 17.e) and spring-like (Figure 17.f) gill covers, as well as the lack of apposition of the branchiostegal membrane to the epithelium at the terminal edge of the branchial cavity generated by different degrees of hyperplasia (Figure 17.h), and folded branchiostegal rays in the gill chamber (Figure 17.i).

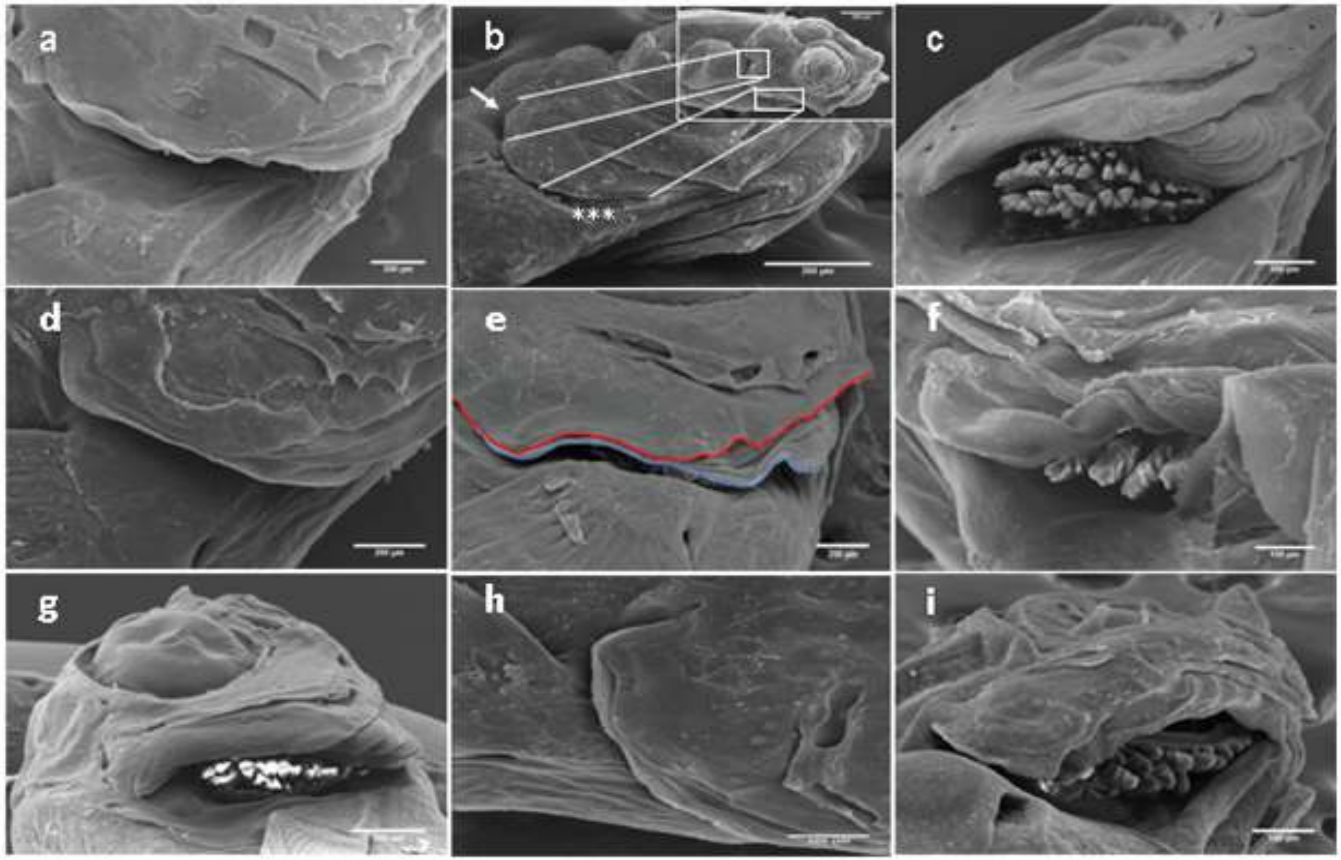

Figure 17. Different forms of the opercular complex abnormalities in gilthead seabream larvae aged 13-53 DPH. (a) Hypoplastic operculum, (b) reduced opercle (white arrows) and lack of interopercle (asterisks), (c) folded opercular bones toward the gills chamber leading to the exposition of gill arches, (d) outside folded operculum, (e) wave-like gill caver (red line) modulating a branchiostegal membrane (blue line), (f) spring-like gill caver with exposed gill arches, (g) combined shortened-folded operculum, (h) hyperplastic branchiostegal membrane, (i) folded branchiostegal rays in the gill chamber. Scale bars: 200 μm.

4.7 SKELETAL DEFORMITIES

The early detection of skeletal deformities in farmed gilthead seabream larvae from the two experimental and control groups was conducted using the acid-free double staining protocol (Figure 18).

The examination of double-stained larvae under the stereomicroscope revealed many typologies of bone deformities (Figure 18). The detected deformities affected the threshold traits of the vertebral column (vertebrae, neural and hemal spin) as well as the meristic characteristics of the caudal fin complex. The vertebral column preserved its normal curvature (no lordosis or kyphosis cases were recorded), and its meristic qualities. It was composed of 24 vertebrae in both experimental and control group larvae. However, several malformations altered vertebrae, and we retrieved a rectangular slender vertebral body (Figure 18.a), cubic thick vertebral body (Figure 18.b), and triangular-shaped vertebrae (Figure 18.c). Neural and hemal spine also exhibited abnormalities such as the bifurcation of the neural spine (Figure 18.a, Figure 18.d) and detached neural and hemal spine (Figure 18.c, Figure 18.e). Skeletal deformities were also revealed in the caudal portion, and abnormalities recorded included the absence of one or all of the three epurals (Figure 18.c, Figure 18.f), and the lack, or fusion of hypural (Figure 18.c). In many cases, we documented multiple deformities in the same sample (Figure 18.a).

The typology and incidence of skeletal deformities detected in MEL1, MEL2, and Ctrl gilthead seabream larvae are shown in Table 3. Out of 90 samples in each group (30 per each sampling time point: 33, 43, and 53 DPH), 84.4% (n= 76), 92.2% (n= 83), and 96.7% (n= 87) of the Ctrl, MEL1, and MEL2 groups larvae, respectively, showed at least one type of deformity. Based on a Chi-square test, when the p-value < 0.05, we concluded that the difference

between the total abnormalities frequencies of Ctrl and MEL1 was not statistically significant, while that of Ctrl and MEL2 was significant (Table 3).

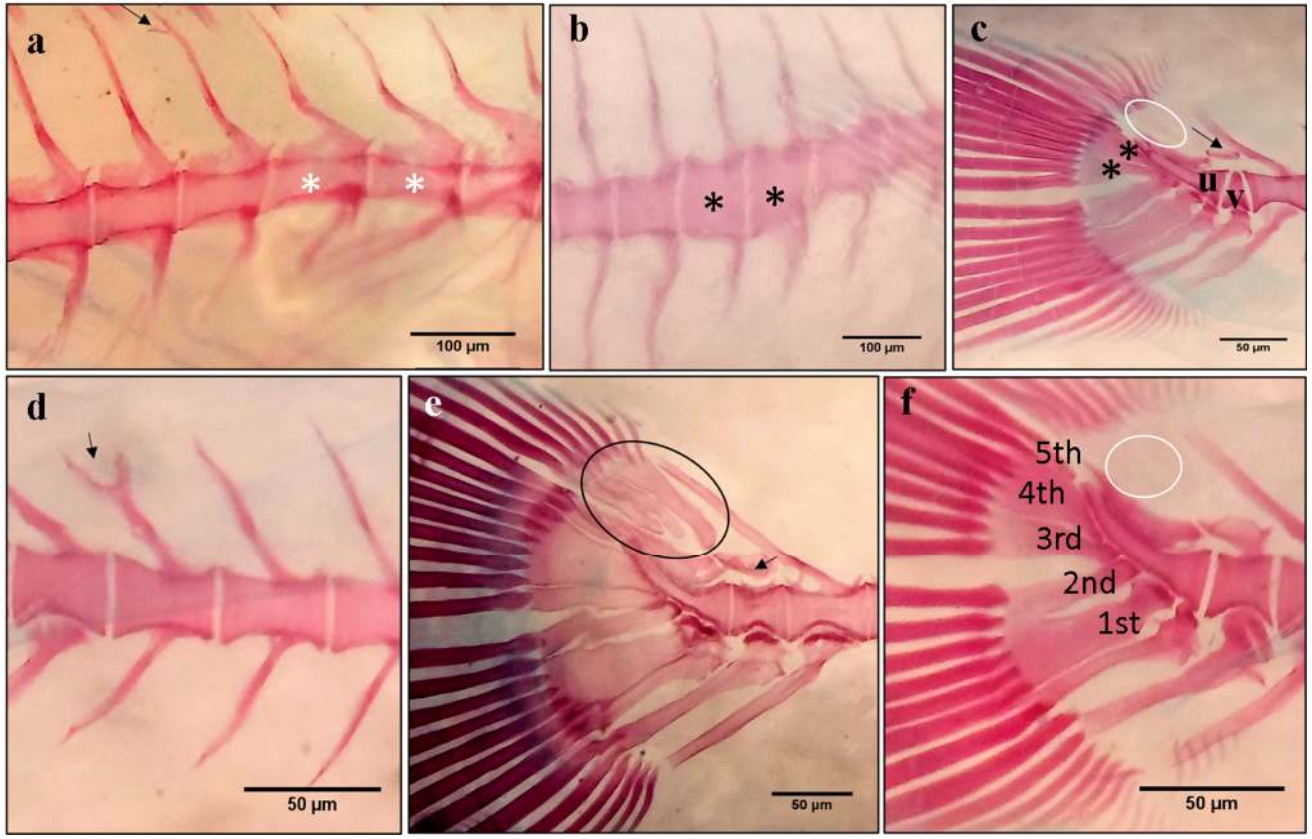

Figure 18. Typical forms of Skeletal abnormalities in gilthead seabream larvae from the three groups of larvae at 53 DPH. (a) Rectangular slender vertebral body (white asterisks), and bifurcated neural spine (arrow); (b) cubic thick vertebral body (black asterisks); (c) The last caudal vertebra (v), preceding the urostyle (u), is triangular shaped with detached neural spine (arrow), The absence of the three epurals (white circle), Lack of the fifth hypural and fusion of the third and fourth hypural (black asteriks); (d) bifurcated neural spine (black arrow); (e) detached neural spine (arrow). The circle indicates a normal epural arrangement; (f) normal hypural arrangment (1st to 5th hypurals) and absence of the three epurals (white circle). Scale bars (a,b): 100 µm, and (c–f): 50 µm.

Abnormalities affecting the caudal fin complex were the most common deformities encountered in 45.6%, 62.2%, and 77.8% of Ctrl, MEL1, and MEL2 larvae, respectively. The statistical differences between the above-mentioned frequencies of the three larval groups were significant. Moreover, the frequency of larvae with at least one vertebral abnormality was 23.3% in both Ctrl and MEL2 groups and 28.9% in MEL1. No statistically significant difference was computed between the frequencies of vertebral abnormalities of the three groups of larvae. We have registered an incidence of hemal and neural spine deformities of 63.3%, 55.6%, and 61.1% respectively, in the MEL1, MEL2, and Ctrl groups, and no statistically significant differences were registered between the different groups.

Table 3. The incidence of skeletal anomalies on gilthead seabream larvae of the three larval groups.

	Control	MEL 1	MEL2
Total Abnormalities	84,4%a	92,2%ab	96,7%b
Vertebral abnormalities	23,3%	28,9%	23,3%
Hemal and neural spin abnormalities	61,1%	63,3%	55,6%
Caudal potion abnormalities	45,6a%	62,2%b	77,8%c

Different letters within the same row show statistically significant differences (Chi-square test, $p < 0.05$).

4.8 EFFECTS OF EXOGENOUS MELATONIN ON BONE AND SKELETAL MUSCLE-SPECIFIC GENE EXPRESSION

Melatonin was administrated in two doses, MEL1 and MEL2, for gilthead seabream larvae to study the responses at the transcriptional level in growth and osteogenesis. For this reason, the expression level of bone-specific genes: bone gamma-carboxyglutamate protein-coding gene (bglap), and parathyroid hormone-related protein-coding gene (PTHrP); skeletal muscle-specific gene: myosin light chain 2 (mlc2), were investigated. In most sampling time points, the expression of both bglap and PTHrP was significantly impacted by MEL administration. Considerable variability in bglap transcript

abundance was detected among both treated groups and between Ctrl and MEL2, while the differences between Ctrl and MEL1 were statistically negligible (Figure 19). Regardless of the significantly decreased expression of bglap over larval development (statistically significant differences between the different sampling time points based in Welch test), the expression pattern was conserved in all treatment groups of each sampling time point, even after the end of MEL administration.

Unlike bglap expression pattern, PTHrP showed a quite constant expression pattern before the metamorphosis. However, a dose-response relationship between MEL concentration and PTHrP transcriptional level was recorded during the first 33 DPH (Figure 20). During the administration of the exogenous MEL period from 13 to 43 DPH, the PTHrP transcriptional levels in MEL1 were more or less comparable to those in Ctrl group. Still, the transcriptional levels of the same gene in MEL2 group larvae showed a statistically significant difference compared to those from the Ctrl group at 13 and 23 DPH. By the end of the MEL treatment period (37 DPH), MEL2's PTHrP expression level decreased and ended by being compared to those of Ctrl samples.

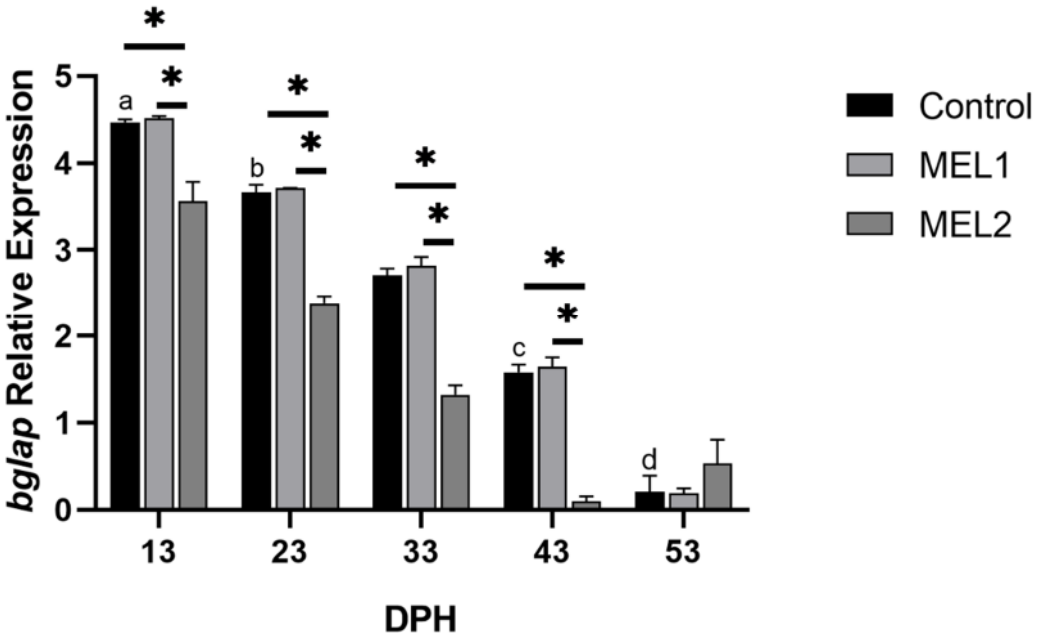

Figure 19. The relative levels of expression of bone gamma-carboxyglutamate protein-coding gene (bglap) in response to MEL administration in gilthead seabream. Gene expression values are expressed as arbitrary units (a.u) for elongation factor 1-alpha (ef1α). Data are expressed as mean ± SD. Different letters indicate statistically significant differences between the different sampling time points of the Ctrl group larvae, and asterisks indicate significant differences between groups for each treatment group (Welch test, $p < 0.05$).

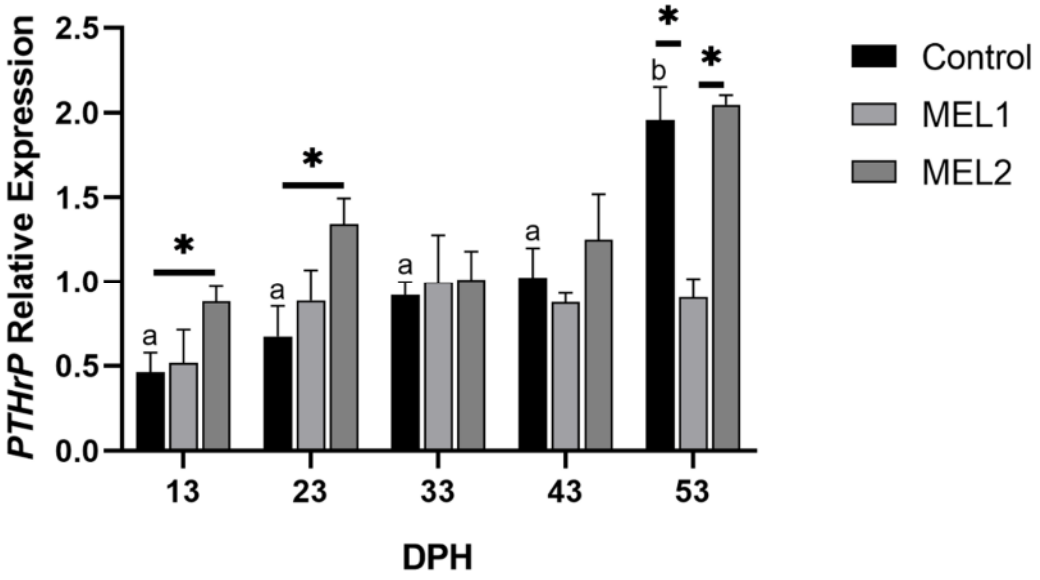

Figure 20. The relative levels of expression of parathyroid hormone-related protein-coding gene (PTHrP) components in response to MEL administration in bone. Gene expression values are expressed as arbitrary units (a.u) for elongation factor 1-alpha (ef1α). Data are expressed as mean±SD. Different letters indicate statistically significant differences between the different sampling time points of the Ctrl group larvae, and asterisks indicate significant differences between groups at each sampling time point (Welch test, $p < 0.05$).

As bglap and PTHrP, mlc2 expression levels showed considerable variability between larvae from the control and the two experimental groups. However, contrarily to the PTHrP expression levels, mlc2 expression was significantly affected by MEL in an inverse dose-response manner during the treatment period from 13 to 33 DPH (Figure 21). At 43 DPH, immediate recovery of mlc2 expression on treated groups temper the expression pattern, which may be explained by the removal of the inhibition exercised by MEL and a possible induction by one of the MEL previously activated pathways.

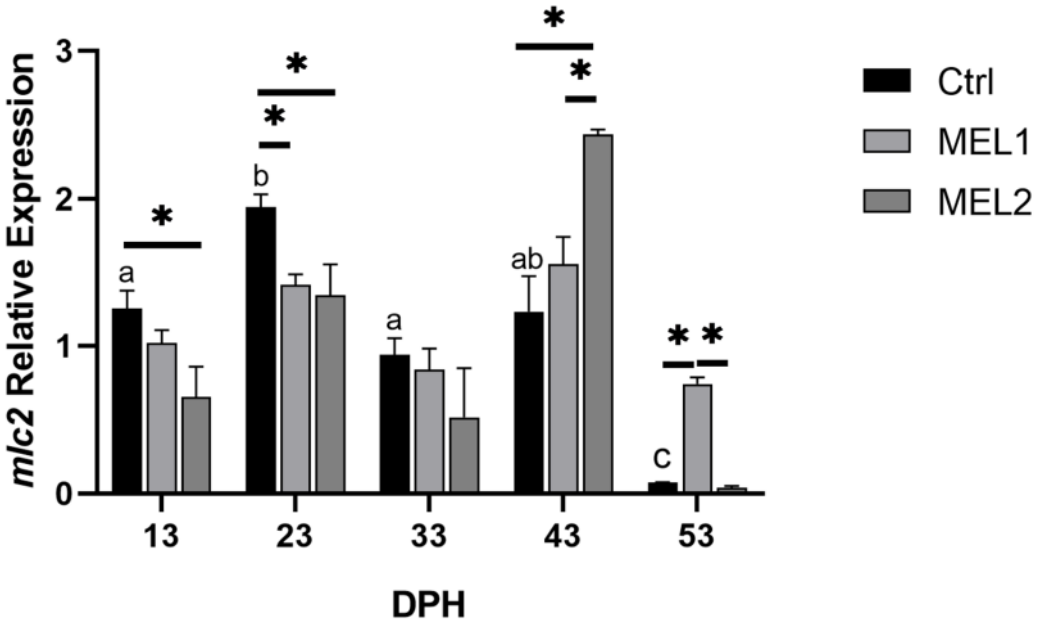

Figure 21. The relative levels of expression of mlc2 components in response to MEL administration in bone. Gene expression values are expressed as arbitrary units (a.u) for elongation factor 1-alpha (ef1α). Data are expressed as mean ± SD. Different letters indicate statistically significant differences between the different sampling time points of the Ctrl group larvae, and asterisks indicate significant differences between groups for each treatment group (Welch test, $p < 0.05$).

Chapter 5: Discussion

5.1 GENERAL DISCUSSION

Skeletal deformities and growth rates in gilthead seabream have been the subject of many research studies. Some authors have associated the skeletal deformities to a defect of inflation of the swim bladder (Peruzzi et al., 2007), others have attributed it to a dietary deficiency of vitamins (Fernández et al., 2008) and fatty acids (Izquierdo et al., 2013) as well as to the larval rearing systems (Roo et al., 2010), and rearing condition (Georgakopoulou et al., 2010). Moreover, the capacity of MEL to induce embryonic development in zebrafish (Danilova et al., 2004; Falcón, Migaud, et al., 2010), and to control several functions related to bone growth in Atlantic salmon (Fjelldal et al., 2004; Porter et al., 1998), was demonstrated. In human adult mesenchymal stem cells/peripheral blood monocytes cocultures, MEL induced osteoblastogenesis and suppressed osteoclastogenesis by the effect of osteoblastic inhibitory lectin derived from osteoblast or by increasing osteoprotegerin and receptor activator of nuclear factor-kB ligand ratios (Maria et al., 2018). Additionally, in a study published in cell biology international, MEL capacity to induce osteoblast differentiation of mice osteoblast precursor cells (MC3T3-E1), and bone formation by upregulating the gene expression of BMP2, BMP6, osteocalcin, and osteoprotegerin was proved (Zhu et al., 2020). However, no study has evaluated exogenous MEL effects on gilthead seabream skeletogenesis and growth during larval development.

In the present study, the two experimental groups of larvae treated with different MEL concentrations and the control group larvae were placed under common hatchery conditions in continuous light to investigate the MEL effect on growth rate and skeletal deformities in gilthead seabream larvae.

In teleosts, the MEL synthesis reported on the pineal gland and gut has daily rhythms that adjust to the relevant photoperiod (Sánchez-Vázquez et al., 2019; Tordjman et al., 2017; Velarde et al., 2010). The retinal MEL, however, acts as a local neuromodulator and is metabolized in situ. Thus, all the differences observed between the control and the two experimental groups of larvae reared in continuous light were only due to the exogenous MEL incorporated into the enrichment fish oil-based emulsion. The main finding of this research is the capacity of exogenous melatonin to affect gilthead seabream larval performance and the incidence of skeletal abnormalities. Indeed, exogenous MEL affected normal skeletogenesis and caused bone deformities. The operculum and caudal fin complex were the most concerned structures. The frequency of opercular anomalies of the Ctrl group larvae in the different sampling time points ranged between 9.7% and 21.3%, figure within the incidence scale extending from 6.3% to 43.2%, registered in prior studies conducted over the past two decades (Beraldo et al., 2003; Ortiz-Delgado et al., 2014). Forthermore, this incidence represents almost a quarter of that reported in an older study published in Aquaculture (Andrades et al., 1996). Those variances may be attributed to the different rearing systems and conditions (Ortiz-Delgado et al., 2014; Roo et al., 2010) and to the accumulation of new knowledge in aquaculture. The incidence of opercular complex deformities was affected by exogenous Mel administration at its lower level and MEL1 group larvae showed the highest incidence of opercular complex abnormalities among the three groups. In agreement with Ortiz-Delgado et al. (Ortiz-Delgado et al., 2014) and Berlado et al. (Beraldo et al., 2003), the deformities were mostly unilateral in all three groups (65 to 100% of specimens). The wide variability of opercular complex deformity typologies, including the new forms reported in this study, hampered the founding of specific patterns of deformities, like those defined by Berlado et al. (Beraldo et

al., 2003). The new forms of operculum deformities reported for the first time in this research, included wave-like gill covers, spring-like gill covers, and the lack of apposition of the branchiostegal membrane to the epithelium at the terminal edge of the branchial cavity, and folded branchiostegal rays in the gill chamber.

In our study, the first sign of opercular complex disorders was detected in 13 DPH larvae, a long time before the ossification process took place and earlier than the timing recorded by Galeotti et al. (Galeotti et al., 2000). The exogenous MEL concentrations increased caudal fin complex defects in a dose-dependent manner. Additionally, the control group's incidence of 45.6% was lower than 47.9% and 48.5% recorded in preceding studies (Boglione et al., 2001; Prestinicola et al., 2013). In the same way, the total frequency of cases with at least one anomaly in the Ctrl group was 84.4%, which was lower than the 87% recorded before (Prestinicola et al., 2013). Both aforementioned data were in favor of an optimized of rearing conditions compared to those used in the reported studies. The increased occurrence of opercular complex, caudal fin complex, and total deformities could be a result of MEL-induced accelerated differentiation of osteoblasts already demonstrated in mice and human MSC/PBMC cells and MC3T3-E1 cells (Maria et al., 2018; Zhu et al., 2020). During teleost embryogenesis, cartilaginous structures are the first element of the skeleton to form, which becomes bone after mineralization (Faustino & Power, 1998; Galeotti et al., 2000; Gavaia et al., 2000). The current study demonstrated that this pattern of development was valid for gilthead seabream larvae in which all skeletal elements remained cartilaginous until shortly before 43 DPH. Under the standard rearing conditions, the same ossification patterns were observed in the two experimental groups as well as in the Ctrl group of larvae, with the ossification process seems to be set up at 43 DPH and ended ten days later. The skeleton ontogenesis in the three groups

of larvae revealed precedency to the onset of the elements which serve in feeding and respiration mechanisms (Maxillary, Meckel's cartilage, cartilaginous branchial arches). These results are in accordance with the finding of (Faustino & Power, 2001; Saka et al., 2008). Studies on gilthead seabream meristic counts reported 24 vertebrae, 13 hemal arches, 23 neural arches, four pairs of parapophyses in the vertebral column region, five hypurals, one parahypural arch, three epurals in the caudal fin complex region beside all structures composing the cephalic skeleton (Faustino & Power, 1998; Prestinicola et al., 2013; Saka et al., 2008). In our study, the three experimental groups mostly conserved the meristics mentioned above (Faustino & Power, 1998; Prestinicola et al., 2013; Saka et al., 2008).

Besides skeletogenesis and bone deformities, exogenous MEL affected larval growth in length and weight. Indeed, MEL2 can ensure higher growth rates than those of the MEL1 and Ctrl groups. Additionally, both concentrations favored a negative allometric growth pattern, which means that larvae were slimmer with increasing length. At 63 DPH, the Ctrl group had higher growth rates than those recorded in the previous studies (Can, 2013; Fernández et al., 2008). The promising values recorded in the Ctrl group (high growth, the absence of kyphotic and lordotic spine curve, and the lower opercular complex abnormalities) compared to the result already published for this species (Beraldo et al., 2003; Boglione et al., 2001; Faustino & Power, 1998; Ortiz-Delgado et al., 2014), showed that the rearing conditions applied in the hatchery were optimal compared to those employed in the studies mentioned above. IGF-1 has been associated with metabolism (Castillo et al., 2004) and growth (Wood et al., 2005). At the beginning of the larval growth, IGF-1 levels were shallow, between 13 to 33 DPH. Our findings were in accordance with the outcomes of Deane et al, and Herrero-Turrion et al (Deane et al., 2003; Herrero-Turrion et al., 2003; Herrero-Turrión et al., 2003),

postulating that during the first 30 days of teleost live, the hormones implicated in growth, and development, i.e., growth hormone and prolactin, are naught, and the number of growth hormone cells and growth hormone expression levels do not increase. This low level of growth hormone in gilthead seabream larvae coincide with a spike in MEL production, initiating immediately after hatching to reach maximum levels between 6 and 10 DPH (Kalamarz et al., 2009). Thus, the high MEL production during the first days post-hatching, when growth hormone and prolactin supplies are still insufficient, suggested a distinct role of MEL in early organogenesis, particularly in skeletogenesis. In some teleosts, tissue levels of IGF-1 mRNA were positively correlated with body growth rate (Beckman et al., 2004). Those finding coincide with our observation on weight and total length increase to 3 times fold while the IGF-1 level grew progressively until 43 DPH, the time by which the metamorphosis and definitive organogenesis were fulfilled, after which the growth hormone concentration declined.

In the present study, we investigated as well the effects of exogenous MEL on bone and skeletal muscle-specific gene expression during the larval stage of gilthead seabream. The marker of muscle development and growth, myosin light chain 2 (mlc2), one of the four light chains of the myosine, exerts its regulatory role in binding calcium (Georgiou et al., 2014). *bglap* gene encodes osteocalcin, a bone protein secreted by osteoblasts during bone formation enabling calcium ion and hydroxyapatite binding activities (Lee et al., 2007). PTHrP is a calcium regulatory factor in gilthead seabream that has a crucial function in several physiological and biochemical processes, including cortisol production (Guerreiro et al., 2006), tissue differentiation and proliferation (Kwong & Perry, 2015), calcium mobilization from internal sources (bone and scales) and via calcium uptake from water and diet (Abbink & Flik, 2007). The lethal deletion of this gene in mice proves its crucial

physiological functions (Karaplis et al., 1994). The dose-response relationship between *PTHrP* expression level and MEL concentration registered at least during the treatment period (MEL1 and MEL2) contradicts the negative correlation of those two parameters stipulated by Abbink et al (Abbink et al., 2008). Indeed, another study on primary BALB/c mouse chondrocytes (Shanqi et al., 2019) supports our finding about MEL's capacity to upregulate PTHrP expression.

Additionally, an association between abnormally developing bones and a high expression of PTHrP on Sparus aurata was already described (Keenan et al., 1998). In light of the abovementioned findings, we can assign the high incidence of bone deformities registered in the treated groups to the *PTHrP* upregulation by the orally supplemented MEL. Myosin, a key component of striated muscle contributing to muscle contraction, is consisted of two heavy chains (MHCs) and four light chains (MLCs). Myosin light chain-2 is a sarcomeric protein expressed in the white muscle of gilthead seabream as two isoforms, mlc2a and mlc2b. Myosin light chain 2a predominates the early larval stages marking new fiber development at the tissue level. In our study, the inverse dose-dependent relationship of *mlc2* expression levels and exogenous MEL concentration during the treatment period was in accord with the negative allometric growth pattern induced by MEL. Our results were in accordance with the significant weight increase registered in Atlantic salmon implanted with melatonin and contrasting the body weight and growth rate reduction induced by implants or injections in both trout and goldfish (De Pedro et al., 2008; Porter et al., 1998; Taylor et al., 2006).

5.2 CONCLUSIONS

Different MEL concentrations, and predominately the high one, affected the normal process of skeletogenesis (but not the ossification rate), and the growth patterns of gilthead seabream larvae. MEL increased the frequency of

skeletal deformities, especially those of the operculum complex, for which we have recorded new typologies. The first signs of the opercular complex deformities were recorded before any sign of mineralization, proving that the abnormalities occur during the onset of the operculum complex bone series. Caudal fin complex was also sensitive to exogenous melatonin administration, and its abnormalities' incidence was increased dose-dependent. In light of our results and bibliographic data, we hypothesize that skeletal deformities detected in experimental groups' larvae can be induced by the augmented *PTHrP* expression level, which is upregulated by exogenous melatonin administration, or by a loss of coordination between skeletal muscle and bone growth. Future research should extend and unmask the melatonin- pathways behind muscle and bone growth in gilthead seabream.

Bibliography

Abbink, W., & Flik, G. (2007). Parathyroid hormone-related protein in teleost fish. *General and Comparative Endocrinology*, *152*(2), 243–251. https://doi.org/10.1016/j.ygcen.2006.11.010

Abbink, W., Kulczykowska, E., Kalamarz, H., Guerreiro, P. M., & Flik, G. (2008). Melatonin synthesis under calcium constraint in gilthead sea bream (Sparus auratus L.). *General and Comparative Endocrinology*, *155*(1), 94–100. https://doi.org/10.1016/j.ygcen.2007.03.002

Acharyya, A., Das, J., & Hasan, K. N. (2021). Melatonin as a Multipotent Component of Fish Feed: Basic Information for Its Potential Application in Aquaculture. *Frontiers in Marine Science*, *8*. https://doi.org/10.3389/fmars.2021.734066

Akyol, O., & Gamsiz, K. (2011). Age and growth of adult gilthead seabream (Sparus aurata L.) in the Aegean Sea. *Journal of the Marine Biological Association of the United Kingdom*, *91*(6), 1255–1259. Cambridge Core. https://doi.org/10.1017/S0025315410001220

Alarcón, J. A., Magoulas, A., Georgakopoulos, T., Zouros, E., & Alvarez, M. C. (2004). Genetic comparison of wild and cultivated European populations of the gilthead sea bream (Sparus aurata). *Aquaculture*, *230*(1), 65–80. https://doi.org/10.1016/S0044-8486(03)00434-4

Al-Harbi, A. H. (2001). Skeletal Deformities in Cultured Common Carp Cyprinus carpio L. *Asian Fisheries Science*, *14*, 247–254.

Altman, D. G., & Bland, J. M. (2005). Standard deviations and standard errors. *BMJ*, *331*(7521), 903. https://doi.org/10.1136/bmj.331.7521.903

Amano, M., Iigo, M., Ikuta, K., Kitamura, S., Okuzawa, K., Yamada, H., & Yamamori, K. (2004). Disturbance of plasma melatonin profile by high dose melatonin administration inhibits testicular maturation of precocious male masu salmon. *Zoological Science*, *21*(1), 79–85. https://doi.org/10.2108/0289-0003(2004)21[79:DOPMPB]2.0.CO;2

Andrades, J. A., Becerra, J., & Fernández-Llebrez, P. (1996). Skeletal deformities in larval, juvenile and adult stages of cultured gilthead sea bream (Sparus aurata L.). *Aquaculture*, *141*(1), 1–11. WorldCat.org. https://doi.org/10.1016/0044-8486(95)01226-5

Atalah, E., Hernández-Cruz, C. M., Ganga, R., Ganuza, E., Benítez-Santana, T., Roo, J., Fernández-Palacios, H., & Izquierdo, M. S. (2012). Enhancement of gilthead seabream (Sparus aurata) larval growth by dietary vitamin E in relation to two different levels of essential fatty acids. *Aquaculture Research*, *43*(12), 1816–1827. https://doi.org/10.1111/j.1365-2109.2011.02989.x

Aydin, M. (2018). Maximum length and age report of Sparus aurata (Linnaeus, 1758) in the Black Sea. *Journal of Applied Ichthyology*, *34*(4), 964–966. https://doi.org/10.1111/jai.13615

Aysun, K., Ali, K., & Sule, G. (2018). Length-weight relationship and condition factor as an indicator of growth and feeding intensity of Sea bream (Sparus aurata L, 1758) given feed with different protein contents. *Indian Journal Of Animal Research*, *53*(4), 510–514. https://doi.org/10.18805/ijar.B-998

Bairwa, M., Saharan, N., Rawat, K. D., Jakhar, J., & Bera, A. (2013). Photoperiod, melatonin and its importance in fish reproduction. *European Journal of Experimental Biology*, *2*, 7–15.

Bardon, A., Vandeputte, M., Dupont-Nivet, M., Chavanne, H., Haffray, P., Vergnet, A., & Chatain, B. (2009). What is the heritable component of spinal deformities in the European sea bass (Dicentrarchus labrax)? *Aquaculture*, *294*(3), 194–201. https://doi.org/10.1016/j.aquaculture.2009.06.018

Beckman, B. R., Shimizu, M., Gadberry, B. A., & Cooper, K. A. (2004). Response of the somatotropic axis of juvenile coho salmon to alterations in plane of nutrition with an analysis of the relationships among growth rate and circulating IGF-I and 41kDa IGFBP. *General and Comparative Endocrinology*, *135*(3), 334–344. https://doi.org/10.1016/j.ygcen.2003.10.013

Beraldo, P., & Canavese, B. (2011). Recovery of opercular anomalies in gilthead sea bream, Sparus aurata L.: Morphological and morphometric analysis. *Journal of Fish Diseases*, *34*(1), 21–30. https://doi.org/10.1111/j.1365-2761.2010.01206.x

Beraldo, P., Pinosa, M., Tibaldi, E., & Canavese, B. (2003). Abnormalities of the operculum in gilthead sea bream (Sparus aurata): Morphological description. *Aquaculture*, *220*(1), 89–99. https://doi.org/10.1016/S0044-8486(02)00416-7

Berillis, P. (2015). FACTORS THAT CAN LEAD TO THE DEVELOPMENT OF SKELETAL DEFORMITIES IN FISHES: A REVIEW. *Journal of Fisheriessciences.Com*, *9*, 17–23.

Berillis, P. (2017). Skeletal Deformities in Seabreams. Understanding the Genetic Origin Can Improve Production? *Journal of FisheriesSciences.Com*, *11*(2). https://doi.org/10.21767/1307-234X.1000118

Björnsson, B. T., Hemre, G. I., Bjørnevik, M., & Hansen, T. (2000). Photoperiod regulation of plasma growth hormone levels during induced smoltification of

underyearling Atlantic salmon. *General and Comparative Endocrinology*, *119*(1), 17–25. https://doi.org/10.1006/gcen.2000.7439

Boeuf, G., & Falcon, J. (2001). Photoperiod and growth in fish. *Vie et Milieu/Life & Environment*, 247–266.

Boglione, C., Gagliardi, F., Scardi, M., & Cataudella, S. (2001). Skeletal descriptors and quality assessment in larvae and post-larvae of wild-caught and hatchery-reared gilthead sea bream (Sparus aurata L. 1758). *Aquaculture*, *192*(1), 1–22. https://doi.org/10.1016/S0044-8486(00)00446-4

Boglione, C., Gavaia, P., Koumoundouros, G., Gisbert, E., Moren, M., Fontagné, S., & Witten, P. E. (2013). Skeletal anomalies in reared European fish larvae and juveniles. Part 1: Normal and anomalous skeletogenic processes. *Reviews in Aquaculture*, *5*(s1), S99–S120. https://doi.org/10.1111/raq.12015

Boglione, C., Gisbert, E., Gavaia, P., E. Witten, P., Moren, M., Fontagné, S., & Koumoundouros, G. (2013). Skeletal anomalies in reared European fish larvae and juveniles. Part 2: Main typologies, occurrences and causative factors. *Reviews in Aquaculture*, *5*(s1), S121–S167. https://doi.org/10.1111/raq.12016

Bolliet, V., Ali, M. A., Lapointe, F.-J., & Falcón, J. (1996). Rhythmic melatonin secretion in different teleost species: An in vitro study. *Journal of Comparative Physiology B*, *165*(8), 677–683. https://doi.org/10.1007/BF00301136

Boursiaki, V., Theochari, C., Zaoutsos, S. P., Mente, E., Vafidis, D., Apostologamvrou, C., & Berillis, P. (2019). Skeletal Deformity of Scoliosis in Gilthead Seabreams (Sparus aurata): Association with Changes to

Calcium-Phosphor Hydroxyapatite Salts and Collagen Fibers. *Water*, *11*(2). https://doi.org/10.3390/w11020257

Bustin, S. A., Benes, V., Garson, J. A., Hellemans, J., Huggett, J., Kubista, M., Mueller, R., Nolan, T., Pfaffl, M. W., Shipley, G. L., Vandesompele, J., & Wittwer, C. T. (2009). The MIQE guidelines: Minimum information for publication of quantitative real-time PCR experiments. *Clinical Chemistry*, *55*(4), 611–622. https://doi.org/10.1373/clinchem.2008.112797

Caballero, M. J., López-Calero, G., Socorro, J., Roo, F. J., Izquierdo, M. S., & Férnandez, A. J. (1999). Combined effect of lipid level and fish meal quality on liver histology of gilthead seabream (Sparus aurata). *Aquaculture*, *179*(1), 277–290. https://doi.org/10.1016/S0044-8486(99)00165-9

Cahill, G. M., & Besharse, J. C. (1995). Circadian rhythmicity in vertebrate retinas: Regulation by a photoreceptor oscillator. *Progress in Retinal and Eye Research*, *14*(1), 267–291. https://doi.org/10.1016/1350-9462(94)00001-Y

Campinho, M. A. (2019). Teleost Metamorphosis: The Role of Thyroid Hormone. *Frontiers in Endocrinology*, *10*, 383. https://doi.org/10.3389/fendo.2019.00383

Can, E. (2013). Effects of Intensive and Semi-Intensive Rearing on Growth, Survival, and V-Shaped (Lordotic) Skeletal Deformities in Juvenile Gilthead Sea Bream (Sparus aurata). *Israeli Journal of Aquaculture - Bamidgeh*, *65*.

Carnevali, O., Mosconi, G., Cardinali, M., Meiri, I., & Polzonetti-Magni, A. (2001). Molecular components related to egg viability in the gilthead sea bream, Sparus aurata. *Molecular Reproduction and Development*, *58*(3), 330–335. https://doi.org/10.1002/1098-2795(200103)58:3<330::AID-MRD11>3.0.CO;2-7

Castillo, J., Codina, M., Martínez, M. L., Navarro, I., & Gutiérrez, J. (2004). Metabolic and mitogenic effects of IGF-I and insulin on muscle cells of rainbow trout. *American Journal of Physiology-Regulatory, Integrative and Comparative Physiology*, *286*(5), R935–R941. https://doi.org/10.1152/ajpregu.00459.2003

Caterina, F., Piccione, G., Marafioti, S., Arfuso, F., Fortino, G., & Fazio, F. (2014). Metabolic response to monthly Variations of Sparus aurata Reared in Mediterranean On-Shore Tanks. *Turkish Journal of Fisheries and Aquatic Sciences*, *14*(2), 567–574. https://doi.org/10.4194/1303-2712-v14_2_28

Cerdà, J., Fabra, M., & Raldúa, D. (2007). Physiological and molecular basis of fish oocyte hydration. In *The Fish Oocyte* (pp. 349–396). Springer.

Chaoui, L., Kara, M. H., Faure, E., & Quignard, J. P. (2006). Growth and reproduction of the gilthead seabream Sparus aurata in Mellah lagoon (north-eastern Algeria). *Scientia Marina*, *70*(3), 545–552. https://doi.org/10.3989/scimar.2006.70n3545

Cicek, E., Avsar, D., Yeldan, H., & Ozutok, M. (2006). Length–weight relationships for 31 teleost fishes caught by bottom trawl net in the Babadillimani Bight (northeastern Mediterranean). *Journal of Applied Ichthyology*, *22*(4), 290–292. https://doi.org/10.1111/j.1439-0426.2006.00755.x

Colloca, f, & Cerasi, s. (2022). Sparus aurata. Cultured Aquatic Species Information Programme. In *FAO*. https://www.fao.org/fishery/en/culturedspecies/Sparus_aurata/en

Conde-Sieira, M., Muñoz, J. L. P., López-Patiño, M. A., Gesto, M., Soengas, J. L., & Míguez, J. M. (2014). Oral administration of melatonin counteracts several of

the effects of chronic stress in rainbow trout. *Domestic Animal Endocrinology*, *46*, 26–36. https://doi.org/10.1016/j.domaniend.2013.10.001

Daniel, P. (1984). *Some simple methods for the assessment of tropical fish stocks* (FAO FISHERIES TECHNICAL PAPER No. 282). FAO. https://www.fao.org/3/x6845e/x6845e00.htm

Danilova, N., Krupnik, V. E., Sugden, D., & Zhdanova, I. V. (2004). Melatonin stimulates cell proliferation in zebrafish embryo and accelerates its development. *FASEB Journal : Official Publication of the Federation of American Societies for Experimental Biology*, *18*(6), 751–753. https://doi.org/10.1096/fj.03-0544fje

De Guzman, M. F., & Geronimo R, R. (2020). *Length-weight relationships of marine fishes caught by danish seine in Lingayen gulf*. *8*(6), 16–18. https://doi.org/10.22271/fish.2020.v8.i6a.2353

De Pedro, N., Martínez-Álvarez, R. M., & Delgado, M. J. (2008). Melatonin reduces body weight in goldfish (Carassius auratus): Effects on metabolic resources and some feeding regulators. *Journal of Pineal Research*, *45*(1), 32–39. https://doi.org/10.1111/j.1600-079X.2007.00553.x

De Vlaming, V. (1980). Effects of pinealectomy and melatonin treatment on growth in the goldfish, Carassius auratus. *General and Comparative Endocrinology*, *40*(2), 245–250. https://doi.org/10.1016/0016-6480(80)90130-6

Deane, E. E., Kelly, S. P., Collins, P. M., & Woo, N. Y. S. (2003). Larval Development of Silver Sea Bream (Sparus sarba): Ontogeny of RNA-DNA Ratio, GH, IGF-I, and Na+-K+-ATPase. *Marine Biotechnology*, *5*(1), 79–91. https://doi.org/10.1007/s10126-002-0052-7

Debes, P. V., Piavchenko, N., Erkinaro, J., & Primmer, C. R. (2020). Genetic growth potential, rather than phenotypic size, predicts migration phenotype in Atlantic salmon. *Proceedings of the Royal Society B: Biological Sciences*, *287*(1931), 20200867. https://doi.org/10.1098/rspb.2020.0867

Desoutter, M., Quero, J. C., Hureau, J. C., Karrer, C., Post, A., & Saldanha, L. (1990). *Check-list of the fishes of the eastern tropical Atlantic (CLOFETA)*. Soleidae.

Dey, R., Bhattacharya, S., Maitra, S. K., & Banerji, T. K. (2003). The Morpho-anatomy and Histology of the Pineal Complex in a Major Indian Carp, Catla catla: Identification of the Pineal Photoreceptor Cells and Their Responsiveness to Constant Light and Constant Darkness During Different Phases of the Annual Reproductive Cycle. *Endocrine Research*, *29*(4), 429–443. https://doi.org/10.1081/ERC-120026949

Downing, G., & Litvak, M. K. (2002). Effects of light intensity, spectral composition and photoperiod on development and hatching of haddock (Melanogrammus aeglefinus) embryos. *Aquaculture*, *213*(1), 265–278. https://doi.org/10.1016/S0044-8486(02)00090-X

Eid, A. M. S., Ali., B. A., Eldahrawy, A. A., Salama, F., & Abd El-Naby, A. S. (2018). GROWTH PERFORMANCE AND SURVIVAL OF GILTHEAD SEABREAM SPARUS AURATA LARVAE FED ROTIFER AND ARTEMIA. *Egyptian Journal of Nutrition and Feeds*, *21*(3), 899–907. https://doi.org/10.21608/ejnf.2018.75831

Ekström, P., & Meissl, H. (1988). Intracellular staining of physiologically identified photoreceptor cells and hyperpolarizing interneurons in the teleost pineal

organ. *Neuroscience*, *25*(3), 1061–1070. https://doi.org/10.1016/0306-4522(88)90059-0

European Food Safety Authority (EFSA). (2008). Animal welfare aspects of husbandry systems for farmed European seabass and gilthead seabream—Scientific Opinion of the Panel. *EFSA Journal*, *6*(11), 844. https://doi.org/10.2903/j.efsa.2008.844

European Union. (2010). Directive 2010/63/EU of the European Parliament and of the Council of 22 September 2010 on the protection of animals used for scientific purposes. *UE Official Journal*, *OJ L 276*, 33–79.

Falcón, J. (1999). Cellular circadian clocks in the pineal. *Progress in Neurobiology*, *58*(2), 121–162. https://doi.org/10.1016/s0301-0082(98)00078-1

Falcón, J., Besseau, L., Fazzari, D., Attia, J., Gaildrat, P., Beauchaud, M., & Boeuf, G. (2003). Melatonin Modulates Secretion of Growth Hormone and Prolactin by Trout Pituitary Glands and Cells in Culture. *Endocrinology*, *144*(10), 4648–4658. https://doi.org/10.1210/en.2003-0707

Falcón, J., Besseau, L., Magnanou, E., Herrero, M., Nagai, M., & Gilles, B. (2011). Melatonin, the time keeper: Biosynthesis and effects in fish. *Cybium*, *35(1)*.

Falcón, J., Besseau, L., Manganou, E., Sauzet, S., Fuentès, M., & Boeuf, G. (2010). The pineal organ of fish. In *Biological clock in fish*. CRC Press, Boca Raton, FL.

Falcón, J., Besseau, L., Sauzet, S., & Boeuf, G. (2007). Melatonin effects on the hypothalamo-pituitary axis in fish. *Trends in Endocrinology and Metabolism: TEM*, *18*(2), 81–88. https://doi.org/10.1016/j.tem.2007.01.002

Falcón, J., Galarneau, K. M., Weller, J. L., Ron, B., Chen, G., Coon, S. L., & Klein, D. C. (2001). Regulation of Arylalkylamine N-Acetyltransferase-2

(AANAT2, EC 2.3.1.87) in the Fish Pineal Organ: Evidence for a Role of Proteasomal Proteolysis. *Endocrinology*, *142*(5), 1804–1813. https://doi.org/10.1210/endo.142.5.8129

Falcón, J., Gothilf, Y., Coon, S. L., Boeuf, G., & Klein, D. C. (2003). Genetic, Temporal and Developmental Differences Between Melatonin Rhythm Generating Systems in the Teleost Fish Pineal Organ and Retina. *Journal of Neuroendocrinology*, *15*(4), 378–382. https://doi.org/10.1046/j.1365-2826.2003.00993.x

Falcón, J., Migaud, H., Muñoz-Cueto, J. A., & Carrillo, M. (2010). Current knowledge on the melatonin system in teleost fish. *Fish Reproduction*, *165*(3), 469–482. https://doi.org/10.1016/j.ygcen.2009.04.026

Falcón, J., Torriglia, A., Attia, D., Viénot, F., Gronfier, C., Behar-Cohen, F., Martinsons, C., & Hicks, D. (2020). Exposure to Artificial Light at Night and the Consequences for Flora, Fauna, and Ecosystems. *Front Neurosci*, *16*(14), 602796. https://doi.org/10.3389/fnins.2020.602796

FAO. (2022a). THE STATE OF WORLD FISHERIES AND AQUACULTURE 2022. *Towards Blue Transformation*. https://doi.org/10.4060/cc0461en

FAO. (2022b, June 28). *Aquaculture Feed and Fertilizer Resources Information System: Gilthead seabream—Sparus aurata* [Database]. https://www.fao.org/fishery/affris/species-profiles/gilthead-seabream/gilthead-seabream-home/en/

Faustino, M., & Power, D. M. (1998). Development of osteological structures in the sea bream: Vertebral column and caudal fin complex. *Journal of Fish Biology*, *52*(1), 11–22. https://doi.org/10.1111/j.1095-8649.1998.tb01548.x

Faustino, M., & Power, D. M. (2001). Osteologic development of the viscerocranial skeleton in sea bream: Alternative ossification strategies in teleost fish. *Journal of Fish Biology*, *58*(2), 537–572. https://doi.org/10.1111/j.1095-8649.2001.tb02272.x

Fernández, I., Hontoria, F., Ortiz-Delgado, J. B., Kotzamanis, Y., Estévez, A., Zambonino-Infante, J. L., & Gisbert, E. (2008). Larval performance and skeletal deformities in farmed gilthead sea bream (Sparus aurata) fed with graded levels of Vitamin A enriched rotifers (Brachionus plicatilis). *Aquaculture*, *283*(1), 102–115. https://doi.org/10.1016/j.aquaculture.2008.06.037

Fjelldal, P. G., Grotmol, S., Kryvi, H., Gjerdet, N. R., Taranger, G. L., Hansen, T., Porter, M. J. R., & Totland, G. K. (2004). Pinealectomy induces malformation of the spine and reduces the mechanical strength of the vertebrae in Atlantic salmon, Salmo salar. *Journal of Pineal Research*, *36*(2), 132–139. https://doi.org/10.1046/j.1600-079X.2003.00109.x

Fragkoulis, S., Batargias, C., Kolios, P., & Koumoundouros, G. (2018). Genetic parameters of the upper-jaw abnormalities in Gilthead seabream Sparus aurata. *Aquaculture*, *497*, 226–233. https://doi.org/10.1016/j.aquaculture.2018.07.071

Fragkoulis, S., Christou, M., Karo, R., Ritas, C., Tzokas, C., Batargias, C., & Koumoundouros, G. (2017). Scaling of body-shape quality in reared gilthead seabream Sparus aurata L. Consumer preference assessment, wild standard and variability in reared phenotype. *Aquaculture Research*, *48*(5), 2402–2410. https://doi.org/10.1111/are.13076

Fragkoulis, S., Economou, I., Moukas, G., Koumoundouros, G., & Batargias, C. (2020). Caudal fin abnormalities in Gilthead seabream (Sparus aurata L.) have a strong genetic variance component. *Journal of Fish Diseases*, *43*(7), 825–828. https://doi.org/10.1111/jfd.13180

Fragkoulis, S., Kerasovitis, D., Batargias, C., & Koumoundouros, G. (2021). Body-shape trajectories and their genetic variance component in Gilthead seabream (Sparus aurata L.). *Scientific Reports*, *11*(1), 16964. https://doi.org/10.1038/s41598-021-95726-9

Fragkoulis, S., Printzi, A., Geladakis, G., Katribouzas, N., & Koumoundouros, G. (2019). Recovery of haemal lordosis in Gilthead seabream (Sparus aurata L.). *Scientific Reports*, *9*(1), 9832. https://doi.org/10.1038/s41598-019-46334-1

Galeotti, M., Beraldo, P., de Dominis, S., D'Angelo, L., Ballestrazzi, R., Musetti, R., Pizzolito, S., & Pinosa, M. (2000). A preliminary histological and ultrastructural study of opercular anomalies in gilthead sea bream larvae (Sparus aurata). *Fish Physiology and Biochemistry*, *22*(2), 151–157. https://doi.org/10.1023/A:1007883008076

Gavaia, P. j, Sarasquete, C., & Cancela, M. L. (2000). Detection of Mineralized Structures in Early Stages of Development of Marine Teleostei Using a Modified Alcian Blue-Alizarin Red Double Staining Technique for Bone and Cartilage. *Biotechnic & Histochemistry*, *75*(2), 79–84. https://doi.org/10.3109/10520290009064151

Georgakopoulou, E., Katharios, P., Divanach, P., & Koumoundouros, G. (2010). Effect of temperature on the development of skeletal deformities in Gilthead seabream (Sparus aurata Linnaeus, 1758). *Aquaculture*, *308*(1), 13–19. https://doi.org/10.1016/j.aquaculture.2010.08.006

Georgiou, S., Makridis, P., Dimopoulos, D., Power, D. M., Mamuris, Z., & Moutou, K. A. (2014). Myosin light chain 2 isoforms in gilthead sea bream (Sparus aurata L.): Molecular growth markers at early stages. *Aquaculture*, *432*, 434–442. https://doi.org/10.1016/j.aquaculture.2014.04.030

Ginés, R., Afonso, J. M., Argüello, A., Zamorano, M. J., & López, J. L. (2004). The effects of long-day photoperiod on growth, body composition and skin colour in immature gilthead sea bream (Sparus aurata L.). *Aquaculture Research*, *35*(13), 1207–1212. https://doi.org/10.1111/j.1365-2109.2004.01126.x

Gkagkavouzis, K., Karaiskou, N., Katopodi, T., Leonardos, I., Abatzopoulos, T. J., & Triantafyllidis, A. (2019). The genetic population structure and temporal genetic stability of gilthead sea bream Sparus aurata populations in the Aegean and Ionian Seas, using microsatellite DNA markers. *Journal of Fish Biology*, *94*(4), 606–613. https://doi.org/10.1111/jfb.13932

Guerreiro, P. M., Rotllant, J., Fuentes, J., Power, D. M., & Canario, A. V. M. (2006). Cortisol and parathyroid hormone-related peptide are reciprocally modulated by negative feedback. *General and Comparative Endocrinology*, *148*(2), 227–235. https://doi.org/10.1016/j.ygcen.2006.03.004

Guo, H., Ma, Z., Jiang, S., Zhang, D., Zhang, N., & Li, Y. (2014). Length-weight relationship of oval pompano, Trachinotus ovatus (Linnaeus 1758)(Pisces: Carangidae) cultured in open sea floating sea cages in South China Sea. *Indian Journal of Fisheries*, *61*(1), 93–95.

Herrero-Turrion, M. J., Rodriguez, R. E., Aijon, J., & Lara, J. M. (2003). Transient expression pattern of prolactin in Sparus aurata. *Journal of Molecular Endocrinology*, *30*(1), 69–84. https://doi.org/10.1677/jme.0.0300069

Herrero-Turrión, M. J., Rodríguez, R. E., Velasco, A., González-Sarmiento, R., Aijón, J., & Lara, J. M. (2003). Growth hormone expression in ontogenic development in gilthead sea bream. *Cell Tissue Res*, *313*(1), 81–91. https://doi.org/10.1007/s00441-003-0735-z

Huysseune, A. (2000). Chapter 18—Skeletal System. In G. K. Ostrander (Ed.), *The Laboratory Fish* (pp. 307–317). Academic Press. https://doi.org/10.1016/B978-012529650-2/50024-X

Izquierdo, M. S., Scolamacchia, M., Betancor, M., Roo, J., Caballero, M. J., Terova, G., & Witten, P. E. (2013). Effects of dietary DHA and α-tocopherol on bone development, early mineralisation and oxidative stress in Sparus aurata (Linnaeus, 1758) larvae. *Br J Nutr*, *109*(10), 1796–1805. https://doi.org/10.1017/s0007114512003935

Jaillon, O., Aury, J.-M., Brunet, F., Petit, J.-L., Stange-Thomann, N., Mauceli, E., Bouneau, L., Fischer, C., Ozouf-Costaz, C., Bernot, A., Nicaud, S., Jaffe, D., Fisher, S., Lutfalla, G., Dossat, C., Segurens, B., Dasilva, C., Salanoubat, M., Levy, M., … Roest Crollius, H. (2004). Genome duplication in the teleost fish Tetraodon nigroviridis reveals the early vertebrate proto-karyotype. *Nature*, *431*(7011), 946–957. https://doi.org/10.1038/nature03025

Jimenez-Jorge, S., Jimenez-Caliani, A. J., Guerrero, J. M., Naranjo, M. C., Lardone, P. J., Carrillo-Vico, A., Osuna, C., & Molinero, P. (2005). Melatonin synthesis and melatonin-membrane receptor (MT1) expression during rat thymus development: Role of the pineal gland. *Journal of Pineal Research*, *39*(1), 77–83. https://doi.org/10.1111/j.1600-079X.2005.00220.x

Kalamarz, H., Nietrzeba, M., Fuentes, J., Martinez-Rodriguez, G., Mancera, J. M., & Kulczykowska, E. (2009). Melatonin concentrations during larval and

postlarval development of gilthead sea bream Sparus auratus: More than a time-keeping molecule? *Journal of Fish Biology*, *75*(1), 142–155. https://doi.org/10.1111/j.1095-8649.2009.02272.x

Kamacı, H. O., Saka, Ş., & Fırat, K. (2005). The Cleavage and Embryonic Phase of Gilthead Sea Bream (Sparus aurata Linnaeus, 1758) Eggs. *Su Ürünleri Dergisi*, *22*(1), 205–209.

Karaplis, A. C., Luz, A., Glowacki, J., Bronson, R. T., Tybulewicz, V. L., Kronenberg, H. M., & Mulligan, R. C. (1994). Lethal skeletal dysplasia from targeted disruption of the parathyroid hormone-related peptide gene. *Genes & Development*, *8*(3), 277–289. https://doi.org/10.1101/gad.8.3.277

Kazemi, R., Yarmohammadi, M., Hallajian, A., Jalilpour, J., & Esmaeili, F. (2020). Influence of the photoperiod and light intensity on growth performance, Melatonin and Insulin-like growth factors gene expression on Acipenser persicus during the embryonic stage. *IFRO*, *19*(3), 1175–1192.

Keenan, L., Ingleton, P., Danks, J., Morton, J., Brown, B., Canario, A., & Power, D. (1998). Immunoreactive parathyroid hormone-related protein (irPTHrP) and PTHrP gene expression in normal and dystrophic sea bream. *J Endocrinol*, *156*, P10.

Kır, M. (2020). Thermal tolerance and standard metabolic rate of juvenile gilthead seabream (Sparus aurata) acclimated to four temperatures. *Journal of Thermal Biology*, *93*, 102739. https://doi.org/10.1016/j.jtherbio.2020.102739

Koumoundouros, G. (2010). Morpho-anatomical abnormalities in Mediterranean marine aquaculture. *Recent Advances in Aquaculture Research*, *661*(2), 125–148.

Koumoundouros, G., Gagliardi, F., Divanach, P., Boglione, C., Cataudella, S., & Kentouri, M. (1997). Normal and abnormal osteological development of caudal fin in Sparus aurata L. fry. *Aquaculture*, *149*(3), 215–226. https://doi.org/10.1016/S0044-8486(96)01443-3

Koumoundouros, G., Oran, G., Divanach, P., Stefanakis, S., & Kentouri, M. (1997). The opercular complex deformity in intensive gilthead sea bream (Sparus aurata L.) larviculture. Moment of apparition and description. *Aquaculture*, *156*(1), 165–177. https://doi.org/10.1016/S0044-8486(97)89294-0

Kraljević, M., & Dulčić, J. (1997). Age and growth of gilt-head sea bream (Sparus aurata L.) in the Mirna estuary, northern Adriatic. *Fisheries Research*, *31*(3), 249–255. https://doi.org/10.1016/S0165-7836(97)00016-7

Kranenbarg, S., Waarsing, J. H., Muller, M., Weinans, H., & van Leeuwen, J. L. (2005). Lordotic vertebrae in sea bass (Dicentrarchus labrax L.) are adapted to increased loads. *Journal of Biomechanics*, *38*(6), 1239–1246. https://doi.org/10.1016/j.jbiomech.2004.06.011

Kwong, R. W. M., & Perry, S. F. (2015). An Essential Role for Parathyroid Hormone in Gill Formation and Differentiation of Ion-Transporting Cells in Developing Zebrafish. *Endocrinology*, *156*(7), 2384–2394. https://doi.org/10.1210/en.2014-1968

Laird, L. M. (2001). Mariculture Overview. In J. H. Steele (Ed.), *Encyclopedia of Ocean Sciences* (pp. 1572–1577). Academic Press. https://doi.org/10.1006/rwos.2001.0474

Lee, N. K., Sowa, H., Hinoi, E., Ferron, M., Ahn, J. D., Confavreux, C., Dacquin, R., Mee, P. J., McKee, M. D., Jung, D. Y., Zhang, Z., Kim, J. K., Mauvais-Jarvis, F., Ducy, P., & Karsenty, G. (2007). Endocrine regulation of energy

metabolism by the skeleton. *Cell*, *130*(3), 456–469. PubMed. https://doi.org/10.1016/j.cell.2007.05.047

Li, Y., Zhou, F., Ma, Z., Huang, J., Jiang, S., Yang, Q., Li, T., & Qin, J. G. (2016). Length-weight relationship and condition factor of giant tiger shrimp, Penaeus monodon (Fabricius, 1798) from four breeding families. *SpringerPlus*, *5*(1), 1279. https://doi.org/10.1186/s40064-016-2979-6

Loizides, M., Georgiou, A. N., Somarakis, S., Witten, P. E., & Koumoundouros, G. (2014). A new type of lordosis and vertebral body compression in Gilthead sea bream, Sparus aurata L.: Aetiology, anatomy and consequences for survival. *Journal of Fish Diseases*, *37*(11), 949–957. https://doi.org/10.1111/jfd.12189

López-Olmeda, J. F., Bayarri, M. J., Rol de Lama, M. A., Madrid, J. A., & Sánchez-Vázquez, F. J. (2006). Effects of melatonin administration on oxidative stress and daily locomotor activity patterns in goldfish. *Journal of Physiology and Biochemistry*, *62*(1), 17–25. https://doi.org/10.1007/BF03165802

Lorenzo-Felipe, Á., Shin, H. S., León-Bernabeu, S., Pérez-García, C., Zamorano, M. J., Pérez-Sánchez, J., & Afonso-López, J. M. (2021). The Effect of the Deformity Genetic Background of the Breeders on the Spawning Quality of Gilthead Seabream (Sparus aurata L.). *Frontiers in Marine Science*, *8*. https://www.frontiersin.org/articles/10.3389/fmars.2021.656901

Loukovitis, D., Sarropoulou, E., Vogiatzi, E., Tsigenopoulos, C. S., Kotoulas, G., Magoulas, A., & Chatziplis, D. (2012). Genetic variation in farmed populations of the gilthead sea bream Sparus aurata in Greece using microsatellite DNA markers. *Aquaculture Research*, *43*(2), 239–246. https://doi.org/10.1111/j.1365-2109.2011.02821.x

Lupatsch, I. (2004). Gilthead seabream. *Aqua Feeds: Formulation and Beyond*, *1*, 16–18.

Mabrouk, H., & Nour, A. al-Aziz. (2011). Effect of Reducing Water Salinity on Survival, Growth performance, chemical composition and nutrients gain of Gilthead Sea bream (Sparus aurata) larvae. *Journal of King Abdulaziz University: Marine Sciences*, *22*(1), 15–29.

Mahamid, J., Sharir, A., Addadi, L., & Weiner, S. (2008). Amorphous calcium phosphate is a major component of the forming fin bones of zebrafish: Indications for an amorphous precursor phase. *Proceedings of the National Academy of Sciences*, *105*(35), 12748–12753. https://doi.org/10.1073/pnas.0803354105

Manchado, M., Planas, J. V., Cousin, X., Rebordinos, L., & Claros, M. G. (2016). 8—Current status in other finfish species: Description of current genomic resources for the gilthead seabream (Sparus aurata) and soles (Solea senegalensis and Solea solea). In S. MacKenzie & S. Jentoft (Eds.), *Genomics in Aquaculture* (pp. 195–221). Academic Press. https://doi.org/10.1016/B978-0-12-801418-9.00008-1

Maria, S., Samsonraj, R. M., Munmun, F., Glas, J., Silvestros, M., Kotlarczyk, M. P., Rylands, R., Dudakovic, A., van Wijnen, A. J., Enderby, L. T., Lassila, H., Dodda, B., Davis, V. L., Balk, J., Burow, M., Bunnell, B. A., & Witt-Enderby, P. A. (2018). Biological effects of melatonin on osteoblast/osteoclast cocultures, bone, and quality of life: Implications of a role for MT2 melatonin receptors, MEK1/2, and MEK5 in melatonin-mediated osteoblastogenesis. *Journal of Pineal Research*, *64*(3), 10.1111/jpi.12465. PubMed. https://doi.org/10.1111/jpi.12465

Maroso, F., Gkagkavouzis, K., De Innocentiis, S., Hillen, J., do Prado, F., Karaiskou, N., Taggart, J. B., Carr, A., Nielsen, E., Triantafyllidis, A., & Bargelloni, L. (2021). Genome-wide analysis clarifies the population genetic structure of wild gilthead sea bream (Sparus aurata). *PloS One*, *16*(1), e0236230. https://doi.org/10.1371/journal.pone.0236230

Masayuki ligo, Ritsuko Ohtani-Kaneko, Masayuki Hara, Kazuaki Hirata, & Katsumi Aida. (1997). Melatonin Binding Sites in the Goldfish Retina. *Zoological Science*, *14*(4), 601–607. https://doi.org/10.2108/zsj.14.601

Mehanna, S. F. (2007). A Preliminary Assessment and Management of Gilthead Bream Sparus aurata in the Port Said Fishery, the Southeastern Mediterranean, Egypt. *Turkish Journal of Fisheries and Aquatic Sciences*, *7*, 123–130.

Mhalhel, K., Germanà, A., Abbate, F., Guerrera, M. C., Levanti, M., Laurà, R., & Montalbano, G. (2020). The Effect of Orally Supplemented Melatonin on Larval Performance and Skeletal Deformities in Farmed Gilthead Seabream (Sparus aurata). *International Journal of Molecular Sciences*, *21*(24). https://doi.org/10.3390/ijms21249597

Mongile, F., Bonaldo, A., Fontanillas, R., Mariani, L., Badiani, A., Bonvini, E., & Parma, L. (2014). Effects of Dietary Lipid Level on Growth and Feed Utilisation of Gilthead Seabream (Sparus Aurata L.) Reared at Mediterranean Summer Temperature. *Italian Journal of Animal Science*, *13*(1), 2999. https://doi.org/10.4081/ijas.2014.2999

Moretti, A., Pedini Fernandez-Criado, M., Cittolin, G., & Guidastri, R. (1999). *Manual on Hatchery Production of Seabass and Gilthead Seabream* (Vol. 1). FAO.

Mylonas, C. C., Zohar, Y., Pankhurst, N., & Kagaw, H. (2011). Reproduction and Broodstock Management. In *Sparidae, Biology and Aquaculture of Gilthead Sea Bream and other Species* (pp. 95–131). https://onlinelibrary.wiley.com/doi/abs/10.1002/9781444392210.ch4

Ndiaye, W., Khady, D., Ousseynou, S., Papa, N., & Jacques, P. (2015). The Length-Weight Relationship and Condition Factor of white grouper (Epinephelus aeneus, Geoffroy Saint Hilaire, 1817) at the south-west coast of Senegal, West Africa. *International Journal of Advanced Research*, *3*.

Negrín-Báez, D., Navarro, A., Lee-Montero, I., Soula, M., Afonso, J. M., & Zamorano, M. J. (2015). Inheritance of skeletal deformities in gilthead seabream (Sparus aurata)—Lack of operculum, lordosis, vertebral fusion and LSK complex. *Journal of Animal Science*, *93*(1), 53–61. https://doi.org/10.2527/jas.2014-7968

NFISS. (2022). *FishStatJ- Software for Fishery and Aquaculture Statistical Time Series* (v4.02.06) [Windows]. FAO. https://www.fao.org/fishery/en/statistics/software/fishstatj/en

Nie, Z., Wu, H., Wei, J., Zhang, X. D., & Ma, Z. (2013). Length-weight relationship and morphological studies in the Kashgarian loach Triplophysa yarkandensis (Day, 1877) from the Tarim River, Tarim River Basin, North-West China. *Indian Journal of Fisheries*, *60*.

Noble, C., Cañon Jones, H. A., Damsgård, B., Flood, M. J., Midling, K. Ø., Roque, A., Sæther, B.-S., & Cottee, S. Y. (2012). Injuries and deformities in fish: Their potential impacts upon aquacultural production and welfare. *Fish Physiology and Biochemistry*, *38*(1), 61–83. https://doi.org/10.1007/s10695-011-9557-1

Ortiz-Delgado, J. B., Fernández, I., Sarasquete, C., & Gisbert, E. (2014). Normal and histopathological organization of the opercular bone and vertebrae in gilthead sea bream Sparus aurata. *Aquatic Biology*, *21*(1), 67–84.

Papandroulakis, N., Divanach, P., & Kentouri, M. (2002). Enhanced biological performance of intensive sea bream (Sparus aurata) larviculture in the presence of phytoplankton with long photophase. *Aquaculture*, *204*(1), 45–63. https://doi.org/10.1016/S0044-8486(01)00643-3

Patruno, M., Radaelli, G., Mascarello, F., & Candia Carnevali, M. D. (1998). Muscle growth in response to changing demands of functions in the teleost Sparus aurata (L.) during development from hatching to juvenile. *Anatomy and Embryology*, *198*(6), 487–504. https://doi.org/10.1007/s004290050199

Pauletto, M., Manousaki, T., Ferraresso, S., Babbucci, M., Tsakogiannis, A., Louro, B., Vitulo, N., Quoc, V. H., Carraro, R., Bertotto, D., Franch, R., Maroso, F., Aslam, M. L., Sonesson, A. K., Simionati, B., Malacrida, G., Cestaro, A., Caberlotto, S., Sarropoulou, E., … Bargelloni, L. (2018). Genomic analysis of Sparus aurata reveals the evolutionary dynamics of sex-biased genes in a sequential hermaphrodite fish. *Communications Biology*, *1*(1), 119. https://doi.org/10.1038/s42003-018-0122-7

Pavlidis, M. A., & Mylonas, C. C. (2011). *Sparidae: Biology and Aquaculture of Gilthead Sea Bream and Other Species* (1st edition). Wiley-Blackwell.

Peruzzi, S., Westgaard, J.-I., & Chatain, B. (2007). Genetic investigation of swimbladder inflation anomalies in the European sea bass, Dicentrarchus labrax L. *Aquaculture*, *265*(1), 102–108. https://doi.org/10.1016/j.aquaculture.2006.10.029

Pita, C., Gamito, S., & Erzini, K. (2002). Feeding habits of the gilthead seabream (Sparus aurata) from the Ria Formosa (southern Portugal) as compared to the black seabream (Spondyliosoma cantharus) and the annular seabream (Diplodus annularis). *Journal of Applied Ichthyology*, *18*(2), 81–86. https://doi.org/10.1046/j.1439-0426.2002.00336.x

Porter, M. J. R., Randall, C. F., Bromage, N. R., & Thorpe, J. E. (1998). The role of melatonin and the pineal gland on development and smoltification of Atlantic salmon (Salmo salar) parr. *Aquaculture*, *168*(1), 139–155. https://doi.org/10.1016/S0044-8486(98)00345-7

Prestinicola, L., Boglione, C., Makridis, P., Spanò, A., Rimatori, V., Palamara, E., Scardi, M., & Cataudella, S. (2013). Environmental Conditioning of Skeletal Anomalies Typology and Frequency in Gilthead Seabream (Sparus aurata L., 1758) Juveniles. *PLOS ONE*, *8*(2), e55736. https://doi.org/10.1371/journal.pone.0055736

Riedel, R., Caskey, L. M., & Hurlbert, S. H. (2007). Length-weight relations and growth rates of dominant fishes of the Salton Sea: Implications for predation by fish-eating birds. *Lake and Reservoir Management*, *23*(5), 528–535. https://doi.org/10.1080/07438140709354036

Roo, J., Hernandez-Cruz, M. C., Socorro, J. A., Fernández-Palacios, H., & Izquierdo, M. S. (2005). *Development of skeletal deformities in Gilthead sea bream (Sparus aurata) reared under different larval culture and dietary conditions*. Larva 2005. Fish and Shellfis Larviculture Symposium., University of Ghent, Belgium. https://doi.org/10.13140/2.1.4093.6960

Roo, J., Socorro, J., & Izquierdo, M. S. (2010). Effect of rearing techniques on skeletal deformities and osteological development in red porgy Pagrus pagrus

(Linnaeus, 1758) larvae. *Journal of Applied Ichthyology*, *26*(2), 372–376. https://doi.org/10.1111/j.1439-0426.2010.01437.x

Rossi, A. R., Perrone, E., & Sola, L. (2006). Genetic structure of gilthead seabream, Sparus aurata, in the Central Mediterranean Sea. *Central European Journal of Biology*, *1*(4), 636–647. https://doi.org/10.2478/s11535-006-0041-3

Roth, J. A., Kim, B. G., Lin, W. L., & Cho, M. I. (1999). Melatonin promotes osteoblast differentiation and bone formation. *The Journal of Biological Chemistry*, *274*(31), 22041–22047. https://doi.org/10.1074/jbc.274.31.22041

Rowlerson, A., Mascarello, F., Radaelli, G., & Veggetti, A. (1995). Differentiation and growth of muscle in the fish Sparus aurata (L): II. Hyperplastic and hypertrophic growth of lateral muscle from hatching to adult. *Journal of Muscle Research & Cell Motility*, *16*(3), 223–236.

Rubio, V. C., Sánchez-Vázquez, F. J., & Madrid, J. A. (2004). Oral administration of melatonin reduces food intake and modifies macronutrient selection in European sea bass (Dicentrarchus labrax, L.). *Journal of Pineal Research*, *37*(1), 42–47. https://doi.org/10.1111/j.1600-079X.2004.00134.x

Ruiz, J. M. A. L. and D. M. V. and L. E. R. R. and N. A. and M. S. I. L. and R. G. (2000). Association of a lordosis-scoliosis-kyphosis deformity in gilthead seabream (Sparus aurata) with family structure. In *Fish Physiology and Biochemistry* (Vol. 22). 0920-1742.

Sadek, S., Osman, M. F., & Mansour, M. A. (2004). Growth, Survival and Feed Conversion Rates of Sea Bream (Sparus aurata) Cultured in Earthen Brackish Water Ponds Fed Different Feed Types. *Aquaculture International*, *12*(4), 409–421. https://doi.org/10.1023/B:AQUI.0000042131.29346.93

Saka, Şahin, Çoban, D., Kamacı, H. O., Süzer, C., & Fırat, K. (2008). Early Development of Cephalic Skeleton in Hatchery-Reared Gilthead Seabream, Sparus aurata. *Turkish Journal of Fisheries and Aquatic Sciences*, *8*, 341–345.

Sánchez-Vázquez, F. J., López-Olmeda, J. F., Vera, L. M., Migaud, H., López-Patiño, M. A., & Míguez, J. M. (2019). Environmental Cycles, Melatonin, and Circadian Control of Stress Response in Fish. *Frontiers in Endocrinology*, *10*, 279. https://doi.org/10.3389/fendo.2019.00279

Sangun, L., Akamca, E., & Akar, M. A. (2007). Weight-Length Relationships for 39 Fish Species from the North-Eastern Mediterranean Coast of Turkey. *Turkish Journal of Fisheries and Aquatic Sciences*, *7*, 37–40.

Sankian, Z., Khosravi, S., Kim, Y.-O., & Lee, S.-M. (2017). Effect of dietary protein and lipid level on growth, feed utilization, and muscle composition in golden mandarin fish Siniperca scherzeri. *Fisheries and Aquatic Sciences*, *20*(1), 7. https://doi.org/10.1186/s41240-017-0053-0

Sfakianakis, D. G., Katharios, P., Tsirigotakis, N., Doxa, C. K., & Kentouri, M. (2013). Lateral line deformities in wild and farmed sea bass (Dicentrarchus labrax, L.) and sea bream (Sparus aurata, L.). *Journal of Applied Ichthyology*, *29*(5), 1015–1021. https://doi.org/10.1111/jai.12248

Shahar, R., & Dean, M. N. (2013). The enigmas of bone without osteocytes. *BoneKEy Reports*, *2*, 343. https://doi.org/10.1038/bonekey.2013.77

Shanqi, F., Miho, K., Yoko, U., Sei, K., Daichi, H., Yuji, S., Asami, T., Takashi, N., Yusuke, M., Mika, I., Atsuhiko, H., Satoshi, K., & Takako, H. (2019). Circadian production of melatonin in cartilage modifies rhythmic gene

expression. *Journal of Endocrinology*, *241*(2), 161–173. https://doi.org/10.1530/JOE-19-0022

Simonneaux, V., & Ribelayga, C. (2003). Generation of the Melatonin Endocrine Message in Mammals: A Review of the Complex Regulation of Melatonin Synthesis by Norepinephrine, Peptides, and Other Pineal Transmitters. *Pharmacological Reviews*, *55*(2), 325. https://doi.org/10.1124/pr.55.2.2

Sola, L., Moretti, A., Crosetti, D., Karaiskou, N., Magoulas, A., Rossi, A. R., Rye, M., Triantafyllidis, A., & Tsigenopoulos, C. S. (2007). Gilthead seabream—Sparus aurata. *Genetic Impact of Aquaculture Activities on Native Populations*, 47.

Sun, T., Li, J., Xing, H. L., Tao, Z. S., & Yang, M. (2020). Melatonin improves the osseointegration of hydroxyapatite-coated titanium implants in senile female rats. *Zeitschrift Für Gerontologie Und Geriatrie*, *53*(8), 770–777.

Taheri, P., Mogheiseh, A., Shojaee Tabrizi, A., Nazifi, S., Salavati, S., & Koohi, F. (2019). Changes in thyroid hormones, leptin, ghrelin and, galanin following oral melatonin administration in intact and castrated dogs: A preliminary study. *BMC Veterinary Research*, *15*(1), 145. https://doi.org/10.1186/s12917-019-1894-9

Taylor, J. F., North, B. P., Porter, M. J. R., Bromage, N. R., & Migaud, H. (2006). Photoperiod can be used to enhance growth and improve feeding efficiency in farmed rainbow trout, Oncorhynchus mykiss. *Aquaculture*, *256*(1), 216–234. https://doi.org/10.1016/j.aquaculture.2006.02.027

Tevfik, C., Okan, A., & Mustafa, E. (2009). Length-Weight Relationships of Fishes from Gökova Bay, Turkey (Aegean Sea). *Turkish Journal of Zoology*, *33*(1), 69–72. https://doi.org/10.3906/zoo-0802-9

The European Commission. (2014). *AquaTrace species leaflet: Gilthead sea bream (sparus auarata)*. Joint Research Centre of the European Commission: AquaTrace. https://fishreg.jrc.ec.europa.eu/web/aquatrace/leaflets/gilthead

Thorland, I., Papaioannou, N., Kottaras, L., Refstie, T., Papasolomontos, S., & Rye, M. (2007). Family based selection for production traits in gilthead seabream (Sparus aurata) and European sea bass (Dicentrarchus labrax) in Greece. *Supplement: Genetics in Aquaculture IX*, *272*, S314. https://doi.org/10.1016/j.aquaculture.2007.07.193

Thuong, N. P., Verstraeten, B., Kegel, B. D., Christiaens, J., Wolf, T. D., Sorgeloos, P., Bonte, D., & Adriaens, D. (2017). Ontogenesis of opercular deformities in gilthead sea bream Sparus aurata: A histological description. *Journal of Fish Biology*, *91*(5), 1419–1434. https://doi.org/10.1111/jfb.13460

Tordjman, S., Chokron, S., Delorme, R., Charrier, A., Bellissant, E., Jaafari, N., & Fougerou, C. (2017). Melatonin: Pharmacology, Functions and Therapeutic Benefits. *Current Neuropharmacology*, *15*(3), 434–443. PubMed. https://doi.org/10.2174/1570159X14666161228122115

Torno, C., Staats, S., Fickler, A., de Pascual-Teresa, S., Soledad Izquierdo, M., Rimbach, G., & Schulz, C. (2019). Combined effects of nutritional, biochemical and environmental stimuli on growth performance and fatty acid composition of gilthead sea bream (Sparus aurata). *PloS One*, *14*(5), e0216611. https://doi.org/10.1371/journal.pone.0216611

Tsakogiannis, A., Manousaki, T., Lagnel, J., Papanikolaou, N., Papandroulakis, N., Mylonas, C. C., & Tsigenopoulos, C. S. (2019). The Gene Toolkit Implicated in Functional Sex in Sparidae Hermaphrodites: Inferences From Comparative

Transcriptomics. *Frontiers in Genetics*, *9*, 749. https://pubmed.ncbi.nlm.nih.gov/30713551/

Vardar, H., & Yildirim, Ş. (2012). Effects of Long-term Extended Photoperiod on Somatic Growth and Husbandry Parameters on Cultured Gilthead Seabream (Sparus aurata, L.) in the Net Cages. *Turkish Journal of Fisheries and Aquatic Sciences*, *12*, 225–231. https://doi.org/10.4194/1303-2712-v12_2_05

Velarde, E., Cerdá-Reverter, J. M., Alonso-Gómez, A. L., Sánchez, E., Isorna, E., & Delgado, M. J. (2010). Melatonin-synthesizing enzymes in pineal, retina, liver, and gut of the goldfish (Carassius): MRNA expression pattern and regulation of daily rhythms by lighting conditions. *Chronobiology International*, *27*(6), 1178–1201. https://doi.org/10.3109/07420528.2010.496911

Verhaegen, Y., Adriaens, D., Wolf, T. D., Dhert, P., & Sorgeloos, P. (2007). Deformities in larval gilthead sea bream (Sparus aurata): A qualitative and quantitative analysis using geometric morphometrics. *Larvi 2005*, *268*(1), 156–168. https://doi.org/10.1016/j.aquaculture.2007.04.037

Villamizar, N., Blanco-Vives, B., Migaud, H., Davie, A., Carboni, S., & Sánchez-Vázquez, F. J. (2011). Effects of light during early larval development of some aquacultured teleosts: A review. *Aquaculture*, *315*(1), 86–94. https://doi.org/10.1016/j.aquaculture.2010.10.036

Villamizar, N., García-Alcazar, A., & Sánchez-Vázquez, F. J. (2009). Effect of light spectrum and photoperiod on the growth, development and survival of European sea bass (Dicentrarchus labrax) larvae. *Aquaculture*, *292*(1), 80–86. https://doi.org/10.1016/j.aquaculture.2009.03.045

Walker, M. B., & Kimmel, C. B. (2007). A two-color acid-free cartilage and bone stain for zebrafish larvae. *Biotechnic & Histochemistry : Official Publication of the Biological Stain Commission*, *82*(1), 23–28. https://doi.org/10.1080/10520290701333558

Wang, T., Wang, H.-S., Sun, G.-W., Huang, D., & Shen, J.-H. (2012). Length–weight and length–length relationships for some Yangtze River fishes in Tian-e-zhou Oxbow, China. *Journal of Applied Ichthyology*, *28*(4), 660–662. https://doi.org/10.1111/j.1439-0426.2012.01971.x

Webster, C. D., & Lim, C. E. (2002). *Nutrient Requirements and Feeding of Finfish for Aquaculture* (First). CABI.

Wood, A., Duan, C., & Bern, H. (2005). Insulin-Like Growth Factor Signaling in Fish. *International Review of Cytology*, *243*, 215. https://doi.org/10.1016/S0074-7696(05)43004-1

Wright, M. L., Cuthbert, K. L., Donohue, M. J., Solano, S. D., & Proctor, K. L. (2000). Direct influence of melatonin on the thyroid and comparison with prolactin. *The Journal of Experimental Zoology*, *286*(6), 625–631. https://doi.org/10.1002/(sici)1097-010x(20000501)286:6<625::aid-jez9>3.0.co;2-q

YAMANO, K. (2005). The Role of Thyroid Hormone in Fish Development with Reference to Aquaculture. *Japan Agricultural Research Quarterly: JARQ*, *39*(3), 161–168. https://doi.org/10.6090/jarq.39.161

Ye, J., Coulouris, G., Zaretskaya, I., Cutcutache, I., Rozen, S., & Madden, T. L. (2012). Primer-BLAST: a tool to design target-specific primers for polymerase chain reaction. *BMC Bioinformatics*, *13*, 134. https://doi.org/10.1186/1471-2105-13-134

Ytteborg, E., Baeverfjord, G., Torgersen, J., Hjelde, K., & Takle, H. (2010). Molecular pathology of vertebral deformities in hyperthermic Atlantic salmon (Salmo salar). *BMC Physiology*, *10*(1), 12. https://doi.org/10.1186/1472-6793-10-12

Yúfera, M., Halm, S., Beltran, S., Fusté, B., Planas, J. V., & Martínez-Rodríguez, G. (2012). Transcriptomic characterization of the larval stage in gilthead seabream (Sparus aurata) by 454 pyrosequencing. *Marine Biotechnology (New York, N.Y.)*, *14*(4), 423–435. https://doi.org/10.1007/s10126-011-9422-3

Zachmann, A., ALI, M., & FALCON, J. (1992). *MELATONIN AND ITS EFFECTS IN FISHES - AN OVERVIEW* (M. Ali, Ed.; WOS:A1992BX69B00012; Vol. 236, pp. 149–165).

Zarantoniello, M., Bortoletti, M., Olivotto, I., Ratti, S., Poltronieri, C., Negrato, E., Caberlotto, S., Radaelli, G., & Bertotto, D. (2021). Salinity, Temperature and Ammonia Acute Stress Response in Seabream (Sparus aurata) Juveniles: A Multidisciplinary Study. *Animals : An Open Access Journal from MDPI*, *11*(1). https://doi.org/10.3390/ani11010097

Zhu, G., Ma, B., Dong, P., Shang, J., Gu, X., & Zi, Y. (2020). Melatonin promotes osteoblastic differentiation and regulates PDGF/AKT signaling pathway. *Cell Biol Int*, *44*(2), 402–411. https://doi.org/10.1002/cbin.11240

Zilberman-Peled, B., Appelbaum, L., Vallone, D., Foulkes, N. S., Anava, S., Anzulovich, A., Coon, S. L., Klein, D. C., Falcón, J., Ron, B., & Gothilf, Y. (2007). Transcriptional regulation of arylalkylamine-N-acetyltransferase-2 gene in the pineal gland of the gilthead seabream. *Journal of*

Neuroendocrinology, *19*(1), 46–53. https://doi.org/10.1111/j.1365-2826.2006.01501.x

Zohar, Y., Abraham, M., & Gordin, H. (1978). The gonadal cycle of the captivity-reared hermaphroditic teleost Sparus aurata (L.) during the first two years of life. *Annales de Biologie Animale Biochimie Biophysique*, *18*(4), 877–882.

Appendice

International Journal of
Molecular Sciences

MDPI

Article

The Effect of Orally Supplemented Melatonin on Larval Performance and Skeletal Deformities in Farmed Gilthead Seabream (*Sparus aurata*)

Kamel Mhalhel *, Antonino Germanà, Francesco Abbate, Maria Cristina Guerrera, Maria Levanti, Rosaria Laurà and Giuseppe Montalbano *

Zebrafish Neuromorphology Lab, Department of Veterinary Sciences, University of Messina, 98168 Messina, Italy; agermana@unime.it (A.G.); abbatef@unime.it (F.A.); mcguerrera@unime.it (M.C.G.); mblevanti@unime.it (M.L.); laurar@unime.it (R.L.)

* Correspondence: kmhalhel@unime.it (K.M.); gmontalbano@unime.it (G.M.); Tel.: +39-379-104-7406 (K.M.); +39-090-676-6822 (G.M.)

Received: 27 November 2020; Accepted: 13 December 2020; Published: 16 December 2020

check for updates

Abstract: The gilthead seabream larval rearing in continuous light is common in most Mediterranean hatcheries to stimulate larval length growth and increase food consumption. Several studies have shown that continuous light affects larval development and increases the prevalence of skeletal deformities. Melatonin is a crucial pineal neurohormone that displays daily secretion patterns, stimulates cell proliferation and embryonic development in Atlantic salmon and zebrafish, and improves osseointegration in mice and humans. However, no studies have examined the effects of orally supplemented melatonin on skeletal deformities in *Sparus aurata* larvae. We administered exogenous melatonin to gilthead seabream larvae via enriched rotifers and nauplii of Artemia. Exogenous melatonin induced bone deformities and stimulated parathyroid hormone-related protein-coding gene (*PTHrP*) mRNA expression. In addition to the melatonin-induced *PTHrP* high expression level, the recorded non coordinated function of skeletal muscle and bone during growth can be the fountainhead of bone deformities. Both myosin light chain 2 (*mlc2*) and bone gamma-carboxyglutamate protein-coding gene (*bglap*) expression levels were significantly affected by melatonin administration in an inverse dose–response manner during the exogenous melatonin administration. This is the first study to report the effect of inducing melatonin bone deformities on *Sparus aurata* larvae reared under ordinary hatchery conditions.

Keywords: melatonin; opercular complex; bone deformity; growth; *Sparus aurata*; *PTHrP*; *mlc2*; *bglap*

1. Introduction

The presence of morphological abnormalities in farmed gilthead seabream (*Sparus aurata*) is a major problem for current aquaculture as it entails significant economic losses [1–3]. Skeletal deformities are the most relevant deformities, and they include head and vertebral column anomalies. Opercular complex abnormalities are the most frequent skeletal anomalies in this species, with an incidence of 80% [2–4]. As the opercular complex's function is the water ventilation and the gill's protection, opercular deformities indirectly cause gill diseases by a lowered resistance to environmental stress [5]. Therefore, exposed gills can decrease respiratory efficiency, as well as reduce market value [2,5]. To improve the profitability of rearing gilthead seabream of commercial size, a rapid and early recognition of anomalies' development is of prime importance for aquaculturists. A wide range of physical, chemical, and biological factors can cause skeletal deformities in farmed fish. Some authors have correlated the opercular deformities with a defect of inflation of the swim bladder [6], others have

attributed it to a dietary deficiency of vitamins, amino acids [7]; or the rearing conditions (density, salinity, temperature, oxygenation, brightness) [8]. Additionally, according to some studies, heritability is central to the etiology of operculum complex anomalies [3]. Opercular complex deformities are induced during the embryonic and post-embryonic periods of life, long before osteological deformities are externally visible, and its development is still not well understood [9,10]. The larval rearing of gilthead seabream in continuous light is a common practice in the majority of Mediterranean hatcheries. Indeed, several studies have shown that continuous light accelerates the depletion of yolk sac reserves, stimulates larval length growth, and increases food consumption by around 40% [11]. However, several other studies have shown that continuous light affects larval development and increases the prevalence of skeletal deformities [12]. The circadian rhythm alternation has a major role in synchronizing daily behavioral processes in fish (locomotor activity, sedation, food intake, shoaling behavior), skin pigmentation, oxygen consumption, thermoregulation, and melatonin synthesis [13]. In fish, as in mammals, melatonin is the output signal of the circadian clock, a crucial hormone produced by the pineal gland that displays daily and seasonal patterns of secretion with a peak level during the dark-phase and basal level during the photo-phase [14]. The synthesis of melatonin also occurs in the retina. Retinal melatonin acts as a local neuromodulator within the eye, and it could be metabolized in situ, which prevents retinal melatonin from being released into the blood [14]. In addition, mRNA transcripts of melatonin synthesis enzymes have been reported in the digestive tracts of several teleosts with daily rhythms that adjust to the prevalent photoperiod [13–16]. The involvement of melatonin in larval development and growth has been demonstrated by several in vivo and in vitro studies [17–22] showing that melatonin stimulates cell proliferation and embryonic development in a dose-dependent manner in zebrafish [17,18]. Moreover, melatonin has several functions related to vertebral bone growth in Atlantic salmon [19], promotes osteoblastic differentiation in mice, human mesenchymal stem cells (MSC)/peripheral blood mononuclear cells and MC3T3-E1 cells by increased messenger RNA levels of osteogenic markers and improved osseointegration in mice [20–22]. In gilthead seabream larvae, melatonin production begins immediately after hatching to reach maximum levels between the 6th and 10th day after hatching [23]. At this time, levels of hormones involved in growth, metabolism and development, i.e., growth hormone and prolactin, are very low [24,25]. Additionally, it has been demonstrated that the number of growth hormone cells and growth hormone mRNA expression does not increase until 30 days post hatching [26]. When growth hormone and prolactin supply is still insufficient, melatonin may play a role in stimulation of cell proliferation and differentiation processes, as it has been postulated in zebrafish *Danio rerio* [18]. In light of all these bibliographic data, we thought that the inhibition of melatonin by continuous light, especially during the first days after hatching, increases the prevalence of skeletal deformities (especially operculum deformities) and alter larvae growth and development. To our knowledge, no study has been conducted on the effect of exogenous melatonin intake on the gilthead seabream skeletogenesis. Therefore, in the present study we evaluated the effect of an exogenous melatonin supplementation on skeletal deformities (especially the opercular complex abnormalities) and larval performance of gilthead seabream.

2. Results

2.1. Effect of Orally Supplemented Melatonin on Growth Rate

At 13 days post hatching (DPH), we did not record statistically significant differences between the three larvae groups for both length and weight (Figures 1 and 2). At 23 DPH, the highest length was recorded in the Ctrl group (0.614 ± 0.0155 cm) which was statistically different only from MEL1 (Mann–Whitney U test, $p < 0.05$) (Figure 1). The growth in weight showed the same growth pattern in length and no statistically significant differences between all the experimental groups of larvae was recorded (Mann–Whitney U test, $p < 0.05$) (Figure 2). At 33 DPH, the Ctrl group showed the highest ponderal growth, while the MEL1 registered the lowest weight value. A significant difference between

Ctrl and both treated groups for the weight was discerned (Mann–Whitney U test, $p < 0.05$) (Figure 1). However, those differences were absent for the growth in length (Figure 1). At 43 DPH, the length showed a statistically significant difference only between Ctrl and MEL1 (Mann–Whitney U test, $p < 0.05$). MEL2 displayed the highest growth in weight (0.0179 ± 0.001148 g), while MEL1 registered the lowest value. We noted statistically significant differences between the three groups of larvae for growth in weight (Mann–Whitney U test, $p < 0.05$) (Figure 2). At 53 DPH, the larvae of MEL2 group showed the highest length (2.17 ± 0.0163 cm), while MEL1 group larvae showed the lowest growth in length among the three groups of larvae (Figure 1). At this age, the weight distribution between the three groups corresponded well to the growth in length. The differences between the three groups for both weight and length were statistically significant (Mann–Whitney U test, $p < 0.05$) (Figures 1 and 2). Ten days later, the larval growth in MEL1 exceeded that in Ctrl but was lower than that of MEL2 (Mann–Whitney U test, $p < 0.05$). At 73 DPH, the length in MEL1 continued to increase and reached 4.06 ± 0.0224 cm while in the Ctrl and MEL2 groups it did not exceed, respectively, 3.380 ± 0.0197 cm and 3.295 ± 0.197 cm (Figure 1). The length crest in MEL1 went with a weight crest of 1.021 ± 0.0196 g, which was 44.47%, and 50.66% higher, respectively, than that of the Ctrl group and MEL2 group (Mann–Whitney U test, $p < 0.05$). At the end of the experience, MEL1 and MEL2 larvae showed almost the same growth rate (4.48 cm/1.323 g–4.47 cm/1.342 g) and were statistically 6.40% longer and 22.38% heavier than that of the Ctrl group (Mann–Whitney U test, $p < 0.05$) (Figures 1 and 2).

The length–weight relationship expressed by the equation $W = aL^b$ was calculated in the three groups from the natural logarithmic equivalent $\log W = b \log L + \log a$. The regression equation for Ctrl, MEL1, and MEL2 groups was, respectively, $\log W = 3.055 \log L - 4.383$, $\log W = 1.087 \log L - 1.18$, $\log W = 0.954 \log L - 0.992$. In both groups supplemented with melatonin, the b values ($b_{MEL1} = 1.087$, $b_{MEL2} = 0.954$) were inferior to three, which means that larvae fed with the different levels of melatonin gained less weight than the cube of its length, reflecting a negative allometric growth pattern and larvae were slimmer with increasing length. On the other hand, Ctrl group larvae showed a positive allometric growth pattern with a b value of 3.05, which means that while weight was still progressing, gains in length stopped.

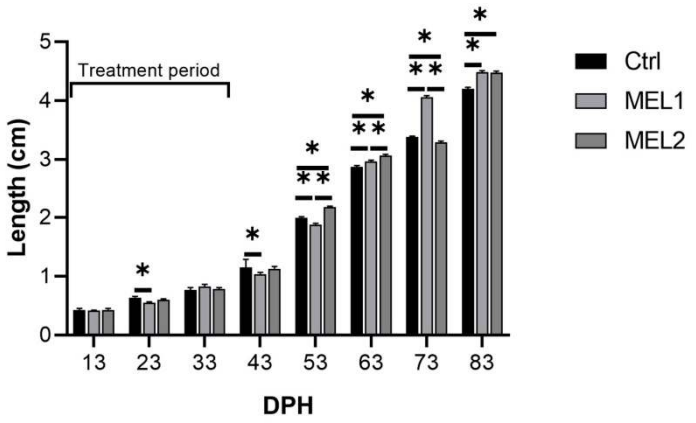

Figure 1. Total length variation in gilthead seabream larvae fed with rotifers (*Brachionus picatilis)* and Artemia (*Artemia salina*) enriched with two graded levels of melatonin (MEL1 and MEL2) (treatment period: from 3 to 38 days post hatching (DPH)). Data are expressed as mean ± SEM. Asterisks indicate significant differences between treatment and control groups (Mann–Whitney U test, $p < 0.05$).

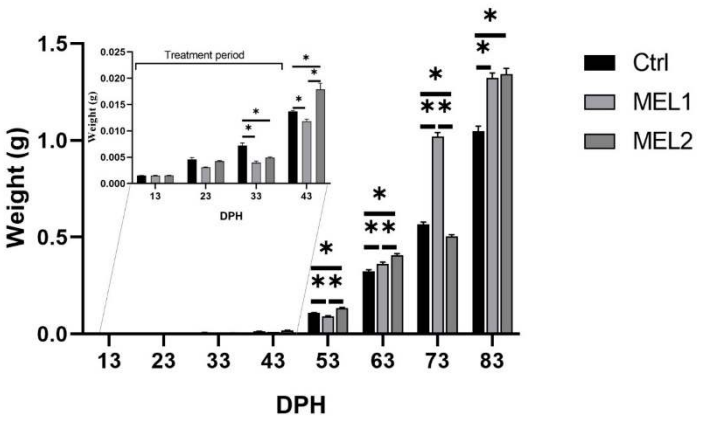

Figure 2. Weight variation in gilthead seabream larvae fed with (*Brachionus picatilis)* and Artemia (*Artemia salina*) enriched with two graded levels of melatonin (MEL1 and MEL2) (treatment period: from 3 to 38 DPH). Data are expressed as mean ± SEM. Asterisks indicate significant differences between treatment and control groups (Mann–Whitney U test, $p < 0.05$).

2.2. *Effect of Exogenous Melatonin on Insulin-Like Growth Factor 1 Concentration*

The insulin-like growth factor 1 (IGF-1) concentration on gilthead seabream larvae fed with a graded level of MEL is shown in Figure 3. The bell-shaped histogram manifested peaks at 43 DPH, after which the IGF-1 rate dropped. At 23, 33, and 43 DPH, MEL2 larvae showed a higher concentration on IGF-1 than the Ctrl group. Still, that difference was statically significant only at 23 and 43 DPH (Mann–Whitney U test, $p < 0.05$). Additionally, MEL1 larvae showed a higher IGF-1 concentration than that of Ctrl group at 23 and 43 DPH but the differences were statically not significant. After the late metamorphosis (43 DPH), there were no statistically significant differences between the three experimental groups for the IGF-1 level (Mann–Whitney U test, $p < 0.05$).

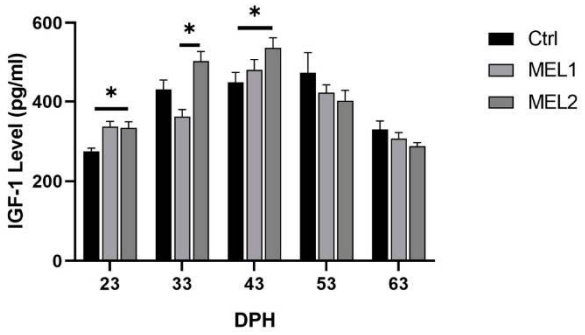

Figure 3. Insulin-like growth factor 1 (IGF-1) level of gilthead seabream larvae fed with rotifers (*Brachionus picatilis)* and Artemia (*Artemia salina*) enriched with two graded levels of melatonin (MEL1 and MEL2). Data are expressed as mean ± SD. Asterisks indicate significant differences between treatment and control groups (Mann–Whitney U test, $p < 0.05$).

2.3. Effects of Melatonin Oral Supplementation on the Ossification Pattern

The ossification state in cultured gilthead seabream larvae was studied using acid-free double staining. Figure 4 shows the chronology of the ossification in Ctrl, MEL1, and MEL2 larvae. Until 33 DPH, the double staining solution reveals only cartilaginous structures such as coraco scapular cartilage, branchiostegal rays, dentary, maxillary, premaxillary, rostral cartilage, lamina precerebralis, sclerotic, and epiphysial tectum in the cranial region (Figure 4a,d,g). On the vertebral column, we identified 23 neural arches and three epurals beside three parapophyses, 13 hemal arches, and five hypural cartilages (Figure 4a,d,g). At 43 DPH, all cartilaginous structures gained volume, and the ossification process was initiated in the dentary, maxillary, opercular complex on the head region (Figure 4b,e,h). A saltatory ossification process was initiated on the vertebral column on centra 1 to 4, 8 to 10, and 14 to 19 (Figure 4b,e,h). The peroration of ossification process occurred at 53 DPH when alizarin red staining had ascendancy over the larva (Figure 4c,f,i). Under the present experimental conditions, the same ossification patterns were observed between the three groups of larvae (Ctrl, MEL1, and MEL2), a continuous process (from 43 to 53 DPH) with the same ossification rate (Figure 4).

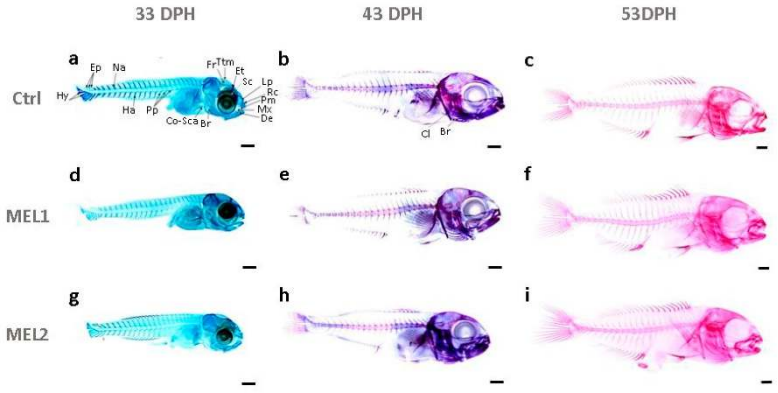

Figure 4. The ossification state in gilthead seabream larvae of Ctrl at 33 DPH (**a**), at 43 DPH (**b**), at 53 DPH (**c**); of MEL1 at 33 DPH (**d**), at 43 DPH (**e**), at 53 DPH (**f**); of MEL2 at 33 DPH (**g**), at 43 DPH (**h**), at 53 DPH (**i**). Double stained larvae showed alician blue-stained cartilaginous structures and alizarin red-stained bony structures. Br, branchiostegal rays; Cl, cleithrum; Co-Sc, coraco scapular cartilage; De, dentary; Ep, epural; Et, epiphysial tectum; Ha, hemal arches; Hy, hypural; Lp, lamina precerebralis; Mx, maxillary; Na, neural arches; Pm, premaxillary; Pp, parapophyse; Rc, rostral cartilage; Sc, sclerotic; Tmp, taenia marginalis posterior. Scale bar:0.5 mm.

2.4. Opercular Complex Deformity: Gross Anatomy

Since 53 DPH, larvae were completely ossified in Ctrl, MEL1, and MEL2, all forms of operculum complex anomalies at this stage were definitive. Figure 5 shows some forms of operculum complex deformities recorded in 53 DPH larvae from the three experimental groups. Opercular complex anomalies were registered as various gill cover irregularities and different degrees of gill chamber exposure. Those abnormalities can be the result of a reduction (Figure 5a,e,i), folding (Figure 5d,h,l), or both reduction and folding (Figure 5b,c,f,g,j,k) of one or more bones composing the opercular complex. The wide variability of malformation typologies arose in this study, and their severity did not allow the definition of accurate, specific patterns of the opercular complex deformities. Additionally, no type of abnormality was defined as group-specific.

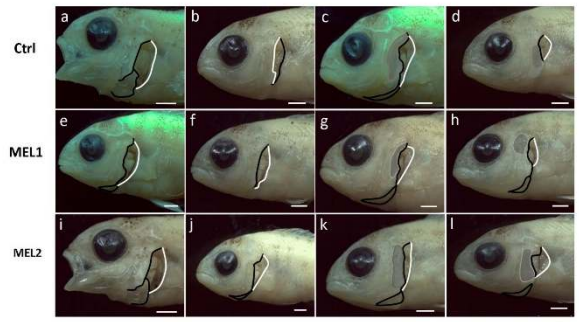

Figure 5. Some forms of opercular complex anomalies registered in Ctrl (**a**–**d**), in MEL1 (**e**–**h**), and in MEL2 (**i**–**l**) gilthead seabream larvae of 53 DPH. (**a**,**e**,**i**) Severe reduction in gills cover (opercle, subopercle, and interopercle); (**b**,**f**,**j**) severe reduction in gills cover (opercle and subopercle); (**c**,**g**,**k**) folded opercle upper corner and reduced subopercle and opercle lower corner; (**d**,**h**,**l**) folded gills cover leading to gills exposition. Black lines indicate the loose edge of the operculum and branchiestegal rays while white lines mark the limits of the normal pattern of the branchial chamber. Grey-shaded areas indicate folded bones. Scale bar: 1mm.

The incidence of opercular complex deformities and the nature of this disorder as being unilateral or bilateral in the treated larvae of gilthead seabream are shown in Figure 6. The incidence of the opercular complex deformities in larvae fed the lower dose of MEL was significantly higher than those observed in the control group larvae (Chi-square test, $p < 0.05$) at 53, 63, and 83 DPH. Still, at 73 DPH, this difference was not statistically significant. Regarding the incidence of opercular complex deformities between MEL2 larvae and Ctrl group larvae, there was no significant statistical difference (Chi-square test, $p < 0.05$) at 53, 63, and 73 DPH, but there was at 83 DPH. In all groups, the anomalies were mostly unilateral (65.6 to 100% of cases) and (in some cases) were bilateral.

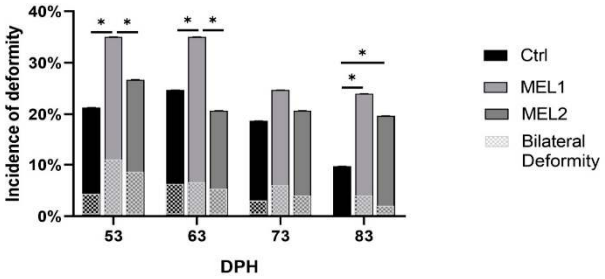

Figure 6. Incidence of opercular complex deformities on gilthead seabream larvae fed with rotifers (*Brachionus picatilis)* and Artemia (*Artemia salina*) enriched with two levels of melatonin (MEL1 and MEL2). Asterisks indicate significant differences between the three experimental groups of larvae (Chi-square test, $p < 0.05$).

2.5. Opercular Complex Anomalies under Scanning Electron Microscope

SEM observation provided a better perception and understanding of different forms of opercular complex deformity compared to stereomicroscope observation. The detected opercular complex anomalies involved the different opercular bones (opercle, subopercle, interopercle, and preopercle)

and branchiostegal rays and membrane. The protective wall for the orobranchial chamber can be reduced in different levels, with references to a reduction or even lack of various bones of the operculum series (Figure 7a,b). Other types of anomalies are attributed to inside or outside folding of one or more opercular bones (Figure 7c,d) or a combined shortened-folded operculum (Figure 7g). Additionally, wave-like (Figure 7e) and spring-like (Figure 7f) gill cavers have been observed for the first time in some gilthead seabream larvae. We report, for the first time, the lack of apposition of the branchiostegal membrane to the epithelium at the terminal edge of the branchial cavity resulting from different degrees of hyperplasia (Figure 7h) and folded branchiostegal rays in the gill chamber (Figure 7i).

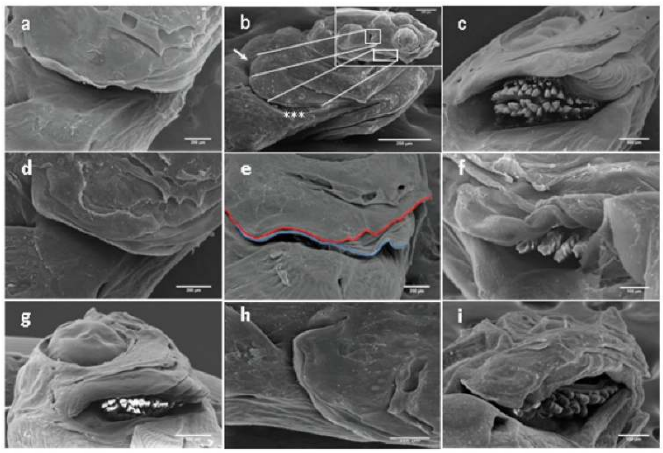

Figure 7. Gilthead seabream larvae aged 13-53 DPH. Different forms of abnormalities in the opercular complex. (**a**) Hypoplastic operculum, (**b**) reduced opercle (white arrows) and lack of interopercle (asterisks), (**c**) folded opercular bones toward the gills chamber leading to exposed gill arches, (**d**) outside folded operculum, (**e**) wave-like gill caver (red line) modulating a branchiostegal membrane (blue line), (**f**) spring-like gill caver with exposed gill arches, (**g**) combined shortened-folded operculum, (**h**) hyperplastic branchiostegal membrane, (**i**) folded branchiostegal rays in the gill chamber. Scale bars: 200 µm.

2.6. Skeletal Deformities

The early detection of skeletal deformities in cultured gilthead seabream larvae was studied using acid-free double staining (Figure 8).

The observation of double-stained larvae under a stereomicroscope revealed many typologies of bone deformities (Figure 8). Detected deformities affected meristic and threshold traits of the vertebral column (vertebrae, neural and hemal spin) and caudal fin complex. The vertebral column conserved its normal curvature (no lordose or kyphotiose cases were recorded), its meristics characteristics, and it was composed of 24 vertebrae in all larvae from the three experimental groups. However, several malformations affected vertebrae, and we retrieved a rectangular slender vertebral body (Figure 8a), cubic thick vertebral body (Figure 8b), and triangular-shaped vertebrae (Figure 8c). Neural and hemal spine also presented abnormalities such as: bifurcated neural spine (Figure 8a,d) and detached neural and hemal spine (Figure 8c,e). Skeletal deformities were also detected in the caudal portion, such as the absence of one or all of the three epurals (Figure 8c,f), and the lack, or fusion of hypural (Figure 8c). In many cases, we recorded multiple deformities in the same sample (Figure 8a).

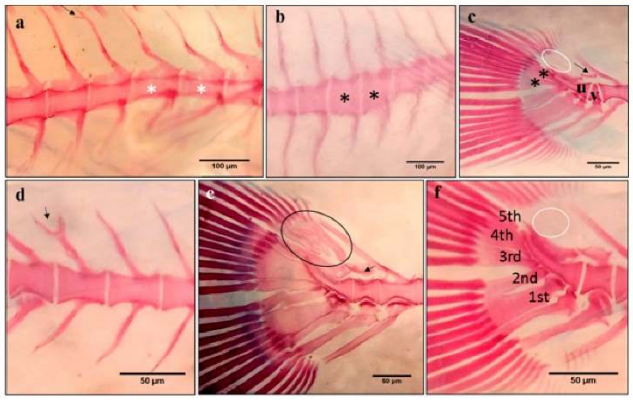

Figure 8. Representative forms of skeleton anomalies in gilthead seabream larvae from the different experimental groups at 53 DPH. (**a**) Rectangular slender vertebral body (white asterisks) and bifurcated neural spine (arrow), (**b**) cubic thick vertebral body (black asterisks), (**c**) last caudal vertebrae (v) preceding urostyle (u) is triangular shaped with detached neural spine (arrow) and the absence of the three epurals (white circle), lack of the fifth hypural and fusion of the third and fourth hypural (black asteriks), (**d**) bifurcated neural spine (black arrow), (**e**) detached neural spine (arrow). The circle indicates normal epural arrangement, (**f**) normal hypural arrangment (1st to 5th hypurals) and absence of the three epurals (white circle). Scale bars (**a**,**b**): 100 µm. Scale bars (**c**–**f**): 50 µm.

The typology and incidence of skeletal abnormalities in gilthead seabream larvae fed with different levels of melatonin are shown in Table 1. Out of a total of 90 samples in each group (30 per each sampling point: 33, 43 and 53 DPH), 76 (84.4%), 83 (92.2%), and 87 (96.7%) from the Ctrl, MEL1, and MEL2 groups, respectively, showed at least one type of deformity, and we have recorded a significant statistical difference between the above-mentioned frequencies of Ctrl and MEL2 groups. Deformities affecting the caudal fin complex were the most common abnormalities encountered with 45.6% in Ctrl larvae, 62.2% in MEL1 group, and 77.8% in MEL2 larvae. The statistical difference between aforementioned frequencies was significant. The frequency of larvae with at least one vertebral anomaly was 23.3% in Ctrl and MEL2 groups and 28.9% in MEL1. No statistically significant difference was registered between the different groups. We have registered an incidence of hemal and neural spine deformities of 61.1%, 63.3%, and 55.6%, respectively, in Ctrl, MEL1, and MEL2 groups, and no statistically significant difference was registered between the different groups.

Table 1. The incidence of bone anomalies on gilthead seabream larvae of the three experimental groups.

	Ctrl	Mel1	MEL2
Total abnormalities	84.4%a	92.2%ab	96.7%b
Vertebral abnormalities	23.3%	28.9%	23.3%
Hemal and neural spine abnormalities	61.1%	63.3%	55.6%
Caudal portion abnormalities	45.6%a	62.2%b	77.8%c

Different letters within the same row show statistically significant differences (Chi-square test, $p < 0.05$).

2.7. *Effects of Exogenous Melatonin on Gene Expression*

Melatonin was administrated in two doses MEL1 and MEL2, for gilthead seabream larvae to study the response at the transcriptional level in osteogenesis and growth. Tissue-specific genes for bone—bone gamma-carboxyglutamate protein-coding gene (*bglap*), and parathyroid hormone-related

protein-coding gene (*PTHrP*)—and for skeletal muscle—myosin light chain 2 (*mlc2*)—were analyzed. In most sampling points, the expression of both *bglap* and *PTHrP* was significantly affected by melatonin administration. Considerable variability in *bglap* transcript abundance was detected between treated groups, and between Ctrl and MEL2 as well, while the differences between Ctrl and MEL1 were statistically non-significant (Figure 9). Despite the significantly decreased expression of *bglap* over larval development, the expression pattern was conserved in all treatment groups of each sampling point, even after the end of melatonin administration (by starting weaning larvae onto dry pellets).

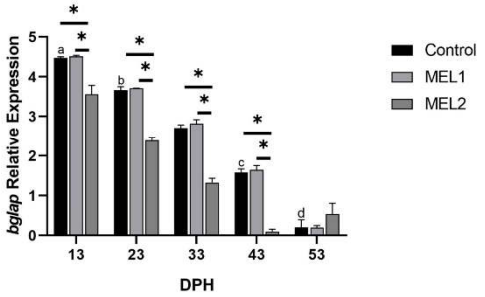

Figure 9. Gene expression of bone gamma-carboxyglutamate protein-coding gene (*bglap*) components in response to MEL administration in bone. Gene expression values are expressed as arbitrary units (a.u) for elongation factor 1-alpha (*ef1α*). Data are expressed as mean ± SD. Different letters indicate statistically significant differences throughout time within groups and asterisks indicate significant differences between groups for each treatment group (Welch test, $p < 0.05$).

Unlike *bglap*, *PTHrP* showed an increasing expression over time. Furthermore, a dose–response relationship between melatonin concentration and *PTHrP* transcriptional level was recorded during the first 33 DPH (Figure 10). During the experimental period, when the melatonin was administrated via live feeds, the *PTHrP* transcriptional levels in MEL1 were comparable to those in Ctrl group. However, the transcriptional levels of the gene mentioned above in MEL2 samples showed a statistically significant difference compared to those in the Ctrl group at 13 and 23 DPH, which decreased by the end of melatonin treatment period (37 DPH) and ended by being compared to those of Ctrl samples.

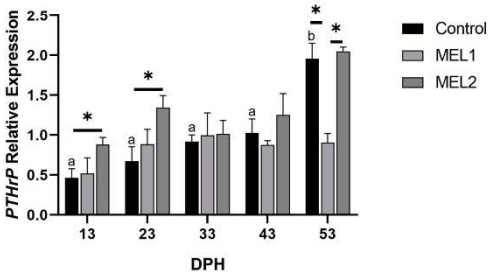

Figure 10. Gene expression of parathyroid hormone-related protein-coding gene (*PTHrP*) components in response to MEL administration in bone. Gene expression values are expressed as arbitrary units (a.u) for elongation factor 1-alpha (*ef1α*). Data are expressed as mean±SD. Different letters indicate statistically significant differences throughout time within groups and asterisks indicate significant differences between groups at each sampling point (Welch test, $p < 0.05$).

As with *bglap* and *PTHrP*, *mlc2* showed considerable variability between control and treated groups. However, *mlc2* expression was significantly affected by melatonin administration in an inverse dose–response manner during the exogenous melatonin administration (Figure 11). At 43 DPH, an abrupt recovery of *mlc2* expression on treated groups temper the expression pattern in favor of a dose–response relationship with exogenous melatonin.

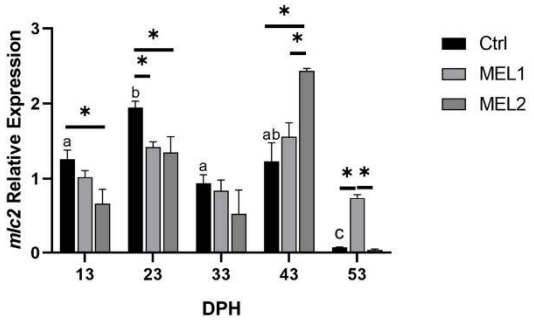

Figure 11. Gene expression of *mlc2* components in response to MEL administration in bone. Gene expression values are expressed as arbitrary units (a.u) for elongation factor 1-alpha (*ef1α*). Data are expressed as mean ± SD. Different letters indicate statistically significant differences throughout time within groups and asterisks indicate significant differences between groups for each treatment group (Welch test, $p < 0.05$).

3. Discussion

Skeletal abnormalities and growth rates in gilthead seabream have been the subject of many research studies. Some authors have correlated the skeletal deformity with a defect of inflation of the swim bladder [6], others have attributed it to a dietary deficiency of vitamins [7], and fatty acids [27] as well as to the larval rearing systems [28], and rearing condition [8]. Additionally, the capacity of melatonin to induce embryonic development in zebrafish [17,18], and to control several functions related to bone growth in Atlantic salmon [19], was proved. In human adult mesenchymal stem cells/peripheral blood monocytes cocultures, MEL was able to induce osteoblastogenesis and suppress osteoclastogenesis by the effect of osteoblast-derived osteoblastic inhibitory lectin or by increasing osteoprotegerin and, receptor activator of nuclear factor-kB ligand ratios [20]. In mice osteoblast precursor cells (MC3T3-E1) as well, MEL induced osteoblast differentiation and bone formation by upregulating the gene expression of BMP2, BMP6, osteocalcin, and osteoprotegerin [21]. However, no study has evaluated exogenous melatonin effects on gilthead seabream skeletogenesis and growth during larval development. In the present study, the three groups of larvae (control group and two groups treated with different concentrations of melatonin) were placed under common hatchery conditions in continuous light to investigate the melatonin effect on skeletal abnormalities and growth rate in gilthead seabream. In teleosts, the melatonin synthesis reported on the pineal gland and gut has daily rhythms that adjust to the relevant photoperiod [14–16]. Additionally, the retinal melatonin acts as a local neuromodulator, and it is metabolized in situ. In light of this, we can gather that all the differences observed between the control and the two treatment groups of larvae maintained under continuous light were only due to the exogenous MEL incorporated into the commercial preparation of enrichment. The main finding from this study is the capacity of exogenous melatonin to affect gilthead seabream larval performance and the incidence of skeletal deformities. Thus, exogenous MEL affected normal skeletogenesis and caused bone deformities. Operculum complex and caudal fin complex were the most influenced structures. In gilthead seabream and many other species, operculum complex deformities

are frequent [9,29–32]. The frequency of opercular anomalies on Ctrl groups (9.7 and 21.3%) was in the range of 6.3 to 43.2% as registered in previous studies conducted over the past two decades [9,30]. However, this represents almost a quarter of what was recorded in older studies [32]. Those differences may be attributed to the different rearing systems and conditions [9,28] and the acquisition of new knowledge in aquaculture. Additionally, the lower concentration of MEL affected the incidence of opercular complex deformities, while MEL2 did not. In fact, larvae fed with the lowest concentration showed the highest incidence of opercular complex deformities among the three groups. In agreement with Ortiz-Delgado et al. [9] and Berlado et al. [30], the deformities were mostly unilateral in all three groups (65 to 100% of cases). The wide variability of operculum deformity typologies, including the new forms registered in this study, hampered the establishment of specific patterns of deformities, like those defined by Berlado et al. [30]. In our study, the first sign of opercular complex alteration was detected on 13 DPH larvae, a long time before the ossification process took place, and earlier than that recorded by Galeotti et al. [29]. The exogenous melatonin concentrations increased caudal fin complex abnormalities in a dose-dependent manner. However, the control group had a frequency of 45.6% lower than 47.9% and 48.5% recorded in previous studies [33,34]. Additionally, the total frequency of individuals affected by at least one anomaly in the Ctrl group was 84.4%, which was lower than the 87% registered earlier [34]. The increased frequency of opercular complex, caudal fin complex, and total deformities might be a result of melatonin-induced osteoblasts accelerated differentiation already demonstrated on mice and human MSC/PBMC cells and MC3T3-E1 cells [20,21]. During teleost embryogenesis, cartilaginous structures are the first element of the skeleton to form, which becomes bone after mineralization [29,35,36]. The current study demonstrated that this pattern of development was valid for gilthead seabream larvae in which all skeletal elements remained cartilaginous until 43 DPH. Under the present experimental conditions, the same developmental patterns were observed between the three groups of larvae (Ctrl group, MEL1, and MEL2). The skeleton ontogenesis in the three groups of larvae revealed a priority to the onset of the elements which serve in feeding and respiration mechanisms (Maxillary, Meckel's cartilage, cartilaginous branchial arches). These results agreed with those of earlier published studies [37,38]. Literature data on gilthead seabream meristic counts reported 24 vertebrae, 13 hemal arches, 23 neural arches, 4 pairs of parapophyses on the vertebral column region and 5 hypurals, 1 parahypural arch, 3 epurals on the caudal fin complex region beside all structures composing the cephalic skeleton [34,35,38]. In this study, the three experimental groups mostly conserved the meristics recorded in previous studies [34,35,38]. Exogenous MEL affected larval growth in length and weight in a dose-dependent manner. Indeed, MEL2 can ensure higher growth rates than those of the MEL1 and Ctrl groups. Additionally, both concentrations were in favor of a negative allometric growth pattern, which means that larvae were slimmer with increasing length. At 63 DPH, the Ctrl group had higher growth rates than those recorded in the previous studies [7,39]. The promising values recorded on the Ctrl group (high growth, the absence of lordotic kyphotic spine curve, and the lower opercular complex deformities), compared to the result already published for this species [9,30,33,35], indicated that the rearing conditions applied in the hatchery were optimal compared to those employed in the above-mentioned studies. IGF-1 has been associated with metabolism [40] and growth [41]. In some teleost species, tissue levels of its mRNA positively correlate with body growth rate [42]. Nevertheless, during this study, while the weight and total length continued to increase with age, the IGF-1 level increased until 43 DPH (shortly after the end of exogenous melatonin administration), after which it decreased. This variability registered during the first period (from 13 to 43 DPH) is in favor of an evident influence on IGF-1 production by the exogenous melatonin administration. In the present study, we investigated as well the exogenous melatonin-induced gene responses in skeletal muscle and bone tissue during the larval stage. The marker of muscle development and growth—myosin light chain 2 (*mlc2*)—one of the four light chains of the myosine, exerts its regulatory role binding calcium [43]. *bglap* is secreted by osteoblasts during bone formation and represents up to 1–2% of the total bone protein with a strong affinity for calcium [44]. *PTHrP* is a calcium regulatory factor in gilthead seabream, has a

crucial function in several physiological and biochemical processes including cortisol production [45], tissue differentiation and proliferation [46], calcium mobilization from internal sources (bone and scales) and via calcium uptake from water and diet [47]. The lethal deletion of this gene on mice proves its crucial physiological functions [48]. The dose–response relationship between *PTHrP* expression level and melatonin concentration registered at least during the treatment period (MEL1 and MEL2) contradicts the negative correlation of those two parameters stipulated by Abbink et al. [49]. Indeed, another study on primary BALB/c mouse chondrocytes [50] supports our finding about melatonin's capacity to upregulate *PTHrP* expression. Additionally, an association between abnormally developing bones and a high expression of *PTHrP* on *Sparus aurata* was already described [51]. In light of the aforesaid findings, we can assign the bone deformities registered in the treated groups to PTHrP expression product, which was induced by the orally supplemented melatonin. Myosin, a major component of striated muscle contributing to muscle contraction, is consisted of two heavy chains (MHCs) and four light chains (MLCs). Myosin light chain-2 is a sarcomeric protein which exists in white muscle of gilthead seabream as two isoforms *mlc*2a and *mlc*2b. Myosin light chain 2a predominates the early larval stages marking new fiber formation at the tissue level. In our study, the inverse dose-dependent relationship of *mlc2* expression levels and exogenous melatonin concentration was in accordance with the negative allometric growth pattern induced by melatonin, which means that larvae were slimmer with increasing length.

4. Materials and Methods

4.1. Larval Rearing

The experiment was conducted at the facilities of the hatchery AQUACULTURE TUNISIENNE at Sousse (Tunisia), according to the Guidelines on the Handling and Training of Laboratory Animals by the Universities Federation for Animal Welfare (UFAW). The experimental protocol was in accordance with the principles outlined in the declaration of Helsinki, and was approved by the local ethics committee (Identification code: 1400192; date of approval: 4 April 2017). Gilthead seabream larvae were raised under standard hatchery conditions in 2.5 m^3 cylindroconical tanks (initial density of 120 larvae/L). Daily water renewal in the rearing tank was 3–15%/h with gentle and continuous aeration. The light intensity at water surface was 150 lux and the temperature was 20–21 °C. Rotifers *Brachionus picatilis* were cultured and enriched with green algae and added to tanks daily as an early live food from 3 to 25 DPH. *Artemia salina* nauplii were introduced from 26 to 38 DPH. One day before being fed to the larvae, rotifers and metanauplii were enriched with a commercial emulsion for enrichment Red Pepper (Bern Aqua, Olen, Belgium) with phytoproteins and highly unsaturated fatty acids. At 38 days, larvae were weaned onto dry pellets.

4.2. Experimental Design

The studies were carried out on 2400 gilthead seabream larvae, which were randomly divided after hatching into three groups of 800 larvae per group placed under ordinary hatchery conditions: a control group (Ctrl), and two melatonin-treated groups (MEL1) and (MEL2). The exogenous supply of melatonin was ensured via rotifers and nauplii of Artemia from 3 to 38 DPH. Rotifers and Artemia were enriched with 0.04 g/kg (MEL1) or 0.2 g/kg (MEL2) of neurohormone added in an ethanol solution to the commercial emulsion for enrichment. The choice of both concentrations was made considering the fact that no studies on melatonin administration have shown an LD50 (lethal dose for 50% of the subjects) [52], and considering as well the range of previously tested doses with positive responsiveness in other species of teleost [53–55]. The lipophilic nature of melatonin facilitates its solubility in this lipid emulsion. The experiment was performed in triplicate. Sampling was performed every ten days from 13 to 83 days post hatching (DPH) from each experimental group and larvae were sacrificed with an overdose of tricaine methane sulfonate (MS222); 1000–10,000 mg L^{-1}.

4.3. Sampling

At each sampling point (from 13 to 83 DPH), 100 larvae per experimental group were collected for analyzing opercular complex abnormalities by stereomicroscope or scanning electron microscopy (SEM) for the smaller larvae (15 larvae of 13–53 DPH), the total length and weight measurement. Thirty larvae from those already investigated for operculum complex anomalies were double stained with alcian blue and alizarin red acid-free staining solution. For gene expression analyses, total RNA was extracted from pools of gilthead seabream larvae (5 to 20 individuals per tank depending on fish size).

4.4. Morphological Studies

At each sampling point, the study of operculum complex anomalies was performed using Leica M205C stereomicroscope (Leica, Milan, Italy) or scanning electron microscope Zeiss EVO LS 10 (Carl Zeiss NTS, Oberkochen, Germany) for the smaller larvae (larvae of 13-53 DPH: 15 larvae). Additionally, the total length was measured using a digital camera Leica IC80 HD (Leica, Milan, Italy) mounted on a stereo-microscope (Leica, Milan, Italy) and weight was determined with the analytical scale KERN 770 (KERN & Sohn, Balingen, Germany).

4.4.1. Scanning Electron Microscopy

The samples were fixed in 2.5% glutaraldehyde in Sörensen phosphate buffer 0.1 M. After several rinsing steps in the same buffer, they were dehydrated in a graded alcohols series, critical-point dried in a Balzers CPD 030 (BAL-TEC AG, Balzers, Liechtenstein), sputter coated with 3 nm gold in a SCD 050 sample coater (BAL-TEC AG, Balzers, Liechtenstein) and examined under a Zeiss EVO LS 10 (Carl Zeiss NTS, Oberkochen, Germany) as described by Abbate et al. [56].

4.4.2. Acid-Free Double Staining

The double staining procedure was performed according to an adjusted protocol of Walker and Kimmel [57]. Acid-free double staining solution was made in two parts. The first part for cartilage staining was done by adding together 0.2% alcian blue 8 GX (C.I. 58,005 from Sigma, St. Louis, MO, USA) in 70% ethanol, and 100 mM MgCl2 (for mucosubstances differentiation by competition with alician blue for the negative charges of acidic mucopolysaccharides). The second part for bone staining was 0.5% alizarin red S (C.I. 74,240 from Sigma, St. Louis, MO, USA). The final acid-free staining solution contained 10 mL of the first part and 100 µL of the second. Larvae of 23, 33, 43 and 53 DPH were fixed for 2 h in 4% paraphormaldehyde in phosphate buffered saline (PBS). After washing, larvae were dehydrated with 1 mL ethanol 50%, at room temperature for 10 min. After removing the ethanol, specimens were transferred directly to the acid-free double stain solution, and rocked at room temperature overnight to incorporate the stain adequately. Next, pigmentation was removed at room temperature for 20 min with a bleach solution made of 1.5% H_2o_2 and 1% KOH. Clearing was achieved by transferring specimens in 20% glycerol and 0.25% KOH solution overnight after which the solution was replaced with 50% glycerol and 0.25% KOH solution (overnight). Larvae were viewed and photographed with M205C stereomicroscope (Leica, Milan, Italy) in the same solution.

4.5. IGF-1 Quantification

IGF-1 quantification was performed using tissue homogenates (25% *w/v*) made from 40–55 larvae in each experimental group. The tissue homogenates were prepared in 0.05 mol/L phosphate buffered saline, pH 7.4 with the use of a knife homogenizer (Polytron) at 4 °C. Homogenates were centrifuged at 16,000× g for 20 min at 4 °C. Supernatant (tissue extract) was used for assays.

The quantification of IGF-1 in larvae was performed using Fish IGF-1 ELISA kit (catalog Num. CSB-E12122Fh, Cusabio Biotech, Wuhan, China) according to the manufacturer's instructions. The assay employs the competitive inhibition enzyme immunoassay technique. The microtiter plate provided

in the kit was pre-coated with goat-anti-rabbit antibody. Standards and samples were added to the appropriate microtiter plate wells with an antibody specific for IGF-1- and horseradish peroxidase (HRP)-conjugated IGF-1. The competitive inhibition reaction is launched between HRP-labeled IGF-1 and unlabeled IGF-1 with the antibody. A substrate solution was added to the wells and the colorimetric reaction developed by negative correlation with the amount of IGF-1 in the sample. The color development was stopped and the intensity of the color was measured.

4.6. Gene Expression Analyses

Gene expression analyses were carried out in compliance with the minimum information for publication of quantitative real-time pcr experiments, MIQE guidelines [58]. Total RNA was extracted from pools of gilthead seabream larvae (5 to 20 individuals per sample time and tank depending on fish size), in which head regions were taken off and muscle/bone tissues were separated, using the TRIzol reagent (Invitrogen, Carlsbad, CA, USA); then, 2 µg of total RNA was reverse transcribed into cDNA using the High-Capacity cDNA Archive Kit (Applied Biosystems, Foster City, CA, USA). The mRNA levels of bone-specific genes, bone gamma-carboxyglutamate protein-coding gene (*bglap*), parathyroid hormone-related protein-coding gene (*PTHrP*) and skeletal muscle specific gene, myosin light chain 2 (*mlc2*), were analyzed by qPCR using a SYBR® Premix DimerEraser™ (Perfect Real Time) (Cat. #RR091A, TAKARA BIO INC, Otsu, Shinga, Japan). The primers were designed based on the published gilthead seabream mRNA sequences for the genes analyzed. Table 2 lists the GenBank accession numbers and primer sequences. Reactions were performed in triplicate using a 7500 PCR real-time system (Applied Biosystems). The results were calculated using the 2-ΔΔCt algorithm against elongation factor 1 alpha (*ef1α*) and expressed as the n-fold difference compared to an arbitrary calibrator, chosen as a higher value than ΔΔCts. Cycling parameters were as follows: 95 °C for 10 min, (95 °C for 15 s, Ta for 30 s, 72 °C for 40 s) (40 cycles), 95 °C for 15 s at the end of the amplification phase.

Table 2. Primers used for real-time quantitative PCR. F, Forward primer, R, reverse primer; Tm, annealing temperature.

Gene	Primer Sequences (5′-3′)	Tm°C	Accession Number
bglap	F: AGT GAC AAC CCT GCT GAT GA	58	AF289506
	R: TCC CTC AGT GTC CAT CAT GT		
PTHrP	F: CCC AGA GCC AAA CAT TCA GT	58	AF197904
	R: CGG CCT AAC CTC ACC TTT TT		
mlc2	F: TGG CAT CAT CAG CAA GGA	54	AF150904
	R: TTG AAA GCG CTC ACG ATG		
ef1α	F: CTTCAACGCTCAGGTCATCA	58	AF184170
	R: GTGGGTGCAGTTTGACAATG		

4.7. Statistics

Statistical analyses of all parameters were performed in IBM SPSS Statistics for Windows version 22, (IBM Corp, Armonk, NY, USA). Normality was analyzed using the Shapiro–Wilk test and homogeneity of variance using Levene's test. Statistical significance was assessed by Chi-Square test for incidence of bone deformities, by Mann–Whitney U Test for growth parameters and Welch test for gene expression analysis. Values were considered statistically significant when $p < 0.05$. Data calculated for each group were expressed as mean± Standard error of the mean (SEM) or mean± standard deviation (SD).

5. Conclusions

Our data showed that the different MEL concentrations, and predominately the high one, affected the normal process of skeletogenesis, and the growth patterns on gilthead seabream larvae. MEL increased the frequency of skeletal abnormalities, especially those of the operculum complex,

for which we have recorded new typologies. The first signs of the operculum complex deformity were recorded before any sign of mineralization, proving that the abnormality occurs during the onset of the operculum complex bone series. Caudal fin complex was also sensitive to exogenous melatonin administration in a dose-dependent manner. In light of our results and bibliographic data, we hypothesize that skeletal deformities detected in experimental groups' larvae can be induced by the increased *PTHrP* expression level, which is upregulated by exogenous melatonin administration, or by a loss of co-ordination between skeletal muscle and bone function. Future studies should extend and unmask the melatonin-regulated pathways in gilthead seabream bone.

Author Contributions: Conceptualization, K.M. and G.M.; methodology, K.M. and G.M.; validation, G.M., A.G. and K.M.; formal analysis, K.M., G.M., F.A. and A.G.; investigation, K.M., G.M., F.A. and A.G.; resources, G.M., K.M. and A.G.; data curation, G.M., K.M. and A.G.; writing—original draft preparation, K.M. and G.M.; writing—review and editing, G.M., K.M. and A.G.; visualization, K.M. and G.M.; supervision, G.M. and K.M. and A.G.; project administration, F.A., R.L., M.L. and M.C.G.; funding acquisition, G.M. All authors have read and agreed to the published version of the manuscript.

Funding: This research was funded by FISH PAT NET (Grant of Sicily Region) CUP n. G47B18000130009, grant number SIPA 01/MS/18.

Acknowledgments: We are most grateful to AQUACULTURE TUNISIENNE for providing the samples and to Sergio Torre for his collaboration.

Conflicts of Interest: The authors declare no conflict of interest. The funders had no role in the design of the study; in the collection, analyses, or interpretation of data; in the writing of the manuscript, or in the decision to publish the results.

References

1. Bardon, A.; Vandeputte, M.; Dupont-Nivet, M.; Chavanne, H.; Haffray, P.; Vergnet, A.; Chatain, B. What is the heritable component of spinal deformities in the European sea bass (*Dicentrarchus labrax*)? *Aquaculture* **2009**, *294*, 194–201. [CrossRef]
2. Beraldo, P.; Canavese, B. Recovery of opercular anomalies in gilthead sea bream, *Sparus aurata* L.: Morphological and morphometric analysis. *J. Fish Dis.* **2011**, *34*, 21–30. [CrossRef] [PubMed]
3. Negrín-Báez, D.; Navarro, A.; Lee-Montero, I.; Soula, M.; Afonso, J.M.; Zamorano, M.J. Inheritance of skeletal deformities in gilthead seabream (*Sparus aurata*)–lack of operculum, lordosis, vertebral fusion and LSK complex1. *J. Anim. Sci.* **2015**, *93*, 53–61. [CrossRef] [PubMed]
4. Verhaegen, Y.; Adriaens, D.; Wolf, T.D.; Dhert, P.; Sorgeloos, P. Deformities in larval gilthead sea bream (*Sparus aurata*): A qualitative and quantitative analysis using geometric morphometrics. *Aquaculture* **2007**, *268*, 156–168. [CrossRef]
5. Thuong, N.P.; Verstraeten, B.; Kegel, B.D.; Christiaens, J.; Wolf, T.D.; Sorgeloos, P.; Bonte, D.; Adriaens, D. Ontogenesis of opercular deformities in gilthead sea bream *Sparus aurata*: A histological description. *J. Fish Biol.* **2017**, *91*, 1419–1434. [CrossRef]
6. Peruzzi, S.; Westgaard, J.-I.; Chatain, B. Genetic investigation of swimbladder inflation anomalies in the European sea bass, *Dicentrarchus labrax* L. *Aquaculture* **2007**, *265*, 102–108. [CrossRef]
7. Fernández, I.; Hontoria, F.; Ortiz-Delgado, J.B.; Kotzamanis, Y.; Estévez, A.; Zambonino-Infante, J.L.; Gisbert, E. Larval performance and skeletal deformities in farmed gilthead sea bream (*Sparus aurata*) fed with graded levels of Vitamin A enriched rotifers (*Brachionus plicatilis*). *Aquaculture* **2008**, *283*, 102–115. [CrossRef]
8. Georgakopoulou, E.; Katharios, P.; Divanach, P.; Koumoundouros, G. Effect of temperature on the development of skeletal deformities in Gilthead seabream (*Sparus aurata* Linnaeus, 1758). *Aquaculture* **2010**, *308*, 13–19. [CrossRef]
9. Ortiz-Delgado, J.B.; FernÃƒÂ¡ndez, I.; Sarasquete, C.; Gisbert, E. Normal and histopathological organization of the opercular bone and vertebrae in gilthead sea bream *Sparus aurata*. *Aquat. Biol.* **2014**, *21*, 67–84. [CrossRef]
10. Berillis, P. Skeletal Deformities in Seabreams. Understanding the Genetic Origin Can-Improve Production? *J. FisheriesSciences.com* **2017**, *11*, 57–59. [CrossRef]

11. Villamizar, N.; Blanco-Vives, B.; Migaud, H.; Davie, A.; Carboni, S.; Sánchez-Vázquez, F.J. Effects of light during early larval development of some aquacultured teleosts: A review. *Aquaculture* **2011**, *315*, 86–94. [CrossRef]
12. Villamizar, N.; García-Alcazar, A.; Sánchez-Vázquez, F.J. Effect of light spectrum and photoperiod on the growth, development and survival of European sea bass (*Dicentrarchus labrax*) larvae. *Aquaculture* **2009**, *292*, 80–86. [CrossRef]
13. Falcón, J.; Besseau, L.; Sauzet, S.; Boeuf, G. Melatonin effects on the hypothalamo-pituitary axis in fish. *Trends Endocrinol. Metab.* **2007**, *18*, 81–88. [CrossRef] [PubMed]
14. Sánchez-Vázquez, F.J.; López-Olmeda, J.F.; Vera, L.M.; Migaud, H.; López-Patiño, M.A.; Míguez, J.M. Environmental Cycles, Melatonin, and Circadian Control of Stress Response in Fish. *Front. Endocrinol.* **2019**, *10*, 279. [CrossRef]
15. Tordjman, S.; Chokron, S.; Delorme, R.; Charrier, A.; Bellissant, E.; Jaafari, N.; Fougerou, C. Melatonin: Pharmacology, Functions and Therapeutic Benefits. *Curr. Neuropharmacol.* **2017**, *15*, 434–443. [CrossRef]
16. Velarde, E.; Cerdá-Reverter, J.M.; Alonso-Gómez, A.L.; Sánchez, E.; Isorna, E.; Delgado, M.J. Melatonin-synthesizing enzymes in pineal, retina, liver, and gut of the goldfish (Carassius): mRNA expression pattern and regulation of daily rhythms by lighting conditions. *Chronobiol. Int.* **2010**, *27*, 1178–1201. [CrossRef]
17. Falcón, J.; Migaud, H.; Muñoz-Cueto, J.A.; Carrillo, M. Current knowledge on the melatonin system in teleost fish. *Gen. Comp. Endocrinol.* **2010**, *165*, 469–482. [CrossRef]
18. Danilova, N.; Krupnik, V.E.; Sugden, D.; Zhdanova, I.V. Melatonin stimulates cell proliferation in zebrafish embryo and accelerates its development. *FASEB J.* **2004**, *18*, 751–753. [CrossRef]
19. Fjelldal, P.G.; Grotmol, S.; Kryvi, H.; Gjerdet, N.R.; Taranger, G.L.; Hansen, T.; Porter, M.J.R.; Totland, G.K. Pinealectomy induces malformation of the spine and reduces the mechanical strength of the vertebrae in Atlantic salmon, *Salmo salar*. *J. Pineal Res.* **2004**, *36*, 132–139. [CrossRef]
20. Maria, S.; Samsonraj, R.M.; Munmun, F.; Glas, J.; Silvestros, M.; Kotlarczyk, M.P.; Rylands, R.; Dudakovic, A.; van Wijnen, A.J.; Enderby, L.T.; et al. Biological effects of melatonin on osteoblast/osteoclast cocultures, bone, and quality of life: Implications of a role for MT2 melatonin receptors, MEK1/2, and MEK5 in melatonin-mediated osteoblastogenesis. *J. Pineal Res.* **2018**, *64*. [CrossRef]
21. Zhu, G.; Ma, B.; Dong, P.; Shang, J.; Gu, X.; Zi, Y. Melatonin promotes osteoblastic differentiation and regulates PDGF/AKT signaling pathway. *Cell Biol. Int.* **2020**, *44*, 402–411. [CrossRef] [PubMed]
22. Sun, T.; Li, J.; Xing, H.L.; Tao, Z.S.; Yang, M. Melatonin improves the osseointegration of hydroxyapatite-coated titanium implants in senile female rats. *Z. Gerontol. Geriat.* **2019**, *53*, 770–777. [CrossRef] [PubMed]
23. Kalamarz, H.; Nietrzeba, M.; Fuentes, J.; Martinez-Rodriguez, G.; Mancera, J.M.; Kulczykowska, E. Melatonin concentrations during larval and postlarval development of gilthead sea bream Sparus auratus: More than a time-keeping molecule? *J. Fish Biol.* **2009**, *75*, 142–155. [CrossRef]
24. Herrero-Turrión, M.J.; Rodríguez, R.E.; Velasco, A.; González-Sarmiento, R.; Aijón, J.; Lara, J.M. Growth hormone expression in ontogenic development in gilthead sea bream. *Cell Tissue Res.* **2003**, *313*, 81–91. [CrossRef]
25. Herrero-Turrion, M.J.; Rodriguez, R.E.; Aijon, J.; Lara, J.M. Transient expression pattern of prolactin in *Sparus aurata*. *J. Mol. Endocrinol.* **2003**, *30*, 69–84. [CrossRef]
26. Deane, E.E.; Kelly, S.P.; Collins, P.M.; Woo, N.Y.S. Larval development of silver sea bream (*Sparus sarba*): Ontogeny of RNA-DNA ratio, GH, IGF-I, and Na+-K+-ATPase. *Mar. Biotechnol.* **2003**, *5*, 79–91. [CrossRef]
27. Izquierdo, M.S.; Scolamacchia, M.; Betancor, M.; Roo, J.; Caballero, M.J.; Terova, G.; Witten, P.E. Effects of dietary DHA and α-tocopherol on bone development, early mineralisation and oxidative stress in *Sparus aurata* (Linnaeus, 1758) larvae. *Br. J. Nutr.* **2013**, *109*, 1796–1805. [CrossRef]
28. Roo, J.; Hernandez-Cruz, C.M.; Socorro, J.; Fernández-Palacios, H.; Izquierdo, M. Effect of rearing techniques on skeletal deformities and osteological development in red porgy *Pagrus pagrus* (Linnaeus, 1758) larvae. *J. Fish Biol.* **2010**, *77*, 1309–1324. [CrossRef]
29. Galeotti, M.; Beraldo, P.; de Dominis, S.; D'Angelo, L.; Ballestrazzi, R.; Musetti, R.; Pizzolito, S.; Pinosa, M. A preliminary histological and ultrastructural study of opercular anomalies in gilthead sea bream larvae (*Sparus aurata*). *Fish Physiol. Biochem.* **2000**, *22*, 151–157. [CrossRef]
30. Beraldo, P.; Pinosa, M.; Tibaldi, E.; Canavese, B. Abnormalities of the operculum in gilthead sea bream (*Sparus aurata*): Morphological description. *Aquaculture* **2003**, *220*, 89–99. [CrossRef]

31. Sajan, S.; Anna-Mercy, T.V. Morphological and osteological malformations in hatchery bred redline torpedo fish, *Sahyadria denisonii* (Day 1865) (Cyprinidae). *Anales Biol.* **2016**, *38*, 73–80. [CrossRef]
32. Andrades, J.A.; Becerra, J.; Fernández-Llebrez, P. Skeletal deformities in larval, juvenile and adult stages of cultured gilthead sea bream (*Sparus aurata* L.). *Aquaculture* **1996**, *141*, 1–11. [CrossRef]
33. Boglione, C.; Gagliardi, F.; Scardi, M.; Cataudella, S. Skeletal descriptors and quality assessment in larvae and post-larvae of wild-caught and hatchery-reared gilthead sea bream (*Sparus aurata* L. 1758). *Aquaculture* **2001**, *192*, 1–22. [CrossRef]
34. Prestinicola, L.; Boglione, C.; Makridis, P.; Spanò, A.; Rimatori, V.; Palamara, E.; Scardi, M.; Cataudella, S. Environmental conditioning of skeletal anomalies typology and frequency in gilthead seabream (*Sparus aurata* L., 1758) juveniles. *PLoS ONE* **2013**, *8*, e55736. [CrossRef] [PubMed]
35. Faustino, M.; Power, D.M. Development of osteological structures in the sea bream: Vertebral column and caudal fin complex. *J. Fish Biol.* **1998**, *52*, 11–22. [CrossRef]
36. Gavaia, P.J.; Sarasquete, C.; Cancela, M.L. Detection of mineralized structures in early stages of development of marine teleostei using a modified alcian blue-alizarin red double staining technique for bone and cartilage. *Biotech. Histochem.* **2000**, *75*, 79–84. [CrossRef] [PubMed]
37. Faustino, M.; Power, D.M. Osteologic development of the viscerocranial skeleton in sea bream: Alternative ossification strategies in teleost fish. *J. Fish Biol.* **2001**, *58*, 537–572. [CrossRef]
38. Saka, Ş.; Çoban, D.; Kamacı, H.O.; Süzer, C.; Fırat, K. Early development of cephalic skeleton in hatchery-reared gilthead seabream, *Sparus aurata*. *Turk. J. Fish. Aquat. Sci.* **2008**, *8*, 341–345.
39. Can, E. Effects of Intensive and Semi-Intensive Rearing on Growth, Survival, and V-Shaped (Lordotic) Skeletal Deformities in Juvenile Gilthead Sea Bream (*Sparus aurata*). *Isr. J. Aquac. Bamidgeh* **2013**, *65*, 1–7, IJA_65.2013.798.
40. Castillo, J.; Codina, M.; Martínez, M.L.; Navarro, I.; Gutiérrez, J. Metabolic and mitogenic effects of IGF-I and insulin on muscle cells of rainbow trout. *Am. J. Physiol. Regul. Integr. Comp. Physiol.* **2004**, *286*, R935–R941. [CrossRef]
41. Wood, A.; Duan, C.; Bern, H. Insulin-like growth factor signaling in fish. *Int. Rev. Cytol.* **2005**, *243*, 215. [CrossRef] [PubMed]
42. Beckman, B.R.; Shimizu, M.; Gadberry, B.A.; Cooper, K.A. Response of the somatotropic axis of juvenile coho salmon to alterations in plane of nutrition with an analysis of the relationships among growth rate and circulating IGF-I and 41kDa IGFBP. *Gen. Comp. Endocrinol.* **2004**, *135*, 334–344. [CrossRef] [PubMed]
43. Georgiou, S.; Makridis, P.; Dimopoulos, D.; Power, D.M.; Mamuris, Z.; Moutou, K.A. Myosin light chain 2 isoforms in gilthead sea bream (*Sparus aurata* L.): Molecular growth markers at early stages. *Aquaculture* **2014**, *432*, 434–442. [CrossRef]
44. Lee, N.K.; Sowa, H.; Hinoi, E.; Ferron, M.; Ahn, J.D.; Confavreux, C.; Dacquin, R.; Mee, P.J.; McKee, M.D.; Jung, D.Y.; et al. Endocrine regulation of energy metabolism by the skeleton. *Cell* **2007**, *130*, 456–469. [CrossRef]
45. Guerreiro, P.M.; Rotllant, J.; Fuentes, J.; Power, D.M.; Canario, A.V.M. Cortisol and parathyroid hormone-related peptide are reciprocally modulated by negative feedback. *Gen. Comp. Endocrinol.* **2006**, *148*, 227–235. [CrossRef]
46. Kwong, R.W.M.; Perry, S.F. An essential role for parathyroid hormone in gill formation and differentiation of ion-transporting cells in developing Zebrafish. *Endocrinology* **2015**, *156*, 2384–2394. [CrossRef]
47. Abbink, W.; Flik, G. Parathyroid hormone-related protein in teleost fish. *Gen. Comp. Endocrinol.* **2007**, *152*, 243–251. [CrossRef]
48. Karaplis, A.C.; Luz, A.; Glowacki, J.; Bronson, R.T.; Tybulewicz, V.L.; Kronenberg, H.M.; Mulligan, R.C. Lethal skeletal dysplasia from targeted disruption of the parathyroid hormone-related peptide gene. *Genes Dev.* **1994**, *8*, 277–289. [CrossRef]
49. Abbink, W.; Kulczykowska, E.; Kalamarz, H.; Guerreiro, P.M.; Flik, G. Melatonin synthesis under calcium constraint in gilthead sea bream (*Sparus auratus* L.). *Gen. Comp. Endocrinol.* **2008**, *155*, 94–100. [CrossRef]
50. Shanqi, F.; Miho, K.; Yoko, U.; Sei, K.; Daichi, H.; Yuji, S.; Asami, T.; Takashi, N.; Yusuke, M.; Mika, I.; et al. Circadian production of melatonin in cartilage modifies rhythmic gene expression. *J. Endocrinol.* **2019**, *241*, 161–173. [CrossRef]

51. Keenan, L.; Ingleton, P.; Danks, J.; Morton, J.; Brown, B.; Canario, A.; Power, D. Immunoreactive parathyroid hormone-related protein (ir*PTHrP*) and *PTHrP* gene expression in normal and dystrophic sea bream. *J. Endocrinol.* **1998**, *156*, P10.
52. Guardiola-Lemaître, B. Toxicology of melatonin. *J. Biol. Rhythm.* **1997**, *12*, 697–706. [CrossRef] [PubMed]
53. Conde-Sieira, M.; Muñoz, J.L.P.; López-Patiño, M.A.; Gesto, M.; Soengas, J.L.; Míguez, J.M. Oral administration of melatonin counteracts several of the effects of chronic stress in rainbow trout. *Domest. Anim. Endocrinol.* **2014**, *46*, 26–36. [CrossRef] [PubMed]
54. Amano, M.; Iigo, M.; Ikuta, K.; Kitamura, S.; Okuzawa, K.; Yamada, H.; Yamamori, K. Disturbance of plasma melatonin profile by high dose melatonin administration inhibits testicular maturation of precocious male masu salmon. *Zool. Sci.* **2004**, *21*, 79–85. [CrossRef]
55. López-Olmeda, J.F.; Bayarri, M.J.; Rol de Lama, M.A.; Madrid, J.A.; Sánchez-Vázquez, F.J. Effects of melatonin administration on oxidative stress and daily locomotor activity patterns in goldfish. *J. Physiol. Biochem.* **2006**, *62*, 17–25. [CrossRef]
56. Abbate, F.; Guerrera, M.C.; Cavallaro, M.; Montalbano, G.; Germanà, A.; Levanti, M. LM and SEM study on the swordfish (*Xiphias gladius*) tongue. *Tissue Cell* **2017**, *49*, 633–637. [CrossRef]
57. Walker, M.B.; Kimmel, C.B. A two-color acid-free cartilage and bone stain for zebrafish larvae. *Biotech. Histochem.* **2007**, *82*, 23–28. [CrossRef]
58. Bustin, S.A.; Benes, V.; Garson, J.A.; Hellemans, J.; Huggett, J.; Kubista, M.; Mueller, R.; Nolan, T.; Pfaffl, M.W.; Shipley, G.L.; et al. The MIQE Guidelines: Minimum Information for Publication of Quantitative Real-Time PCR Experiments. *Clin. Chem.* **2009**, *55*, 611–622. [CrossRef]